ADDIS ABABA UNIVERSITY

ADDIS ABABA INSTITUTE OF TECHNOLOGY

School of Civil and Environmental Engineering

Evaluation of Climate Change Impact on Hydrology

(A Case Study of Upper Abay Basin)

Using CORDEX-RCP Climate Data and SWAT Model

A thesis Submitted to the School of Graduate Studies in Partial Fulfillment of the Requirements for the Degree of Master of Science in Civil Engineering (Major in Hydraulic Engineering)

By:

Habesh Mohammed Ibrahim

Advisor:

Dr. Daneal F/Sillassie

Addis Ababa University

Addis Ababa, Ethiopia

May, 2018

ADDIS ABABA UNIVERSITY

ADDIS ABABA INSTITUTE OF TECHNOLOGY

School of Civil and Environmental Engineering

Evaluation of Climate Change Impact on Hydrology

(A Case Study of Upper Abay Basin)

Submitted in partial fulfillment for the degree of Masters of Science in Civil Engineering

(Major in Hydraulic Engineering)

By:

Habesh Mohammed Ibrahim

Advisor:

Dr. Daneal F/Sillassie

May, 2018

Declaration and Copyright

I, Habesh Mohammed, do here by declare to the Senate of Addis Ababa University that this thesis is entirely original work and all other materials are duly acknowledged. This work has not been submitted for any academic degree award at any University.

Declaration

ADDIS ABABA UNIVERSITY

ADDIS ABABA INSTITUTE OF TECHNOLOGY

School of Civil and Environmental Engineering

Evaluation of Climate Change Impact on Hydrology

(A Case Study of Upper Abay Basin)

Submitted in partial fulfillment for the degree of Masters of Science in Civil Engineering (Major in Hydraulic Engineering)

By: Habesh Mohammed Ibrahim

Approval by Board of Examiners

---------- ---------- --------

Chairman (department of graduate committee) Signature Date

---------- ---------- --------

Advisor

---------- ---------- -------

Internal Examiner

---------- ---------- ------

External Examiner

ACKNOWLEDGMENT

First of all, I would like to thank 'Almighty Allah' who made it possible, to begin and finish this work successfully.

I would like to express my deepest gratitude to Dr. Daneal F/Sillassie for his patient, continuous guidance, encouragement and motivation in conducting this thesis work.

I would like to extend my sincere thanks to Haileyesus Belay, who helped me to boost up my knowledge in hydrology and gave me opportunity to work in this subject and provided me with the necessary materials.

I am thankful to Eyobe Yeheyes for his tireless efforts in training me basics of SWAT and SWAT-CUP models without which I would not even dare working on this topic.

I am very grateful to Ethiopian Road Authority (ERA) for sponsoring me and Addis Ababa Institute of Technology Department of Civil Engineering for allowing me to take part in the Master Program.

I am most grateful to my Dad Mohammed Ibrahim for encouraging me throughout my studies and always reminding me that sky is just the lower limit. My heartfelt thanks to my Mam, wife, brothers and sisters whose love, sacrifice and prayers kept me going during last few years.

At last a special group of friends who supported me through their friendship and professional help especially Abera Molla and Belay Gedamu deserves special thanks.

DEDICATION

To my beloved father Mohammed Ibrahim

ABSTRACT

Climate change is becoming one of the most arguable and threatening issues in terms of global context and their socio/economic driver. This study aims to assess the Annual, seasonal, monthly and extreme Discharge trend of Abay River at Kesse Gauging station by creating Hydrological response model under changing rainfall and temperature using data from an ensemble of downscaled climate data based on the Coordinated Regional climate Downscaling Experiment over African domain (CORDEX-Africa) with Coupled Model Inter-comparison Project Phase 5 (CMIP5) simulations under Representative Concentration Pathway's viz. RCP2.6, RCP4.5 and RCP8.5 climate scenarios.

Observed climate data from different stations within the Upper Abay basin were collected, Bias correction was performed for the RCP climate data (temperature and rainfall data), soil and water assessment Tool (SWAT) was calibrated and validated for stream flow simulation using SWAT-CUP with a method of SUFI2.The performance of the model was assessed through calibration and validation process and resulted R^2 = 0.91and E_{NS} = 0.9 during calibration and R^2 = 0.76 and E_{NS} = 0.74 during validation for monthly base simulation and R^2 = 0.84, E_{NS} = 0.81 during calibration R^2 = 0.72, E_{NS} = 0.69 for daily base simulation

The future projection period were divided in to three viz. 2030s (2031–2040), 2050s (2051–2060, and 2090s (2091–2100) and compared with the historical or base period (2001–2010) to explore the changes in Precipitation, Potential evapotranspiration and stream flow. From the results obtained, the mean monthly, seasonal and annual rainfall and Potential evaporation is expected to increase in all the future time series for all RCP scenarios. The projected annual mean precipitation and Potential Evaporation shows an increasing trend from the base period by (+9.4%), (+14.6%) and (+20.7%) for precipitation and by (+3.8%), (+3.9%) and (+3.6%) for potential evaporation during 2030s, 2050s and 2090s respectively under RCP2.6.For RCP4.5 the projected annual mean precipitation shows an increase by (+9.9%), (+15.6%) and (+25.2%) and potential evaporation by (+4.8%), (+6%) and (+6.6%) during 2030s, 2050,and 2090s respectively. The change in magnitude for RCP8.5 shows an increasing trend for precipitation with (+18.1%), (+23.4%) and (+36.6%) and potential evaporation by (+4.3%), (+8.5%) and (+18.2%) during 2030s, 2050, and 2090s respectively.

The projected stream flow for mean monthly, seasonal and annual flows shows an increasing trend when compared to the base period. Stream flow is expected to increase in the future, at 2030s average annual stream flow projection change may increase by (+7.8%) for RCP2.6, (+11.1%) for RCP4.5 and (+15.28%) for RCP 8.5 scenarios. At 2050s the corresponding average annual stream flow percentage changes increase by (+11.7%) for RCP 2.6, (+14.5%) for RCP4.5 and (+23.64%) for RCP8.5 scenarios. At 2090s average annual Stream flow projection change may increase up to (+22.0%) for RCP2.6, +24.5% for RCP4.5 and +41.24% for RCP8.5 scenarios.

The seasonal flow pattern also shows an increasing trend from the base period with maximum increment in Belg by (+62.6%) and Bega by (+33.1%) and Kiremt by (+12.9%) for RCP2.6 in 2090s. For RCP4.5 the maximum increase in stream flow shows (+40.9%) for Belg, (+30.7) for Bega and (+20.3%) for Kiremt season in 2090s. For RCP8.5 the maximum change in seasonal stream flow shows (+66.6%) for Belg, and (+70.8%) and (+29%) in 2090s.

Annual Peak flow pattern shows an increasing trend in all future time series under all RCP scenarios except for RCP2.6 with (-1.4%) decrease in2036.Max increase by (+26.7%) for RCP2.6 in 2095, (+24%) for RCP4.5 in2095 and (+30.8%) for RCP 8.5 in 2092. But the annual low flow pattern shows both an increasing and decreasing trend in the future with maximum increase (+145.7%) in 2092 and maximum decrease (-54%) in 2056 for RCP2.6, for RCP4.5 maximum increase (+155.5%) in 2093 and maximum decrease (-36.4%) in 2034 is observed. For RCP8.5 maximum increase (+281.2%) in 2094 and maximum decrease (-33.5%) in 2037 is observed.

From this study, it was concluded that the changing climate cloud have an impact on the availability of water and the increased in flow volume in the basin cloud be useful for water resources management and policy making so that climate change cloud be incorporated in the plans and management of future and existing water resource projects in the basin.

Keywords: Upper Abay basin; Climate Change; CORDEX-Africa; CMIP5; RCP; SWAT; Scenario; SWAT-CUP,SUFI2

TABLE OF CONTENTS PAGES

LIST OF FIGURES PAGES

LIST OF TABLES PAGES

LIST OF ACRONYMS

IPCC- Intergovernmental Panel on Climate Change

NMSA-National Meteorological Service Agency

RCP -Representative concentration pathway

SERS- Special Report on Emission Scenario

GCM-Global Circulation Model

RCM-Regional Climate Model

AR4- Assessment report No.4

AR5- Assessment report No 5

FAO- Food and Agricultural Organization

WCRP-World Climate Research Program

CORDEX- Coordinated Regional Downscaling Experiment

GHG- Green House Gas

SWAT- Soil and Water Assessment Tool

HRU- Hydraulic Reponses Units

DEM- Digital Elevation Model

SUFI-2-Sequential Uncertainty Fitting version-2

SWATCUP-Soil and Water Assessment Tool Calibration and Uncertainty Program

MoWIE- Ministry of water, Irrigation & Electricity

IWMI- International Water Management Institute

SRTM-shutter Radar Topography Mission

USGS- United states Geology Survey

UNESCO-United Nation Education, Science and Cultural Organization

NBI- Nile Basin Initiatives

CMIP5-Coupled Model Inter-comparison Project Phase 5

SDLM-Statistical Downscaling Model

CHAPTER ONE

1. INTRODUCTION

1.1 BACKGROUND

Climate change has been a burning issue among global scientific community since last two decades because of its potential serious impacts on human, society and environment. The Intergovernmental Panel on Climate Change (IPCC) fifth assessment report has shown an increase of 0.85° C in the global mean temperature since 1880 until 2012 *(IPCC 2013a),*

These changes in global temperature have been accompanied by changes in climate in different ways *(Feng et al. 2014).* Many regions have experienced changes in precipitation leading to frequent occurrence of floods *(Min et al. 2008, 2011)* and droughts *(Dai 2011, 2012).* These changes in climate system will have a strong impact on local and regional hydrological regimes in many regions of the world *(Dibike and Coulibaly 2005, Hu et al. 2013).*

The oceans and glaciers have experienced considerable changes *(Feng et al. 2014),* the arctic sea ice is continuously decreasing and recorded the lowest in 2012 *(Viñas 2014),* while the snow caps and glaciers in the Himalayas are continuously melting *(Yao et al. 2012). IPCC (2014a)* provided robust evidence for the impacts of climate change on reducing surface water and groundwater resources in most of the dry subtropical regions. The continuous shrinkage of glaciers and thawing of permafrost is affecting runoff and water resources downstream *(IPCC 2013a).* If these changes continue and become even more pronounced in the future, they would likely to have serious implications on the ecosystem, environment and the whole society.

In addition to increasing trends observed in the global mean temperature in 20th century, successive IPCC reports *(IPCC, 2007; IPCC, 2013)* have projected a significant increase in the global mean temperature if greenhouse gas emissions continue to increase unabated over the 21st century. Greenhouse gasses have played a great role in changing the climate change at global as well as regional level. The release of these gases to the atmosphere has been disturbing the normal composition of the atmosphere *(.Luqman Atique, Farman Atique and Iran Mohammed, 2014).*

In case of Africa the impacts of climate change on the hydrological cycle in general and on water resources in particular are of high significance due to the fact that all natural and socio/economic

system critically depends on water *(Dagnenet.F and Markus D, 2016)*. The direct impact of climate change can be variation and changing pattern of water resources availability and hydrological extreme events such as floods and the occurrence of severe droughts such as: in West Africa during the 1970s and 1980s *(Lamb, 1982)*, the 1983-85 drought event in Ethiopia *(Africa Watch, 1991)*, the 2011 East African drought *(Lyon, 2011)* and the current 2015-16 severe drought in parts of eastern Ethiopia are some of the events and with many indirect effects on agriculture, food and energy production and overall water infrastructure *(Ebrahim et al., 2013)*.

The impact may be worse for developing countries like Ethiopia because of their economies are strongly dependent on basic forms of natural resources mainly on agriculture and their economic structure is less flexible to adjust to such drastic changes *(NMSA, 2001)*.

In addition, the impact may be worse for trans-boundary Rivers like Upper Blue Nile River where competition for water is becoming high from different economic, political and social interests of the riparian countries and when runoff variability of upstream countries can greatly affect the downstream countries *(Kim, 2008; Semenov and Barrow, 1997)*.And further, previous studies showed that many parts of the Nile basin are sensitive to climatic variations *(Conway and Hulme, 1996; Yates and Strzepek 1996, 1998a, b; Conway, 2005; Kim et al., 2008; Beyene et al., 2010)* implying that climate change will have a considerable impact on the water resource.

It is in these regard , it is extremely important to conduct a research on the impacts of climate change on hydrological regimes so that people and society can foresee and respond the tentative future challenges either by mitigating the worst condition that likely to happen in future or at least be well prepared and resilient to face the possible challenges.

In this study, the hydro-climatic data of CORDEX-Africa RCMs downscaled from different GCMs from CMIP5 simulation under different RCPs scenario (RCP2.6, RCP4.5 and RCP8.5) will be used for the catchment. Then the data will be used as an input to the hydrological model (SWAT2012) to simulate the effect of climate change on the hydrological regimes and analyses the future water availability in the region.

1.2 STATEMENT OF THE PROBLEM

The climate in the Blue Nile basin is marked by significant inter-annual and inter-decadal variability, which has important implications for the management of water resources in the Nile *(Conway, 2005).*In addition, the water resources in the basin are critically sensitive to climate change *(Conway et al., 2007).* It is expected that future climate change may exacerbate the level of water stress or increase the water resource across the basin and it is therefore important to assess and manage the potential effects of such changes.

The freshwater resource of the Upper Blue Nile River Basin is a fundamental basis for the economic growth and social development of the communities in the basin. However, the ongoing global climate change puts further constraint on the already limited water resources in the basin due to high temporal and spatial variability in rainfall, prolonged dry season, global environmental changes and population growth *(NBI, 2013).* Therefore, evaluation of water resources in light of future climate change is very important for sustainable planning and management of the water resources.

Accordingly, a number of studies were conducted on the Abay River basin based on GCM and RCM models through downscaling of the GCM output to catchment level. Most findings of past studies conducted in the basin are mainly based on outdated climate scenario (SERS). Studies conducted on the SRES scenarios concluded that it is linked with exclusive socioeconomic assumptions or emission scenarios and it doesn't assume any polices to control climate change *(IPCC, 2013).*

Representative concentration pathways (RCPs) are new scenarios and these overcome the shortcoming of the SRES. Therefore, application of up-to-date Representative concentration path way (RCPs) emission scenario is essential to make the impact assessment more reliable and valid.

1.3 RESEARCH QUESTIONS

The research questions addressed in this study are:

- What are the temporal climate change trends of Precipitation and PET over the selected catchment of Abay basin (Upper Abey Basin)?
- Which climate variable dominates the future impact trajectory, precipitation change or potential Evapotranspiration change?
- How does the hydrological uncertainty affect climate change impact interpretation?

1.4 OBJECTIVE OF THE STUDY

1.4.1 General Objective

The general objective of this study is to evaluate the impact of climate change on hydrology of the selected catchment in Abay river basin (Upper Abay basin).

1.4.2 Specific Objective

In order to achieve the general objective of the study, the following specific objectives are set for major milestones of the study:

- To assess the impact of climate change (Precipitation and Temperature) on the hydrology of the selected catchment using SWAT Hydrological model and downscaled hydro-climatic data from CORDEX-Africa RCMs under RCP2.6, RCP4.5 and RCP8.5 climate scenario.
- To assess the mean annual, Monthly and seasonal stream flow variation for Abay River compared with the base period
- To assess the extreme (Maximum and minimum) flow pattern variation for Abay River compared with the base period simulated
- Assessment of sensitivity of the selected catchment (upper Abay basin) to climate change.
- Evaluation of impact of hydrological uncertainty on interpretation of climate change.

1.5 SCOPE AND LIMITATION OF THE STUDY

The study focuses on the Upper Abay basin and responds to the impact of climate change on the hydrology of the catchment and its effect on water availability of the river. Owing to data constraint, this study considered 2001 to 2010 as a baseline period. Three different RCP emission scenario data: RCP2.6, RCP4.5 and RCP8.5 divided three future time period: 2030s, 2050s and 2090s were used to generate future impacted flow. The followings are the limitations the study:

- In this study the impact of climate change was assessed for the meteorological terms of Precipitation and Temperature the other climate variables such as Relative Humidity, Solar Radiation and Wind speed were assumed to remain the same in the future.
- In addition the Physiographic terms such as land cover assumed to remain the same for the future. However, in real world the above variables are changing.
- Only data for 15 meteorological stations are available in the basin, and this shows an indication of the data scarcity for the basin and this can cause a lower level of performance by a hydrological model during the calibration and validation processes.
- The climate variables used in this study are results of CORDEX-Africa ensemble RCMs simulations scaled by downscaling different GCM models under different RCPs with a spatial resolution of 50km, which is a little bit coarse.

1.6 OVERVIEW OF THE THESIS

This thesis contains five chapters and organized as follows:

Chapter 1: Introduction

This chapter discusses the background information, problem statement, general and specific objectives, and limitations of the study. It brings to focus the problems experienced in this region in light of the changing environment and climate.

Chapter 2: Literature review

This chapter summarizes literature regarding the subject of climate changes in terms of global, continental and regional aspect, Major previous studies conducted in the Abay basin ,hydrologic modeling for use in impact assessment and Recent climate change scenarios data are also mentioned.

Chapter 3: Materials and Methodology

It describes the various data used in the study, their sources, the methods used for data quality control and also a step-by-step methodology adopted in the research is presented.

Chapter 4: Result and Discussion.

This chapter presents the outcome of model application to assess the impact of climate change. It gives a detailed account of the model set up, sensitivity of model parameters, calibration, validation and interpretation of results.

Chapter 5: The last chapter includes conclusion and Recommendation

This chapter summarizes the contribution of this research with conclusion and recommendation

CHAPTER TWO

2. LITERATURE REVIEW

2.1 OVERVIEW OF CLIMATE CHANGE

2.1.1 Global Climate Change

A simple definition climate is the average weather condition of a region over a long period of time. Therefore, it is safe to say that climate change is the change in the weather condition of a place due to anthropogenic intervention observed over comparable time periods *(United Nations 1992).*However, the *(IPCC, 2013b)* defines climate change as a change in the state of the climate that can be identified by changes in the mean and/or the variability of its properties and persist for an extended period typically a decade or even longer either due to anthropogenic or natural forcing.

Almost the entire globe has been experiencing surface warming and the evidence for this warming comes from multiple climate system indicators from atmosphere to the oceans such as change in temperature of oceans, atmosphere and surface, change in glacier, snow cover, sea ice, sea level and water vapor *(Hartmann et al. 2013).*

There is a total increase of 0.78^{o} C in global temperature from the second half of the 19 century to the 1^{st} decade of 20^{th} century *(IPCC 2013c)* While the number of cold days and cold nights have decreased, the number of warm days and nights have increased globally *(Hartmann et al. 2013).* There is also change in precipitation over the global land areas, particularly Northern Hemisphere has visible increase in precipitation after 1951*(Hartmann et al. 2013).* Due to these changes in temperature and precipitation, glaciers have continued to shrink globally, and arctic sea ice and spring snow cover have decreased remarkably in Northern Hemisphere *(IPCC 2013c).* Most of the regions in the world have experienced decreased snowfall events where winter temperatures have increased *(Hartmann et al. 2013).*

2.1.2 Climate Change Of Africa

Africa has been identified as one of the parts of the world most vulnerable to the impacts of climate change *(IPCC2014; Niang et al. 2014).*

African countries are more affected by climate change because of their reliance on agriculture as well as their lower financial, technical, and institutional capacity to adapt *(Nordhaus, 2006; Rose, 2015; Signgh and Purohit, 2014; Huq et al., 2004).* The African continent is expected to be the most affected by climate change, land degradation, and desertification *(Hummel, 2015).* Though Africa is the lowest source of GHG emissions from inhabited continents (due to low levels of industrial development), it is the most vulnerable to the effects of climate change *(Beg et al., 2011, Huq et al., 2004 and Bewket, 2012).*

The warming in Africa is likely to be somewhat larger than the global, annual mean warming throughout the continent and in all seasons, with drier subtropical regions (especially arid zones) warming more than the moister tropics. Annual rainfall is very likely to decrease in much of North Africa and Northern Sahara, while winter rainfall will very likely decrease in much of Southern Africa. There will likely be an increase in annual mean rainfall in tropical and East Africa *(Impact of Climate Change in Africa, July 2016).*

Sub-Saharan Africa is considered to be the most vulnerable to the impacts of climate change because of its high dependence on agriculture and natural resources, warmer baseline climates, low precipitation, and limited ability to adapt. Several studies have shown that surface water and groundwater evolutions over the past decades in Sub-Saharan Africa have been strongly affected by rainfall variations *(Hassan, R.; Nhemachena, C., 2008)*

2.1.3 Climate change of Ethiopia

Ethiopia is among those countries most vulnerable to climate risks in Africa. Its high vulnerability derives in large measure from the country's heavy dependence on rain-fed, subsistence agriculture. *(USAID, 2011)*

Ethiopia is a country where about 80% of the population is engaged in the agricultural sector *(Dile et al., 2013; Deressa et al., 2011)* and the main source of income for rural communities *(Bryan et al., 2009).* Around 90% of the country's grain is produced by smallholder farms. subsistence and rain-fed farming systems dominate and, with few exceptions, irrigation is not practiced *(FAO, 2009).*Consequently, agricultural and livestock production, people's livelihoods and food security depend strongly on weather conditions mainly on rainfall patterns such as amounts and timing. Hence, a large share of Ethiopia's population is very vulnerable to climate

change and in particular to its inter-annual variability *(Busby et al., 2014; Megersa et al., 2014; Headey et al., 2014; Zaitchik et al., 2012; Simane et al., 2012).*

The Ethiopian Highlands, where the Blue Nile is rising in, are considered as the water tower in East Africa. the Blue Nile, for instance, contributes about 55–65% of the flow of the Nile at the confluence with the White *Nile (King, 2013; Sutcliffe and Parks, 1999).*The river is therefore the most important water resource not only for Ethiopia but also for the downstream riparian countries of Sudan and Egypt. Water politics in the Nile basin have a long history and are a central geopolitical feature in this region *(Gebreluel, 2014; Ibrahim, 2012).* With growing populations, industrialization, climate change and its variability the situation becomes more and more tense *(Gebreluel, 2014).* Therefore, Knowledge about availability of future water resources in this region and studies providing insights of climate change, and their impacts on the hydrology are of outmost importance.

Table 2-1: Overview of Selected historical trend studies of mean, high and low stream flows in the Blue Nile

Data Length	Variables	Basin (Sub-basin)	Results	References
1978-2001	Low and high sstream flows	Gilgel Abay	Low Stream flow index Decreased by 18.1% and 66.6% for the periods 1982-2000 annd 2001-2005 respectively High stream flow index increased by 7.6%and 46.6% for the same periods	Rientjet et (2011)
1957-1998	Low and high sstream flows	Chemoga	Decline at monthly and daily scales a statistically significant decline by 0.6mm/year for dry season strem flow (October-May) annd a 94% decrease at monthly scale for February stream flow No discernible trend of monthly and daily high stream flows	Bewket annd sterk (2005)
1960-2002	Low and high sstream flows	Koga	No change in the hydrology of sub-basin in spite of lad use change	Gebrehiwot et al.(2010)
1968-2008	Mean Seasonal strea flow	Upper BNR	Significant incrase in discharege during kiremt season at Bahirdar, Kessie and EI diem (26%,27% and 10%) No significant trends at Baherdar and kessie but a significant decreasing trend (10%) at EI Diem for the dry season . A significant trend at Bahirdar and kessie (88%and 51%) while no change at I Diem during Belg season	Tesemma et al (2010)
1970-2009	Mean Seasonal stream flow	Upper BNR	Statistically significant increasing trends of annual and kiremt season stream flow significant decreasing trend in the dry season flow.	Gebremicael et al.(2018)
1970-2010	Mean annual, rainy season, dry season and small rainy seaason stream flow. Extreme stream flows given as 1-day annual maxima/minima and 7-day annual maxima/minima	Upper BNR	No significant trends is hydrological variiables are observed for Ribb and Chemoga sub-basins. Significcant decreasiinng trends for monthly stream flows during dry season (December -February) for jedeb sub-basin (-0.015m/s/year)	Tekleab et al. (2018
1960-2004	Annual total, high, low stream flow, run off coefficient and low stream flow index	Upper BNR	Generally, no significant change in twelve sub-basins for all variables. The exceptions are: Significant decreasing trend of Gilgel Abaay low stream flows annd low stream flow index Significant increasing trend of Andasa annd Koga run off coefficient. Significant decreasing trend of Guder annual total stream flow.	Gebrehiwot et al.(2014)

2.1.3.1Current Climate Variability and Observed Trends

I. Rainfall Variability and Trend

According to the study conducted by Ethiopian National Meteorological Services Agency and Ministry of water Irrigation and Electricity (NMSA and MoWIE, 2007) on the climate variability and trend for selected stations in the country , in such a way a baseline climate was developed using historical data of temperature and precipitation from 1971- 2000.The year-to-year variation of rainfall over the country expressed in terms of normalized rainfall anomaly averaged for 42, stations shows the country has experienced both dry and wet years over the last fifty five years (1951-2006)

The trend analysis of annual rainfall shows that rainfall remained more or less constant between 1951-2006 when averaged over the whole country. However, both seasonal and annual rainfall has exhibited high variability.

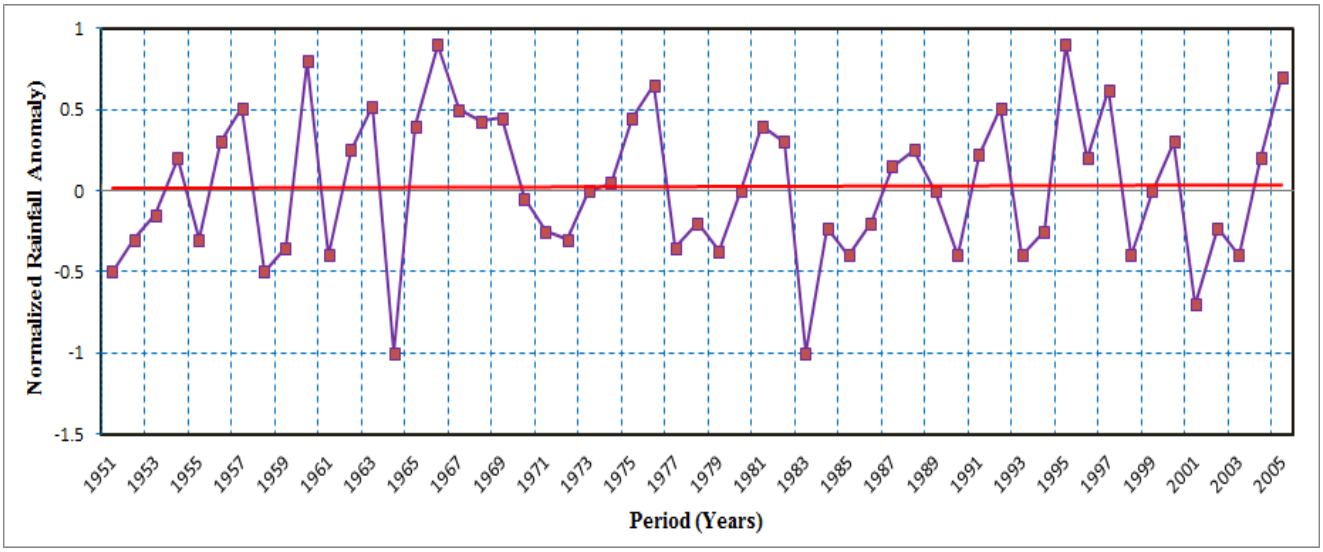

Figure 2-1: Year to year variability of annual Rainfall and trend over Ethiopia expressed in Normalized deviation (NMSA and MoWIE, 2007)

II. Temperature Variability and Trend

The year to year variation of annual minimum temperatures expressed in terms of temperature differences from the mean and averaged over 40 stations shows the country has experienced both warm and cool years over the last 55 years. However, the recent years are the warmest compared to the early years. The Figure 2-2 and 2-3 below clearly reveals that there has been a warming

trend in the annual minimum and maximum temperature over the past 55 years. It has been increasing by about 0.37^0C every ten years. Between 1960 and 2006, the mean annual temperature increased by 1.3℃, at an average rate of 0.28℃ per decade. (NMSA and MoWIE, 2007)

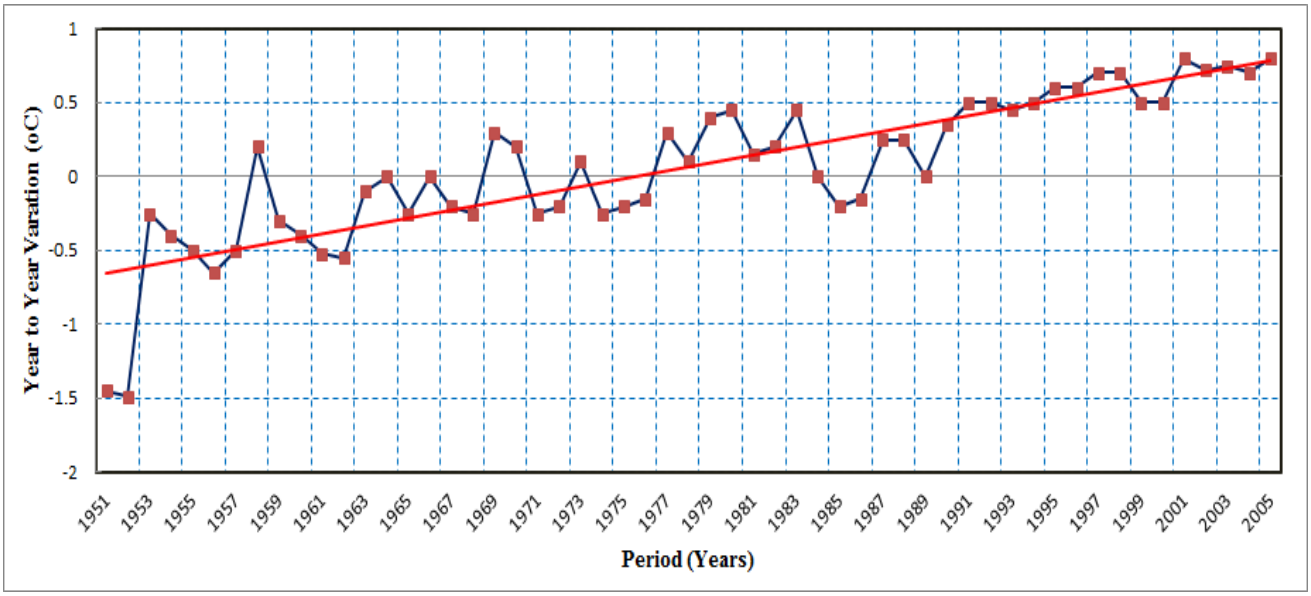

Figure 2-2: Year to year variability of annual Minimum temperature and trend over Ethiopia expressed in temperature Deference (NMSA and MoWIE, 2007)

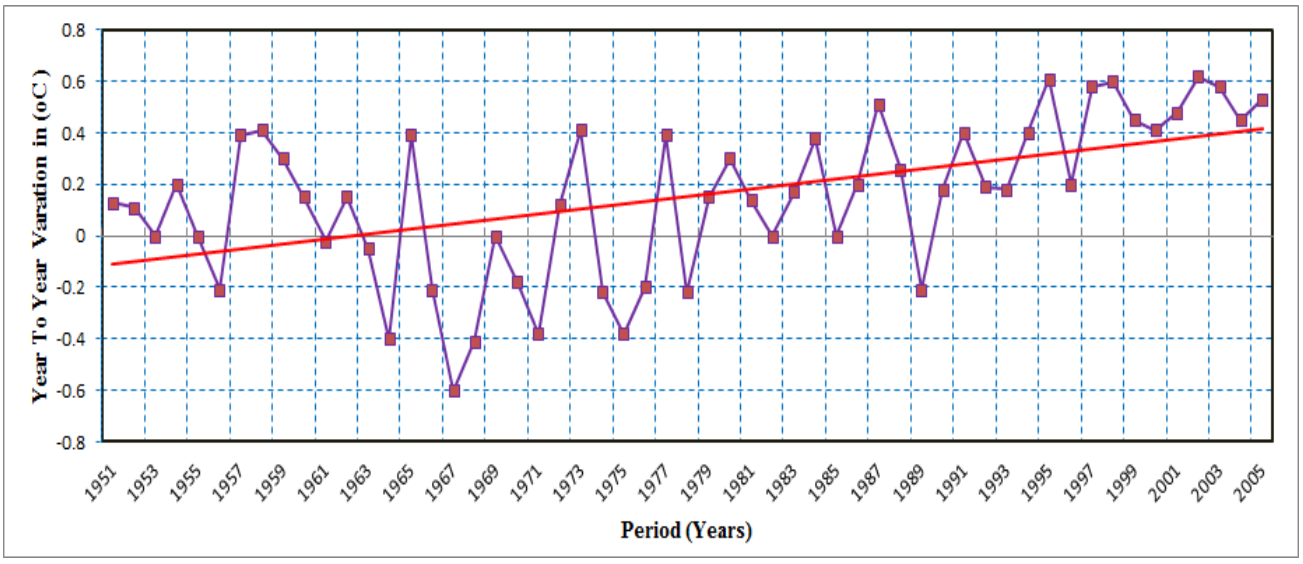

Figure 2-3: Year to year variability of annual Maximum temperature and trend over Ethiopia expressed in temperature Deference (NMSA and MoWIE, 2007)

2.2 CLIMATE SCENARIO

Scenarios have been used by decision makers and planners to analyze the situations where outcomes are uncertain *(Bjørnæs, 2015).* In climate change research, they have become an important element as they allow researchers to understand the long-term consequences (*van Vuuren, Edmonds, Kainuma, Riahi, and Weyant 2011)* and describe plausible pathways of climatic condition and other aspects of future *(Moss et al. 2010).* Over time, different scenarios have been used in climate research from SA92 used in IPCC's first assessment report to Special Report on Emissions and Scenarios (SRES) used in third and fourth assessment report. And recently, the new scenarios called Representative Concentration Pathways were developed and used for preparing fifth assessment report (AR5) of IPCC released in 2015.

2.2.1 Representative Concentration Path way (RCP)

RCPs are time and space dependent trajectories of concentrations and emission of greenhouse gases and pollutants resulting from human activities, including changes in land use. RCPs provide a quantitative description of concentrations of the climate change pollutants in the atmosphere over time, as well as their radiative forcing in 2100. RCP is the latest generation of scenarios that provide input to climate models in climate research. The RCPs were developed by combined efforts of the researchers from different disciplines involved in climate research *(Van Vuuren, Edmonds, Kainuma, Riahi, and Weyant 2011).*

A total of four pathways RCP2.6, RCP4.5, RCP6 and RCP8.5 were developed. They were named based on the radiative forcing target levels of 2.6, 4.5, 6 and 8.5 Watt/m2, by the end of 21st century *(van Vuuren, Edmonds, Kainuma, Riahi, Thomson, et al. 2011).* The estimation of radiative forcing is based on the forcing of GHGs and other agents. All these four pathways were considered to be the representative of all the literature pertinent to change in climate *(van Vuuren, Edmonds, Kainuma, and Riahi, and Weyant 2011, van Vuuren, Edmonds, Kainuma, Riahi, Thomson, et al. 2011, Wayne 2013).* And each RCPs defines a specific emissions trajectory and subsequent radiative forcing *(Wayne2013).*

2.2.1.1 RCP2.6 (mitigation scenario)

The RCP 2.6 was developed by the IMAGE modeling team of the PBL Netherlands Environmental Assessment Agency *(van Vuuren, Edmonds, Kainuma, Riahi, Thomson, et al. 2011, Wayne 2013).* This RCP is representative of the mitigation scenarios which aims to limit

the increase of global mean temperature to 2^{o}C. This pathway is also referred as RCP3PD in which PD stands for peak and decline. This pathway indicates that radiative forcing will reach around 3 W/m^2 in the mid-century and decline afterward to 2.6 W/m by the end of 21 st centuries *(van Vuuren, Stehfest, et al. 2011).* In order to achieve this, emission would need to be significantly reduced. CO_2 emissions need to be reduced by more than 100 % by 2100. This can be achieved only by replacing use of fossil fuel by renewable energy, nuclear power, increased use of bioenergy and use of carbon capture and storage (CCS). The important assumption in this scenario is that new energy efficient technologies can be rapidly transferred to all over the world and implement immediately *(van Vuuren, Stehfest, et al. 2011).*

2.2.1.2 RCP4.5 (stabilization scenario)

The RCP 4.5 was developed by the GCAM modeling group at the Pacific Northwest National Laboratory‘s Joint Global Change Research Institute (JGCRI) in the United States. It is the stabilization scenario *(Wayne, 2013)* in which radiative forcing stabilizes at 4.5W/m^2 (approximately 650 ppm CO_2-equivalent) in 2100 without ever exceeding that value *(Thomson et al. 2011)*. However, it doesn‘t mean that the GHG emissions and concentrations are stable.

The major assumptions of this scenario are the global population reaches a maximum of 9 billion by 2065 and then declines to 8.7 billion in 2100, declines in energy consumption, increase in fossil fuel consumption, substantial increase in renewable energy and nuclear energy use, and large increase in forest area as a mitigation strategy *(Clarke et al. 2007; Smith and Wigley 2006; Wise et al. 2009).*

2.2.1.3 RCP6 (stabilization scenario)

The RCP6 was developed by National Institute for Environmental Studies (NIES) and Japan Agency for Marine-Earth Science and Technology in Japan by using Asia-Pacific Integrated Model (AIM) modeling. It is also stabilization scenario like RCP4.5 but here radiative forcing stabilizes at 6.0 W/m^2 in the year 2100 without exceeding that value in prior years *(Masui et al. 2011).* It is climate policy intervention scenario in which climate policies are implemented to restrain radiative forcing not to exceed 6.0 W/m$^{2.}$ In this scenario, the GHG emissions will be the highest in 2060 and then decline thereafter. The primary assumptions of this RCP are increase in energy demand, shift from coal based to gas based production technologies, increase in use of

non-fossil fuel energy type and increase in population and economic growth in urban area, expansion of cropland and forest area, and decrease in grassland *(Masui et al. 2011).*

2.2.1.4 RCP8.5 (high emission scenario)

The RCP8.5 was developed by Integrated Assessment Framework by the International Institute for Applied System Analysis (IIASA) using MESSAGE model (*van Vuuren, Edmonds, Kainuma, Riahi, Thomson, et al. 2011, Wayne 2013).* This RCP is representative of high emission scenarios in the literature and characterized by increasing GHG emission over time *(Riahi et al. 2011).* It is consistent with future with no change in climate policy to reduce emissions *(Bjørnæs 2015).* This pathway is also called as baseline scenario without including any mitigation target or without explicit climate policy. The GHG emissions increase significantly over time leading to 8.5 W/m^2 of radiative forcing by the end of 21^{st} century. The important assumptions in this pathway are continuous increase in global population reaching 12 billion by 2100, slow income growth with modest rates of technological progress, long-term high energy demand, moving towards coal intensive technologies and high emission in the absence of climate change policies *(Riahi et al. 2011).*

Note; IA Model = Integrated Assessment model; MEASSAGE= Model for Energy Supply strategy Alternatives and their General Environmental Impact; International Institutes for applied Systems, Austria; AIM = Asia-pacific Integrated Model, National Institute for Environmental studies, Japan; GCAM= Global change Assessment Model, Pacific North West National Laboratory, USA(Previously referred to as MiniCAM); IMAGE= Integrated Model to Assess the Global Environment; Netherlands Environmental assessment Agency, The Netherlands.

Table 2-2: Summary of the four RCPs

RCPs	Radiative forcing	Concentration (ppm)	Pathway
RCP 2.6	Peak at ~3 W/m^2 before 2100 and then declines	Peak at ~490 CO_2-equiv. before 2100 and then declines	Peak and decline
RCP 4.5	~4.5 W/m^2 at stabilization after 2100	~650 CO_2-equiv. at stabilization after 2100	Stabilization without overshoot
RCP 6	~6 W/m^2 at stabilization after 2100	~850 CO_2-equiv. at stabilization after 2100	Stabilization without overshoot
RCP 8.5	>8.5 W/m^2 in 2100	>1370 CO_2-equiv. 2100	Rising

(Source: Moss et al. 2010)

2.3 COMPARISONS OF SRES AND RCP CLIMATE SCENARIOS

- The four RCP scenarios used in CMIP5 lead to radiative forcing values that range from 2.6 to 8.5 W m–2 at 2100, a wider range than that of the three SRES scenarios used in CMIP3 (IPCC, 2013).
- The SRES scenarios do not assume any policy to control climate change, unlike the RCP scenarios.
- RCPs represent pathways of radiative forcing, not linked with exclusive socio-economic assumption in contrary to Special Report on Emission Scenarios (SRES). Any single radiative forcing pathway can result from a diverse range of socio-economic and technological development scenarios*(Van Vuuren et.al.,2011)*

2.4 COORDINATED REGIONAL DOWNSCALING EXPERIMENT (CORDEX)

World climate Research program (WCRP) has initiated Global Coordinated Regional Downscaling Experiment (CORDEX: http://wcrp-cordex.ipsl.jussieu.fr/) with the intention of producing an ensemble of high-resolution climate change projections by downscaling GCM simulations from Coupled Model Inter-comparison Project Phase 5 (CMIP5) data archive (Taylor et al., 2012) on 25Km and 50Km grid spacing for 14regions of the Globe. Africa was selected as the first target region. CORDEX-Africa RCMs generate an ensemble of high

resolution historical and future climate projections at regional scale by downscaling different GCMs forced by RCPs based on the Coupled Intercomparison Project Phase 5 (CMIP5).

In this study, results of CORDEX-Africa ensemble RCMs simulations for the historical (1951–2005) and future (2006–2100) climate projections downscaled from different GCMs under RCP2.6, RCP4.5 and RCP8.5 with spatial resolution of 0.44 (50km) is used.

Output form CORDEX-Africa domain have been used for impact studies especially over east Africa such as one carried out by *(Ngaina, et al., 2015)* they found out that all the CORDEX models performed well in simulating rain fall over east Africa and predicted high variation of minimum and maximum temperature for both RCP4.5 and RCP8.5.However, temperature increase was found to be higher during long rainy (LR) season while increase in rainfall was found to be higher during short rainy (SR) season.

A further study carried out in the southern Africa on extreme precipitation events and future climate, found out that the simulated climate output correlates well with the observation of station data *(Christopher, et al., 2015).*

Among, the four RCP (RCP2.6, RCP4.5, RCP6 and RCP8.5) only the RCP6 is not used in the study because the characteristics of RCP6 is more or less similar with that of RCP4.5 as in both case they are stabilizing scenario.

2.5 BIAS CORRECTION

Despite high resolution data provision of RCM models, its limitations are systematic errors during 1st data correction. The theoretical and practical limitations may cause bias and should be corrected by bias correction methods. Bias correction should be applied to compensate for any tendency to overestimate or underestimate the mean of downscaled variables. *(Mentioned in Mulushewa nigatu, 2013).*

Bias correction factors are computed from the statistics of observed and historical simulated variables for the same duration. Bias correction methods are assumed to be stationary, i.e. the correction algorithm and its parameterization for current climate conditions are assumed to be valid for future conditions as well. *(Teutschbein and Seibert, 2012)*

The correction method used in the study was the linear scaling method (LS), as the method aims to perfectly match the monthly average of corrected values with observed ones.

2.6 PREVIOUS RELATED STUDIES IN THE STUDY AREA

Various studies have been conducted in Abay basin to study the effect of climate change. Some of the findings of the studies are discussed below:

1. **Setegn (2011):** projected a uniform temperature increase in Lake Tana Basin for 15 GCMs for all time periods and emission scenarios based upon SRES of AR4. According to the study for the SRES A2 scenario, four out of the nine GCMs showed significant decline in annual stream flow for the 2080–2100 period.
2. **Abdo (2008):** assessed the impact of climate change on the inflow to Lake Tana using the statistical downscaling model (SDSM) and HBV hydrological models (Hydrologiska Byråns Vattenbalansavdelning). According to the IPCC AR4 emission scenarios, He found significant changes of seasonal and monthly flows. A reduction in the runoff volume during the wet-season by approximately 11.6% and 10.1% was predicted for the2080s by the A2 and B2 emission scenarios respectively.
3. **Tarekegn and Tadege(2006):** studied the impact of climate change on water resource of Lake Tana-sub basin accordingly, If the temperature is increased by 2^{o}c and there is no change in rainfall the mean annual flow will be decreased by 11.3%. But if the rainfall is decreased by 10% and 20% the decrease in runoff will be 29.3% and 44.6% respectively. On the other hand, if the rainfall is increased by10%and 20%, the mean annual runoff will increase by 6.6% and 32.5%respectivly. And it was concluded as the basin is more sensitive to change in rainfall than temperature.
4. **Muluneh (2008):** based on hypothetical climate change scenario and using HBV hydrological model. The assessment was done on selected 10 catchment of Abay basin the hypothetical scenario within the range of (-30 to +30) for both precipitation and PET. Evaluation of water resource change shows that, for both scenarios, impact assessment of Chacha is the most sensitive catchment followed by catchments Sechi, Birr, Guder, G/Belese, Teme, Muger, Koga, Neshi, and Little Anger. And from the sensitivity map developed for the whole Basin Jemma, Dabus, part of Belese, Woleka, Wonbera and Beshilo are overstress sensitive sub basins, however; Fincha, Anger and Tana sub basins have relaxed water resource change sensitivity.
5. **Yehun (2009):** using downscaled climate outputs from SDSM as an input to the SWAT model and used to assess the impact of climate change on the Gilgel Abay River and Lake

Tana basin. The result reveals that the impact of climate change may cause a decrease in monthly flow volume up to 46% in the 2020s and increase up to 135% in the 2080s. It is observed that climate change has negligible effect on the low flow condition of the river. Seasonal flow volume may show increase up to 136% and 36% for Belg and Kiremt respectively. It is observed that there may be a net annual increase in flow volume in Gilgel Abay River due to climate change.

6. **Andualem (2009):** assessed the impact of climate change on runoff in upper Gilgel Abay River basin using SDSM model climate output data and SWAT model. The result shows, the changes in the climate variables i.e. the decrease in precipitation and increase in temperature thereby increasing evapotranspiration are likely to have significant impacts on the runoff. As a result, the total average annual runoff might decline significantly up to 43.5%, 56.5% and 75.8% for A2a- and 42.2%, 53.3% and 67.2% for B2a scenario for 2020s, 2050s and 2080s period respectively.

7. **vHailu Sheferaw Ayele et al., Ming-Hsu Li et al., Ching-Pin Tung et al. and Tzu-Ming Liu et al., (2016):** In this study, projections of seven global circulation models (GCMs) associated with high and medium–low Representative Concentration Pathways (RCP8.5 and RCP4.5) for the period 2021–2040 and 2081–2100 were adopted to assess changes on runoffs in the Gilgel Abay sub basin, the upper Blue Nile basin. Despite the projected magnitude of changes varied among different GCMs and RCPs, increasing runoffs in wet-season and decreasing in dry-season are observed in both periods, mainly attributed to the change in projected precipitation. Such changes are profound in cases of RCP8.5 with respect to those of RCP4.5 and in cases of2081–2100 with respect to those of 2021–2040.

8. **V. Aich , S. Lierschv, T. Vetter, S. Huang , J. Tecklenburg (2014)**

   This study aims to compare impacts of climate change on stream flow in four large representatives African river basins: the Niger, the Upper Blue Nile, the Ouban-gui and the Limpopo. Eco-hydrological model SWIM (Soil and Water Integrated Model)

   For the climate impact assessment, outputs of five bias corrected Earth system models of Coupled Model Inter-comparison Project Phase 5 (CMIP5) for the representative concentration pathways (RCPs) 2.6 and 8.5 was used. Regarding the changes in river discharge for Upper Blue Nile Basin a base period (1970–1999) and two future period near (2021–2050) and far (2070–2099) was selected and. In the Upper Blue Nile basin, the

discharge projections for almost all climate models and both RCPs show an increasing trend which corresponds to the precipitation trend with maximum change in discharge ranging from ~10 % to ~50 % for RCP 8.5 in the far period

Despite many research have been made on climate change in Abay river basin, most of them were made using the old climate scenario (SRES) in predicting future impact of climate change. In this research, since anthropogenic climate change poses critical challenges globally and regionally it is very critical to use, up-to-date climate scenario data, to improve our understanding of the potential impacts and implications of climate change. Therefore in order to see the impact of climate change in detail Hydro-climatic data from CORDEX-Africa RCMs based on different RCPs scenarios (RCP2.6, RCP4.5 and RCP8.5) were used in the analysis.

2.7 HYDROLOGICAL MODELING

There are various definitions of a model depending on the field of study. A model represents a simple and complex process in a system or a real world with its output being close to exactly what happen in the real system *(Devi, et., al. 2015). (Schulze, 2000)* defines a hydrological model as; **"Quantifying expression of observation analysis and predication of the interaction of the various hydrological processes which vary in time and over space i.e. Rainfall, infiltration, evaporation or stream flow"**

A hydrological model involves the application of mathematical equations to model the physical response of a watershed to meteorological events in a catchment area *(Rwigi, 2014).*For the purpose of hydrological modeling, the river basin is the most appropriate scale to focus on for analysis of water management issues using hydrological models. Stream flow and runoff are interplays of many physical processes that include: the hydrological, meteorological, topographical, human activitie and soil characteristics. Hydrological model relates stream flow and these parameters and are primarily used for hydrological prediction as well as for understanding the hydrologic process in the catchment area *(Mutua, 1986).*

Hydrological model uses mathematical estimations of stream flow as a function of basin characteristics with rainfall and drainage area being the most important input element in addition to soil characteristics, land cover, topography of the watershed, soil water content and availability of an aquifer therefor hydrological models are vital and necessary for water and environment management *(Devi, et. al., 2015).*

2.7.1 Soil and Water Analysis Tool (SWAT)

SWAT is a physically based semi distributed hydrological model which is a process-based, basin scale and continuous time model developed in early 1990s by Agriculture Research Service of the United States Department of Agriculture (USDA*) (Arnold et al. 1998,Arnold and Fohrer 2005).* This model has been tremendously used in studying the impacts of climate change on hydrological regime of a watershed *(Liu et al. 2011, Wang et al. 2012, Zuo et al. 2015)* as it has proven to be effective for assessing water resources at global and regional scale, and it is also computationally efficient and capable of continuous simulation over long periods *(Gassman et al. 2007).* SWAT divides a river basin into sub-basins and then into multiple units of unique slope, soil and land use characteristics called hydrological response units (HRUs*) (Wang et al.*

2012). HRUs are defined as homogenous spatial units characterize by common climate, land use, geomorphology and hydrological properties *(Flugel 1996).* The water movements and losses are considered individually for each HRUs and aggregated in sub-basin scale and then routed to basin outlets through the channel network *(Zuo et al. 2015).*

The model requires comprehensive input data and currently being applied for climate change studies worldwide with reported success and some of them are listed here:

(Zhang et. al., 2016) studied the impact of climate change and variability on the Head water of River in China. Separate and combined human activities on land and change in climate conditions were studied and it was concluded that SWAT model simulated well historical and future land use and changes in climate change.

(Kim et. al., 2015) studied global climate changes on water projects and stream flow behavior in Geum River. In this study output from regional model were used to provide projected climate data and daily stream flow by SWAT model. The model simulated well runoff during two future periods compared to the base period. In south Africa, *(Dabrowski, 2014)* utilized SWAT hydrological model to study orthophosphate loads and trophic status in some reservoir in South Africa and it provides good estimate of orthophosphate concentration in the four Dams of varying sizes. In Ethiopia, *(Dile, Berndtsson, & Setegn, 2013),* used SWAT to study the response of climate to the hydrology of Gilgel Abay River in, Lake Tana Sub-basin.

2.7.2 Watershed Delineation

The watershed delineation is primary made on the sub-basin level, and is determined based on the relative spatial location of each sub-basin, the direction of hydrologic flow and the natural divisions of stream networks determined by elevation. A digital elevation model (DEM) is the only required dataset for this step. Generally, the smaller the threshold area, the more detailed are the drainage networks, and the larger are the number of sub-basins and HRUs. However, this needs more processing time and space. As a result, an optimum size of a watershed that compromises both should be selected *(ARCSWAT, User manual interference for SWAT2009)*

2.7.3 Weather Generator Data Preparation

Lack of full and realistic long period climatic data is the problem of developing countries. Weather generators solve this problem by generating data having the same statistical properties

as the actual ones *(Danuso, 2002).* SWAT requires daily values of precipitation, maximum and minimum temperature, solar radiation, relative humidity as an input. But most of the time actual recorded date contains too many missing data and for that SWAT has a built in weather generator called WGEN *(Richardson et al., 1984)* that is used to fill the gaps, filled with, -99 identifier to fill the gap. But in this research the missing climate variables data was filled manually using suitable statistical approach.

For the sake of data generation and preparation, weather parameters were developed by using the weather parameter calculator PCPSTAT and dew point temperature calculator DEW02, which were downloaded from the SWAT website.

The PCPSTAT program reads daily values of precipitation it then calculates the daily averages and standard deviations of all variables in month as well as probability of wet and dry days, skew coefficient, and average number of precipitation days in the month. The DEW02 programs reads daily values of relative humidity, and maximum and minimum temperature values and calculates monthly average dew point temperatures.

2.7.4 Determination Of Hydrologic Response Units (HRU's)

The HRU Analysis section takes land use, soil and slope data and divides each sub-basin into hydrologic response units, with specific combinations of the three layers respective characterizations. The layer produced by this process is crucial to the ultimate analysis performed by the SWAT model, because it determines the land, soil and slope category assigned to each HRU. This category determines how land will respond to precipitation, runoff, infiltration and other hydrologic processes during the simulation. Each sub-basin can then have one or more major HRUs defined within it (*ARCSWAT User manual interference for SWAT2009)*

The required land cover and soil data is accompanied by preparing a look-up table with attribute information for each specific land cover and soil type, and provides these tables for each layer. The last layer needed for the HRU Analysis setup is slope, which is determined from the DEM supplied during watershed delineation.

Once each layer is loaded, they must be overlaid to determine the HRU features. For every unique combination of slope, land use and soil class than a HRU will be created, although within the study area there can be multiple HRUs with the same combination.

The last step is to define how HRU classifications will be aggregated or transferred to the sub-basin level. The Multiple HRU option was chosen for defining HRU. This option allows the user to select a threshold for each category individually, starting with land use, then soil class, and finally ending with slope. *(ARCSWAT User manual interference for SWAT2009)*.

According to (*Luzio et al.* 2002) and user manual for SWAT, the threshold levels set for multiple HRUs is a function of the project goal and the amount of detail desired by the modeler. For most applications, the default settings for land use threshold (5 %) soil threshold (20%) and20% slope were applied in this research work

2.7.5 Hydrologic Water Balance

Water balance is the driving force behind everything that happens in the watershed. In SWAT simulation of hydrology of the watershed can be separated in to two major divisions. The first division is the land phase of hydrologic cycle controls the amount of water, sediment, nutrient and pesticide loadings in to the main channel in each sub basin. The second division is the routing phase of hydrological cycle which can be defined as the movement of water, sediments, etc through the channel network of the watershed to the outlet *((Neitsch et al. 2002)*. As far as this research work is concerned the hydrologic cycle mainly focused only on the movement of water, which is the runoff generation.

The hydrologic cycle simulated by SWAT is based on the following water balance equation:

$$SW_t = SW_O + \left[\sum_{i=1}^{t} (R_{day} - Q_{surf} - E_a - W_{seep} - Q_{gw}) \right] \text{----------Eq2.1}$$

In which SW_t is the final soil water content (mm), SW_o is the initial soil water content on Day i (mm), t is the time (days), R_{day} is the amount of precipitation on day i (mm), Q_{surf} is the amount of surface runoff on day i (mm), E_a is the amount of evapotranspiration on day I (mm), W_{seep} is the amount of water entering the vadose.

2.7.6 Surface runoff

Surface runoff occurs whenever the rate of water application to the ground surface exceeds the rate of infiltration. SWAT provides two methods for estimating surface runoff: the SCS curve number procedure (SCS, 1972) and the Green & Ampt infiltration method (1911). For these research work SCS curve number method has been selected

The SCS curve number used (SCS, 1972)

$$Q_{surf} = \left[\frac{(R_{day}-I_a)^2}{(R_{day}-I_a+S)}\right]$$ ----------Eq2.2

Where: Q_{surf} is the accumulated runoff of rainfall excess (mmH_2O), R_{day} is the rainfall depth for the day (mmH_20), I_a is the initial abstractions which includes surface storage, interception and infiltration prior to runoff (mmH_2O), S= is the retention parameter (mm).

The retention parameter varies spatially due to changes in soils, land use, management and slope and temporally due to changes in soil water content. The retention parameter is defined as:

$$S = 25.49\left[\frac{1000}{CN} - 10\right]$$ ----------Eq2.3

Where: CN is the curve number for the day.

The initial abstraction, Ia, is commonly approximated as 0.2S and Eq. (4.1) becomes,

$$Q_{surf} = \left[\frac{(R_{day}-0.2S)^2}{(R_{day}-0.8S)}\right]$$ ---------- Eq2.4

Runoff will only occur when $R_{day} > Ia$.

2.7.7 Peak Runoff Rate

The peak discharge or the peak surface runoff rate is the maximum volume of flow rate passing a particular location during a storm event. SWAT calculates the peak runoff rate with a modified rational method it assumed that a rainfall of intensity I begins at time t=0 and continuous indefinitely, the rate of runoff will increase until the time of concentration t=t_{conc} and mathematically expressed as:

$$q_{peak} = \left(\frac{\alpha_{tc} * Q_{surf} * \text{Area}}{3.6 t_{conc}}\right)$$ ----------Eq2.5

Where: q_{peak} is the peak runoff rate (m^3/s), α_{tc} is the fraction of daily rainfall that occurs during the time of concentration, Q_{surf} is the surface runoff (mm), Area is the sub-basin area in (km^2), and t_{conc} is the time of concentration (hr), and 3.6 is the conversion factor.

SWAT estimates the value of α_{tc} using the following equation:

$$\alpha_{tc} = 1 - exp\left(\frac{-125}{R_{Day}+5}\right)$$ ----------Eq2.6

Where: α_{tc} is the fraction of daily rainfall that occur on a given day, R_{day} is the Rainfall on a given day (mmH_2O)

2.7.8 Time of Concentration

The time of concentration, t_{conc} is the time within which the entire sub basin area is discharging at the outlet point. It is calculated by summing up both the overland flow time of the furthest point in the sub basin to reach a stream channel (t_{ov}) and the upstream channel flow time needed to reach the outlet point. (t_{ch}):

$$t_{conc} = t_{ov} + t_{ch}$$ ----------Eq2.7

The overland flow time (t_{ov}) is computed as:

$$t_{ov} = \left(\frac{L_{slp}}{3600 * V_{ov}}\right)$$ ----------Eq2.8

Where: L_{slp} is the average sub basin slope length (m),

V_{ov} is the overland flow velocity (m/s), and 3600 is a unit conversion factor

The overland flow velocity for a unit width along the slope is calculated by using the manning's equation:

$$V_{ov} = \left(\frac{q^{0.4} * Slp^{0.3}}{n^{0.6}}\right)$$ ----------Eq2.9

Where: q is the average overland flow rate (m^3/s)

Slp is the average slope of the basin (m/m)

n is the manning's roughness coefficient of the basin

Assuming an average flow rate of 6.35mm/hr and substituting the equation of V_{ov} in to t_{ov} the simplified equation of the overland flow becomes:

$$t_{ch} = \left(\frac{L_{slp}^{0.6} * n^{0.6}}{16 * Slp^{0.3}}\right)$$ ----------Eq2.10

Channel flow time is computed as:

$$t_{ch} = \frac{L_c}{3.6 * V_c}$$ ----------Eq2.11

Where: L_c is the average flow channel length (km)

V_c is the average flow velocity (m/s), and 3.6 is a unit conversion factor

The average flow length is calculated as:

$$L_c = \sqrt{L_{cen} * L}$$----------Eq2.12

.

Where: L is the channel length from the furthest point to the sub basin outlet (km)

L_{cen} is the distance along the channel to the sub basin centroid (km)

Assuming L_{cen} = 0.5L, and using manning's equation for V_c for a trapezoidal channel with side slope of 2:1 and bottom width ratio 10:1, channel flow time becomes.

$$t_{ch} = \left(\frac{0.62 * L * n^{0.75}}{\text{Area}^{0.125} * Slp_{ch}{}^{0.375}}\right)$$----------Eq2.13

Where: t_{ch} is the time of concentration for channel flow (hr).

L is the channel length from the most distant point to the sub basin outlet (km),

n is manning's roughness coefficient for the channel,

Area is the sub basin area (km^2), and Slp_{ch} is the channel slope (m/m)

2.7.9 Surface Runoff Lag

In large sub basins with a time of concentration greater than 1 day, only a portion of the surface runoff will reach the main channel on the day it is generated. SWAT incorporates a surface runoff storage feature to lag a part of the surface runoff release to the main channel.

Once surface runoff is calculated, the amount of surface runoff released to the main channel is calculated as:

$$Q_{surf} = \left(Q'_{surf} + Q_{surf,i-1}\right) * \left(1 - exp\left[\frac{-surlag}{t_{conc}}\right]\right)$$----------Eq2.14

Where: Q_{surf} is the amount of surface runoff discharged to the main channel in a day (mm), Q'_{surf} is the amount of surface runoff generated in a sub basin in a day (mm),

$Q_{surf,i-1}$ is the surface runoff stored or lagged from the previous day (mm), $surlag$ is the surface runoff lag coefficient, and t_{conc} is the time of concentration for the sub basin (hr)

2.7.10 Routing

The routing phase is the second division of hydrological cycle which can be defined as the movement of water, sediments, etc through the channel network of the watershed to the outlet. Water is routed through the channel network using the variable storage routing method or the Muskingum River routing method.

The Muskingum routing method models the storage volume in a channel length as function of wedge and prism storages.

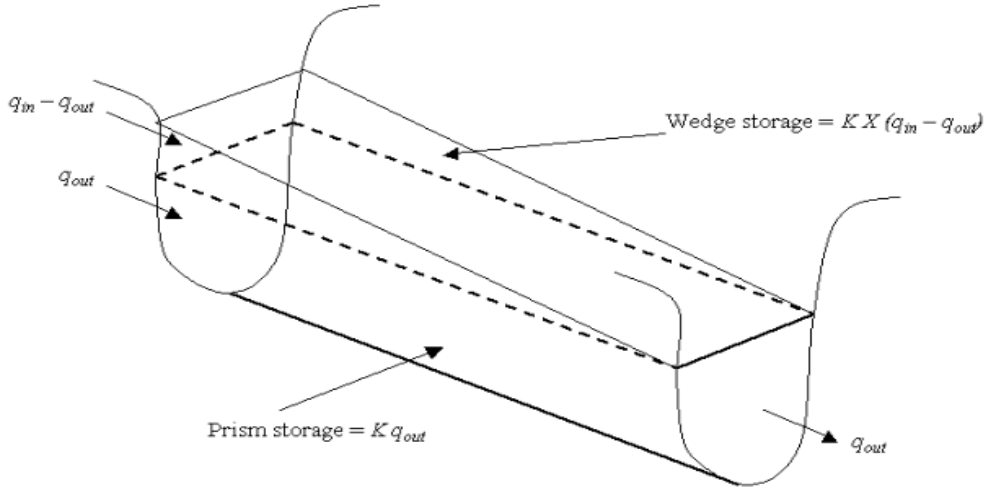

Figure Prism and wedge storages in a reach segment (Chow et al., 1988)

When a flood wave advances in to a reach segment, inflow exceeds out flow and a wedge of storage is produced. As the flood wave recedes, outflow exceeds inflow in the reach segment and a negative wedge is produced. In addition to the wedge storage, the reach segment contains a prism of storage formed by a volume of constant cross-section along the reach segment.

For a given reach segment, the storage routing is based on the continuity equation:

$$(V_{in} - V_{out}) = \Delta V_{stored}$$----------Eq2.15

Where V_{in} is the volume of inflow during the time step (m^3H_2O), V_{out} is the volume of outflow during the time step (m^3H_2O), and $\Delta V_{stored}$is the change in volume of storage during the time step (m^3H_2O), the equation can be written as

$$\Delta t = \left(\frac{q_{in.1}+q_{in.2}}{2}\right) - \Delta t\left(\frac{q_{out.1}+q_{out.2}}{2}\right) = V_{stored.2} - V_{stored.1}$$ ----------Eq2.16

Where: =Δt is the length of the time step (s), $q_{in.1}$ is the of inflow rate at the beginning the time step (m^3/s), $q_{in.2}$ is the of inflow rate at the end of the time step (m^3/s), $q_{out.1}$ is the out flow rate at the beginning of the time step (m^3/s), $q_{out.2}$ is the out flow rate at the end of the time step (m^3/s), $V_{stored.1}$ is the storage volume at the beginning of the time step(m^3H_2O) , and is $V_{stored.2}$ the storage volume at the end of the time step (m^3H_2O).

As defined by Manning's equation, the cross sectional area of flow is directly proportional to the discharge for a given reach segment. Using this assumption the volume of prism storage can be expressed as the function of the discharge, $k * q_{out}$ where K is the ratio of storage to discharge and has a dimension of time. In a similar manner, the volume of wedge storage can be expressed as $KX(q_{in} - q_{out})$, where X is weighting factor that controls the relative importance of inflow and outflow in determining the storage in a reach .Summing these terms gives a value for a total storage.

$$V_{stored} = k * q_{out} + KX(q_{in} - q_{out})$$----------Eq2.17

Where V_{stored} is the storage volume (m^3.H_2O), q_{in} is the inflow rate in (m^3/sec) q_{out} is the discharge rate (m^3/sec), K is the storage time constant for the reach (s) and X is the Weighting factor. The equation can be re arranged to form

$$V_{stored} = K * (xq_{in} + (1-x)q_{out})$$----------Eq2.18

The Weighting factor, X has a lower limit of 0 and an upper limit of 0.5. This factor is a function of wedge storage and a mean value of 0.2 is used

The storage volume in the above equation can be incorporated in to the continuity equation (Eq 3.1) and simplified to

$$q_{out.2} = C_1 * q_{in.2} + C_2 * q_{in.1} + C_3 * q_{out.1}$$ ----------Eq2.19

$q_{in.1}$ is the of inflow rate at the beginning the time step (m^3/s), $q_{in.2}$ is the of inflow rate at the end of the time step (m^3/s), $q_{out.1}$ is the out flow rate at the beginning of the time step (m^3/s), $q_{out.2}$ is the out flow rate at the end of the time step (m^3/s),and

$$C_1 = \frac{\Delta t - 2KX}{2K(1-X)+\Delta t} \quad C_2 = \frac{\Delta t + 2KX}{2K(1-X)+\Delta t} \quad C_3 = \frac{2K(1-X)-\Delta t}{2K(1-X)+\Delta t}$$ ----------Eq2.20

Where: $C_1 + C_2 + C_3 = 1$. To express all values in unit of volume, both sides of the equation (eq 3.3) are multiplied by the time step.

$$V_{out.2} = C_1 * V_{in.2} + C_2 * V_{in.1} + C_3 * V_{out.1}$$ ----------Eq2.21

To maintain numerical stability and avoid the computation of negative outflows, the following condition must be met:

$$2Kx < \Delta t < 2K(1-X)$$ ----------Eq2.22

The value of the weighting factor, X, is the value for storage time constant and estimated as:

$$K = coef_1 * K_{bnkfull} + coef_2 * K_{0.1bnkfull}$$ ----------Eq2.23

Where K is the storage time constant for the reach segment(s) $coef_1$ and $coef_2$ are weighing coefficient, $K_{bnkfull}$ is the storage time constant calculated for the reach segment with bank full flows (s), and $K_{0.1bnkfull}$ is the storage time constant calculated for the reach segment with one- tenth of the bank full flows (s). To calculate $K_{bnkfull}$ and $K_{0.1bnkfull}$,an equation developed by Cung (1969) is use

$$K = \frac{1000 * L_{ch}}{C_k}$$ ----------Eq2.24

Where K is the storage time constant (s), L_{ch} is the channel length in (km), and C_k is the celerity corresponding to the flow for a specified depth (m/s). Celerity is the velocity with which a variation in flow rate travels along the channel. It is defined as

$$C_k = \frac{d}{dA_{ch}}(q_{ch})$$ ----------Eq2.25

Where the flow rate, q_{ch}, is defined by manning's equation, and differentiating with respect to the cross sectional area gives:

$$C_k = \frac{5}{3}\left(\frac{R_{ch}^{2/3} * Slp_{ch}^{1/2}}{n}\right) = \frac{5}{3}V_c$$ ----------Eq2.26

Where C_k is the celerity (m/s), R_{ch} is the hydraulic radius for a given depth of flow (m) , Slp_{ch} is the slope along the channel length (m/m), n is the manning's roughness coefficient for the channel, and V_c is the flow velocity (m/s)

2.7.11 Potential Evapotranspiration

Potential evapotranspiration (PET) was a concept originally introduced by Thornthwaite (1948) as part of a climate classification scheme. He defined PET is the rate at which evapotranspiration would occur from a large area uniformly covered with growing vegetation that has access to an unlimited supply of soil water and that was not exposed to advection or heat storage effects. Because the evapotranspiration rate is strongly influenced by a number of vegetative surface characteristics, Penman (1956) redefined PET as "the amount of water transpired by a short green crop, completely shading the ground, of uniform height and never short of water". Penman used grass as his reference crop, but later researchers (Jensen, et al., 1990) have suggested that alfalfa at a height of30 to 50 cm may be a more appropriate choice.

Numerous methods have been developed to estimate PET. Three of these methods have been incorporated into SWAT: the Penman-Monteith method (Monteith, 1965; Allen, 1986; Allen et al., 1989), the Priestley-Taylor method (Priestley and Taylor, 1972) and the Hargreaves method (Hargreaves et al., 1985).

The three PET methods included in SWAT vary in the amount of required inputs. The Penman-Monteith method requires solar radiation, air temperature, and relative humidity and wind speed. The Priestley-Taylor method requires solar radiation, air temperature and relative humidity. The Hargreaves method requires air temperature only.

2.7.11.1 Penman-Monteith Method.

The Penman-Monteith equation combines components that account for energy needed to sustain evaporation, the strength of the mechanism required to remove the water vapor and aerodynamic and surface resistance terms.

The penman-Monteith equation is:

$$\lambda E = \frac{\Delta(H_{net}-G)+\rho_{air} * C_p * [e_z^{\ 0} - e_z]/r_a}{\Delta+\Gamma*(1+\frac{r_c}{r_a})} \text{----------Eq2.27}$$

Where: λE is the latent heat flux density (MJ m^{-2} d^{-1}), E is the depth rate evaporation (mm d^{-1}), Δ is the slope of the saturation vapor pressure- temperature curve, de/dT (kPa °C^{-1}), H_{net} is the net radiation (MJ m^{-2} d^{-1}), G is the heat flux density to the ground (MJ$m^{-2}d^{-1)}$, ρ_{air} is the air density (kg m^{-3}) , C_p is the specific heat at constant pressure (MJ kg^{-1} °C^{-1}) , $e_z^{\ 0}$ is the saturation vapor pressure of air at height z (kpa), e_z is the water vapor pressure of air at height z (kPa) , Γ is the psychometric constant (kpa °C^{-1}), r_c is the plant canopy resistance (sm^{-1}), and r_a is the diffusion resistance of the air layer (aerodynamic resistance) (s m-1).

For well-watered plants under neutral atmospheric stability and assuming logarithmic wind profiles, the Penman-Monteith equation may be written (Jensen et al., 1990):

$$\lambda E_t = \frac{\Delta(H_{net}-G)+\Gamma* k_1(0.622\lambda \frac{\rho_{air}}{p} * [e_z^{\ 0} - e_z]/r_a}{\Delta+\Gamma*(1+\frac{r_c}{r_a})} \text{----------Eq2.28}$$

Where λ is the latent heat of vaporization (MJ kg^{-1}), E_t is the maximum transpiration rate (mm d^{-1}), K_1 is a dimension coefficient needed to ensure the two terms in the numerator have the same units (for u_z in m s^{-1}, K_1 = 8.64 x 10^4), and P is the atmospheric pressure (kPa).

2.7.12 Groundwater

SWAT assumes two layers of aquifers while simulating the groundwater balance; namely a shallow-unconfined aquifer, and a deep-confined aquifer. The unconfined shallow aquifer is contributes to flow in the main channel or reach of the sub basin, whereas the deep confined aquifer assumed to contribute to stream flows outside the watershed *(Arnold et al. 1995).*

The volume of water available in the shallow aquifer is governed by the recharge from the top soil profile (recharge), the flow into the main stream channels or reach (base flow), the movement into the overlying unsaturated zone (revap) and the flow to the deep aquifer (deep

percolation). Evaporation, pumping withdrawals, seepage to the deep aquifer, and water uptake from the shallow aquifer by deep rooted plants is also components of the groundwater.

The details of the methodology are described in the SWAT Theor

$$aq_{sh,i} = aq_{sh,i-1} + W_{rchrg} - Q_{gw} - W_{revap} - W_{deep} - W_{pump,sh}$$ ---------- Eq2.29

Where: $aq_{sh,i}$ is the amount of water stored in the shallow aquifer on day i (mm),

$aq_{sh,i-1}$ is the amount of water stored in the shallow aquifer on day i-1 (mm),

W_{rchrg} is the amount of recharge entering the aquifer on day i (mm),

Q_{gw} is the groundwater flow, base flow, into the main channel on day i (mm),

W_{revap} is the amount of water moving into the soil zone in response to water deficient on day i (mm),

W_{deep} is the amount of water percolating from the shallow aquifer into the deep aquifer on day i (mm), and

$W_{pump,sh}$ is the amount of water removed from the shallow aquifer by pumping on day i (mm).

CHAPTER THREE

3. MATERIALS AND METHDOLOGY

3.1 DESCRIPTION OF THE STUDY AREA

3.1.1 General

The Nile River is the longest international river system in the world. It flows some 6700 km through ten countries before reaching the Mediterranean Sea. Its headwaters are in Lake Victoria about 4^{o}S latitude and it flows mostly northward to its mouth at 32^{o} N latitude. It is formed by three tributaries, the Blue Nile, the White Nile, and the Atbara. The Blue Nile contributes about 60% of the total flow of the Nile, whereas the Baro-Akobo (Sobat) and Tekeze (Atbara) contribute slightly less than 15% each *(Eman S.A. Soliman et al., 2009).*

Among the three tributaries of the Nile River the headwaters of all the tributaries, the Blue Nile originates from the highlands of Ethiopia, and the bulk of their runoff (70% on average) occurs between July and September *(Conway, 2000).*

Therefore, this study focuses on the selected catchments of the Upper Blue Nile River Basin, commonly known as Upper Abay Basin; it includes 5 major sub basins: Tana sub basin, North Gojam sub basin, Beshilo Sub basin, Welaka Sub basin and Jemma Sub Basin *(Blue Nile Atlas, 2009)*

3.1.2 Location

Upper Abbay basin is part of the Abay basin found in North East part of Ethiopia. Geographically it extends between 12^{o} 44' N to 09^{o} 01' N latitude and from 36^{o} 46'E to 39^{o} 49' E longitude.

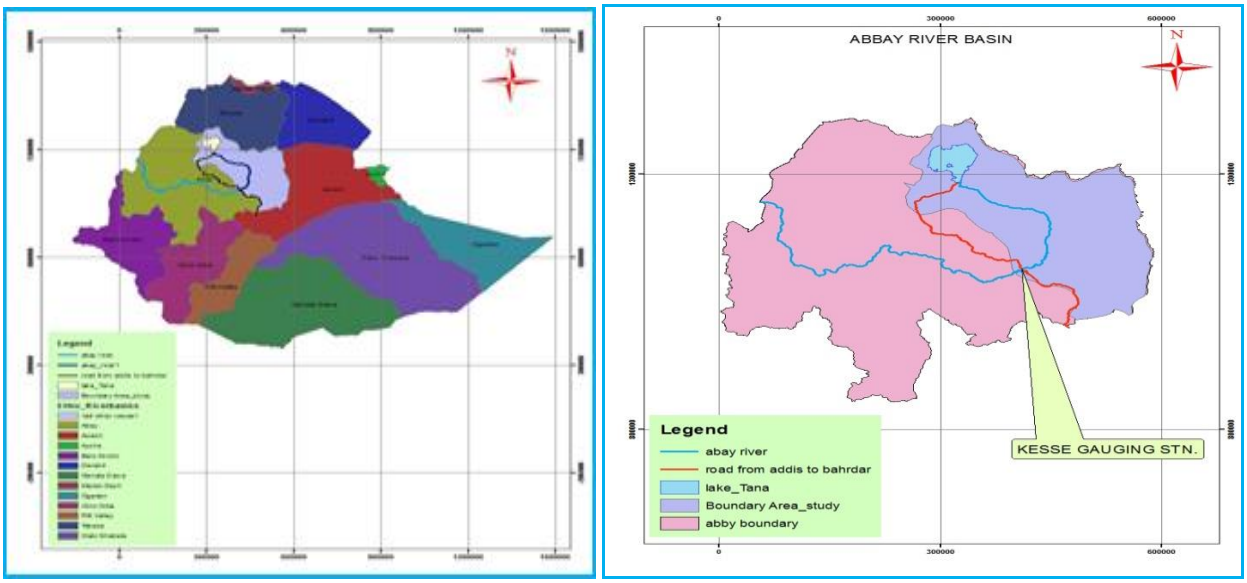

Figure 3-1: Location map of the Blue Nile river Basin

Item	Study Area
Location	12° 44' N to 09° 01' N and 36° 46'E to 39° 49' E
Topography	(997m to 4236m) amsl
Rainfall	725mm to 1584mm
Temprature	Max(19 to 18)°C and Min(-6.6 to16)°C
PET	1042mm to 1103mm
Stream Guging Stn.	1 (Kesse)

Figure3-2 **:** Location map of the Study Area

3.1.3 Topography

The topographic features of Abay basin vary between the highlands in the center and eastern part of the basin and the lowlands in the western part of the basin with altitude ranges from 498 up to 4261 masl. *(Blue Nile Basin Atlas, 2009).*

The research area lays almost in the Easter part of the Blue Nile basin and the elevation of the study area ranges between 997 m to 4234 m +MSL, which is extracted from DEM (30*30m) grid resolution and the mean elevation of the basin is found to be 2255 m +MSL.

3.1.4 Climate

The traditional climate classification of the country which is based on altitude and temperature shows the presence of five climatic zones namely: Wurch (cold climate at more than 3000m altitude), Dega(temperate like climate ;highland with 2500-3000 m altitude), Woina Dega (warm 1500-2500m altitude), Kola (hot and arid type, less than 1500 m in altitude), and Berha (hot and hyper-arid type) climate *(NMSA, 2001).* According to this classification, the study area falls in Wurch, Dega, Woina Dega and Kola climate zone.

I. Rainfall

The rainfall distribution in the research area (middle Abay basin) is found to be a mono-modal pattern i.e. one peak value observed during rainy season especially in July, or August. For the 15 rainfall stations used in the study area which are collected from NMSA for a period of 10 years (2001-2010) shows a mean annual rainfall amount ranges between 725mm in WegelTena and 1584 mm in Dangela.

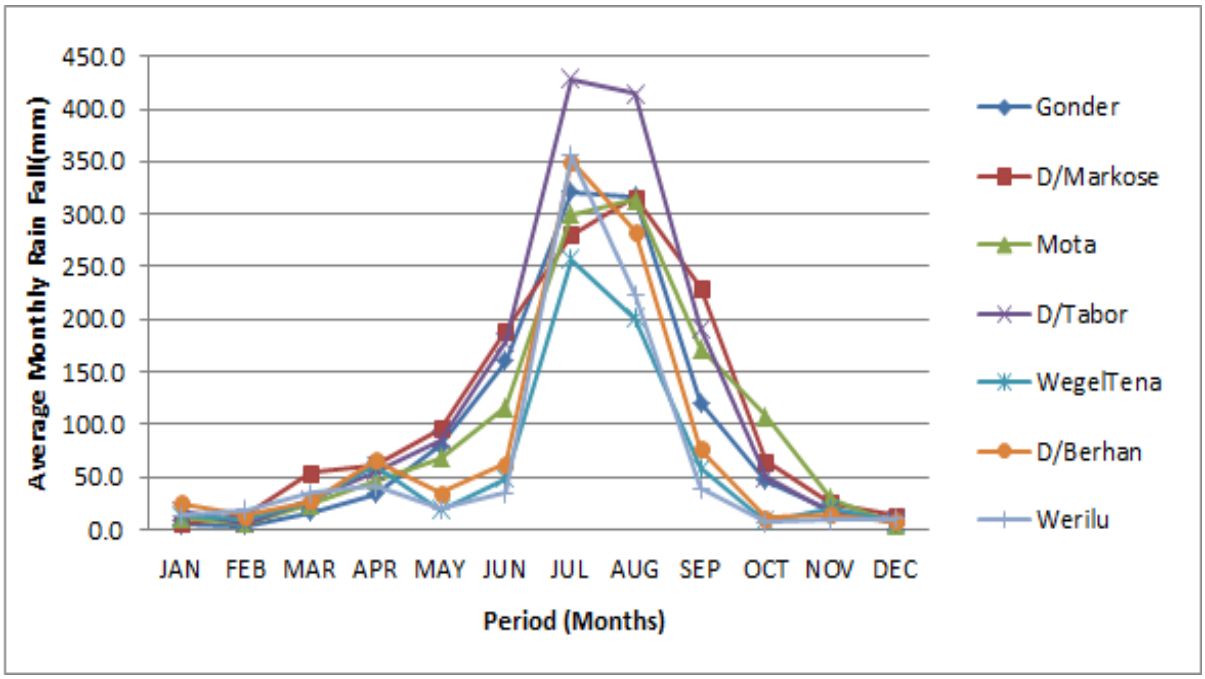

Figure 3-3a

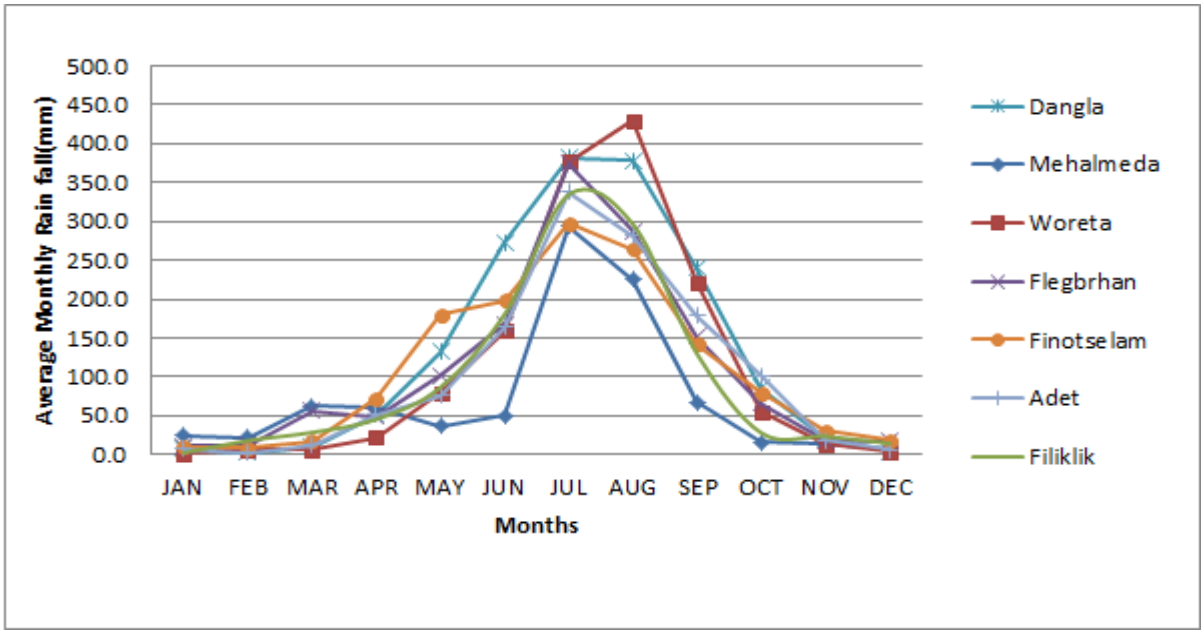

Figure 3-3b

Figure3-3: Average Monthly rainfall of Different Station in the study area for a period of (2001-2010)

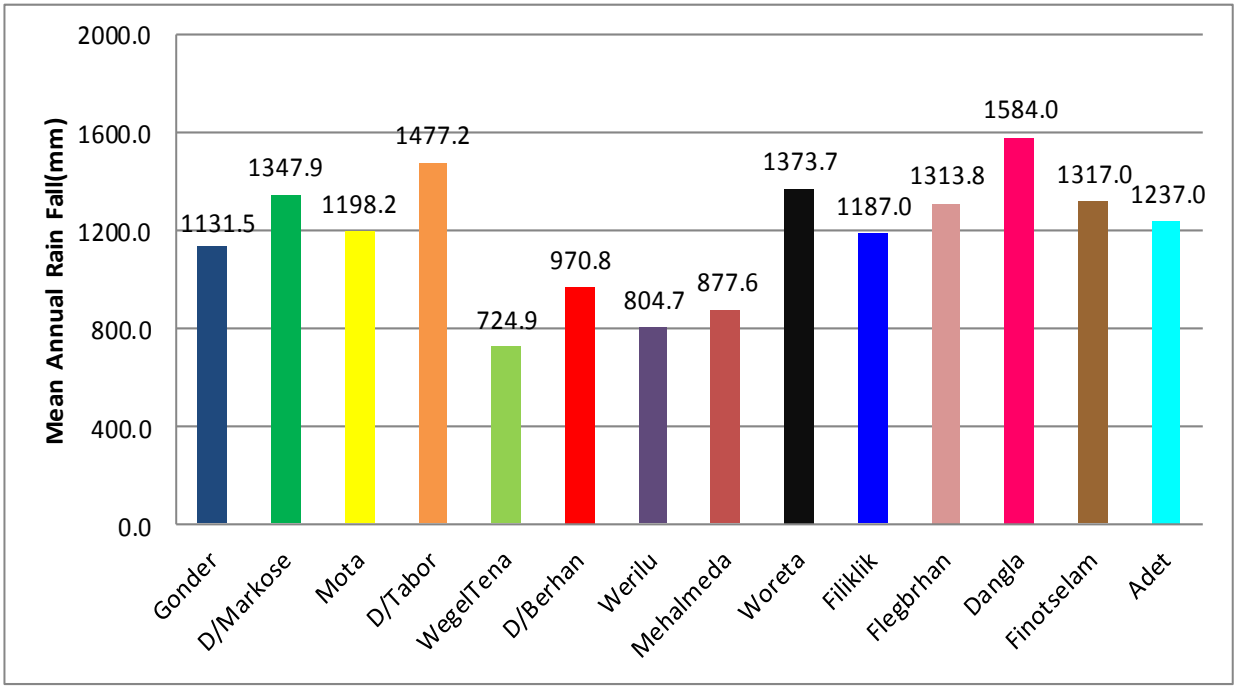

Figure 3-4: Mean Annual Rain Fall for the study Area from a period of (2001 up to 2010)

II. Temperature

The mean annual minimum and maximum temperature ranges between -6.6^{o}C in Debrebrhane and 37.5^{o}C in Filiklik respectively.

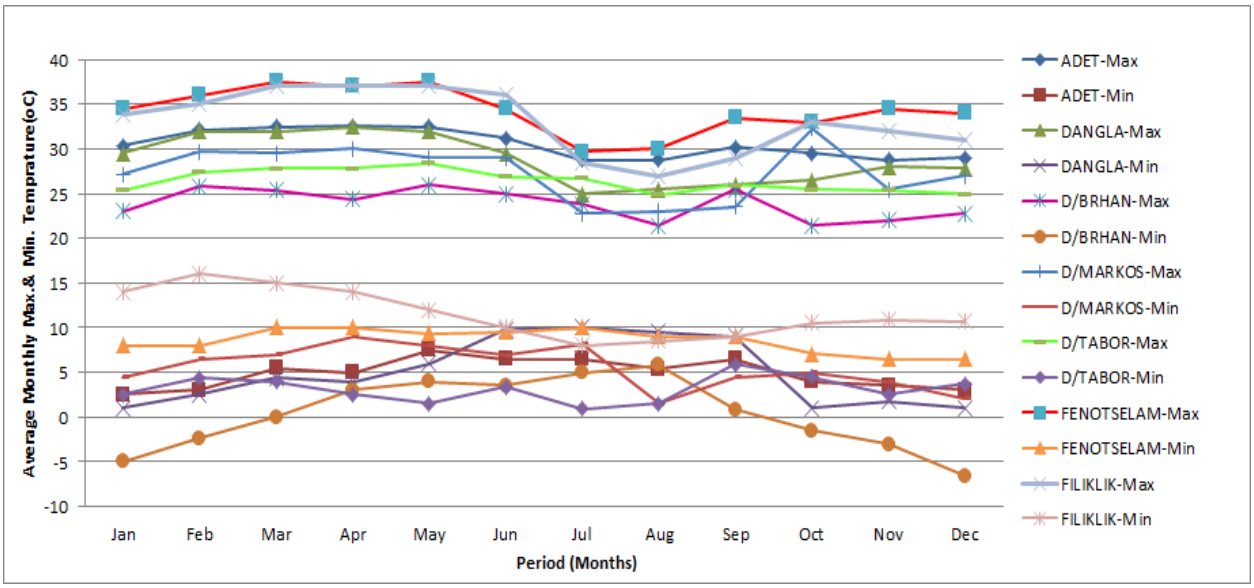

Figure 3.5a

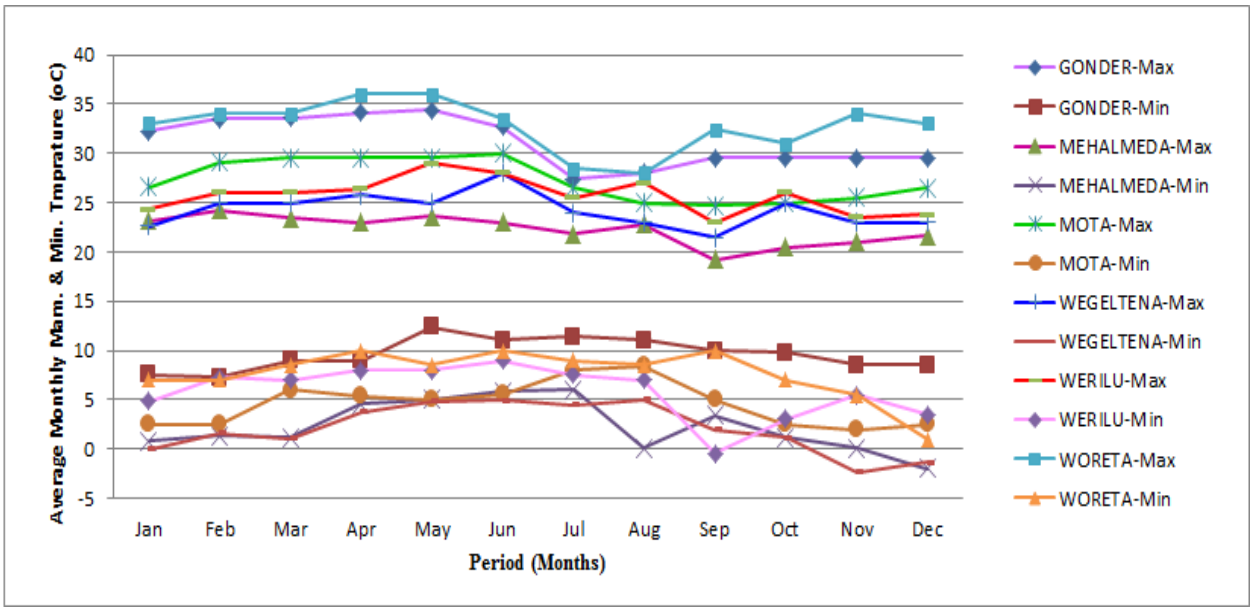

Figure 3.5b)

Figure 3-5: Mean Monthly Minimum and Maximum Temperature of Different Station used in the study Area for a period of 2001-2010

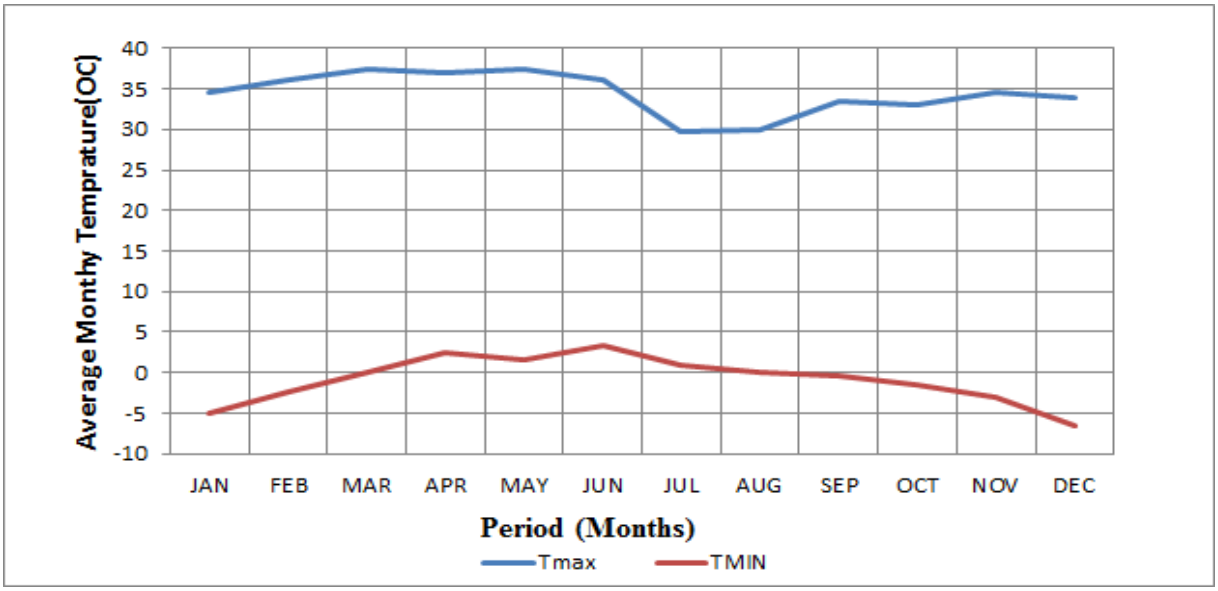

Figure 3-6**:** Mean Monthly Minimum and Maximum Temperature for the Study Area for a period of 2001-2010

3.1.5 Land Use

The land cover for Abay basin is mainly characterized by dominantly cultivated, in the eastern part, and grass land, wood lands, and forest to the western part according to the Ministry of Water ,Irrigation and Electricity land cover classification mentioned in Characterization and Atlas of the Blue Nile Basin and its Sub basins *(IWMI, 2009).*

Accordingly, the Land use characteristics of the study area was classified as about 37.55 % of the watershed area was covered by Agriculture, 47.7 % Agro-pastoral, 0.8 % Agro-slyvicultural, 0.03 % wetland , 8.2 % Pastoral, 0.2 % slyvicultural 0.6 % sylvo-pastora,0.1% Urban, 4.9 % by Lake Tana,

3.1.6 Soil

According to the Ministry of Water Irrigation and Electricity the major dominant soil types in the Abay basin are Alisols and Leptisols, followed by Nitosols, Vertisols, Cambrisols, Fluvisols and Luvisols Mentioned in Characterization and Atlas of the Blue Nile Basin and its Sub basins *(IWMI, 2009).*Based on the classification the following soil types are considered to be the major dominant soil in the study area. Lithic Leptosols covers about 41.84 %, Eutric Vertisols 18.11%, Chromic Luvisols 11.98%, Haplic Luvisols 6.11%, Eutric Cambisols 5%, Water bodies 4.89%, Rendezic leptosols 4.12% Vitric Cambisols 3.7%, Eutric leptosols 2.68%, Humic Nitisols 1.56%, Eutric fluvisols 0.02%

3.2 METHODOLOGY

3.2.1 Data Types And Sources

The data used for this research were varied in types and sources .Daily climate variables of (Rainfall, temperature, Relative humidity, Wind speed and Sunshine hour) were sourced from National Meteorological Service Agency of Ethiopia (NMSA) while Daily discharge of Abay River at KESE gauging Station were obtained from Ministry of Water, Irrigation and Electricity (MoWIE).Regional climate model data from Coordinated Regional Downscaling Experiment (CORDEX) were downloaded via the download node (https://esgf-data.dkrz.de/search/cordex-dkrz). The climate model data includes simulated historical and projected temperature and precipitation data for 1951-2005 and 2006-2100 respectively under RCP2.6, RCP4.5 and RCP8.5 scenarios. Spatial data that included DEM downloaded from the shutter Radar Topography Mission (SRTM) with 30m*30m resolution generated by the United States Geology Survey (USGS).

Table 3-1: Data Sources and Types used in the Study

I	**Meteorological Data**		
S.NO	**Data Type**	**Time Step**	**Data Sources**
1	Rainfall	2001-2010	NMSA
2	Temperature		
3	Wind Speed		
4	Sun Shine Hr.		
5	Relative Humidity		
II	**Hydrological Data**		
1	Stream flow Data	2001-2010	MoWIE
III	**Spatial Data**		
1	DEM		USGS
2	Soil		MoWIE
3	Land cover		MoWIE
IV	**Climate Scenarios Data**		
1	CORDEX- RCP Climate Data	2006-2100	https://esgf-data.dkrz.de/search/cordex-dkrz

3.2.1.1 Meteorology data

Even though Daily data for 25 stations was collected from National Meteorological Service Agency (NMSA), only 15 climate stations which have sufficient data were used for this research. The number of meteorological variables collected varies from station to station. Some stations contain all climate variables of: precipitation, maximum and minimum temperature, Humidity sunshine hours and wind Speed other station may only have climate variables of rain fall and Temperatures Data.

Table 3-2: Summary of selected Meteorological stations within the study area

S/NO	Stations	Latitude (degree)	Longitude (degree)	Altitude (m.a.s.l)	Time Step	% of Missed Data	Basin
1	ADET	11.299	37.499	2175	2001-2010	0.25	Abay Basin
2	DANGLA	11.399	36.799	2113		0.55	
3	DEBREMARKOS	10.299	37.699	2443		0.27	
4	TABOR	11.899	37.999	2606		0.41	
5	DEBRBRHAN	9.599	39.499	2746		0.88	
6	GONDER	12.499	37.399	1967		3.5	
7	MEHALMEDA	10.299	39.699	3078		2.79	
8	MOTA	11.099	37.899	2413		0.22	
9	WGLTENA	11.599	39.199	2945		8.35	
10	FLGBRHAN	10.700	38.100	2710		2.52	
11	FERSBET	10.800	37.600	3000		1.73	
12	FLIKLK	10.100	38.200	1853		8.41	
13	FENOTSLAM	10.700	37.100	1840		21.09	
14	WORETA	11.900	37.700	1819		1.75	
15	WORILU	10.599	39.399	2702		18.71	

3.2.1.2 Hydrological data

Daily flow data for Abay River for a period of 10 years from 2001-2010 recorded at KESE gauging station was collected from Ministry of Water Irrigation & Electricity (MoWIE). The missing discharge data was filled using linear regression.

Table 3-3: Summary of Hydrological Data for Kesse Gauging station

S.No	Stations Identification		River	Latitude (degree)	Longitude (degree)	Years of Data Used	% of Missed Data
	Name	Code					
1	KESSIE	112001	Abay	11.4	38.11	2001-2010	1.94

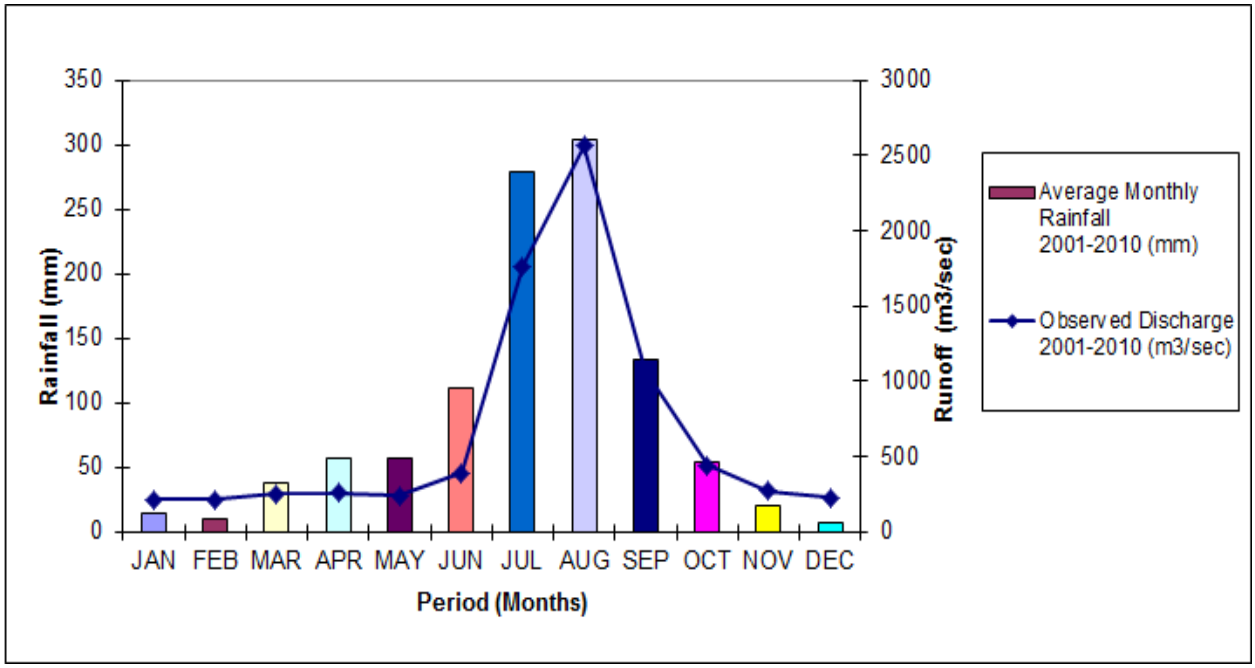

Figure 3-7: Mean Monthly observed Runoff and Rainfall of the study area for a period of (2001-2010)

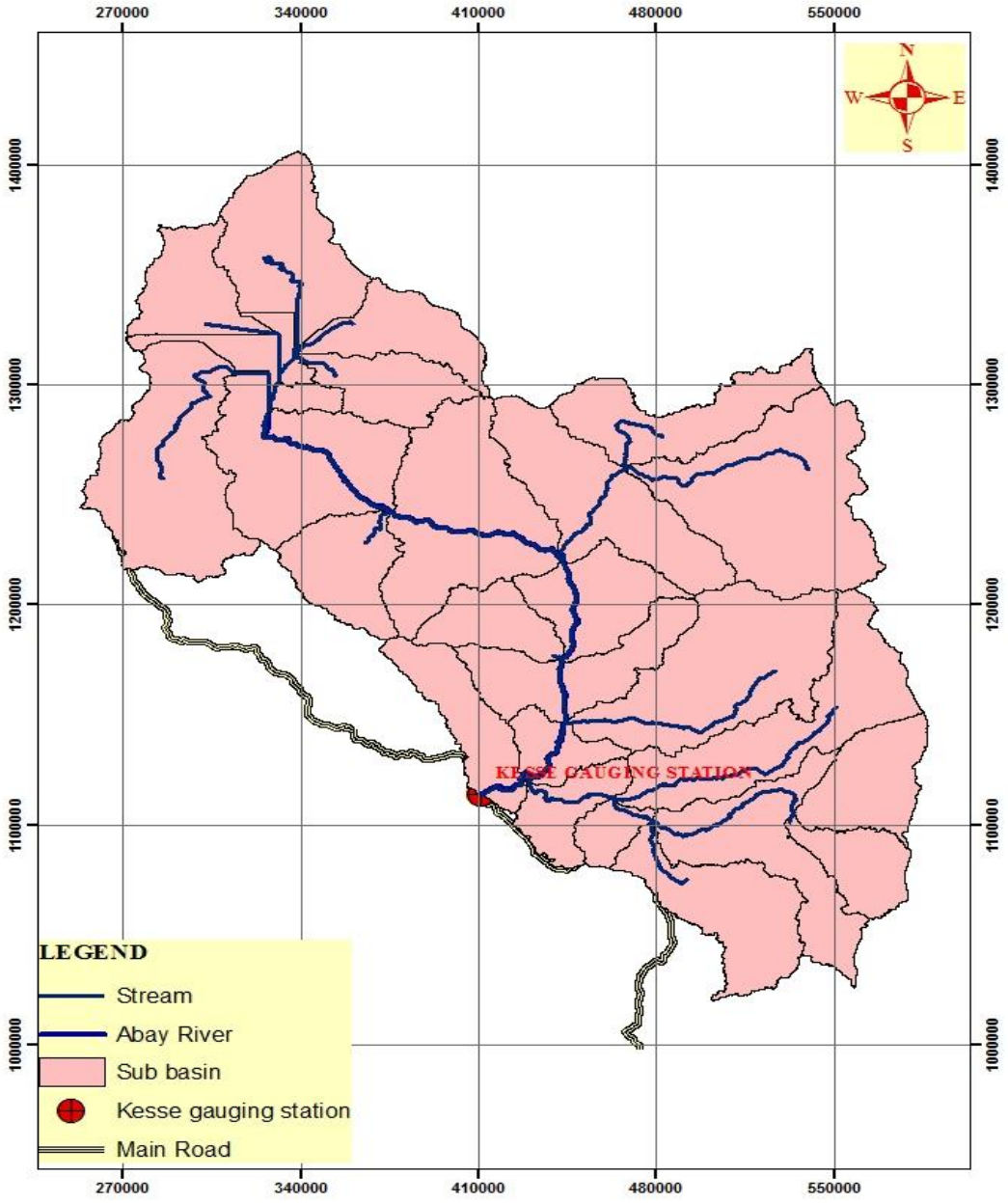

Figure 3-8: Location map of Metrological station Used in the Study Area

3.2.1.3 Filling missing rainfall data

Before the observation data for both climate and discharge were used for analysis, data quality control was carried out to get rid of errors in the result. This is because consistency of data is an indispensible perquisite in any analysis. Inadequate climate and discharge data results in unrealistic output. Incomplete records of hydro metrological data sometimes occurs possibly due to operator error or equipment malfunction further the personal to take readings are either too few or unreliable this the problem to many developing countries *(Opera,1991)*

Estimation of the missing records of climate and discharge data sets was essential since they are utilized to drive and adjust the SWAT model that requires consistent data records.

3.2.1.4 Checking the Consistency of Data

The most common method of checking for inconsistency of recorded data is Double Mass Curve analysis (DMC). The curve is a plot of cumulative rainfall collected at a particular gauge where measurement condition may have changed significantly against the average of the cumulative rainfall for the same period of record collected at several gauges in the same region. The data is arranged in the reverse order that is the latest record as the first entry and the oldest record as the last entry in the list. A change in the proportionality between the measurements at the suspect station and those in the region is reflected in a change in the slope of the trend of the plotted points. The data series, which is inconsistent, adjusted to consistent values by proportionality.

Double mass curve plot were made for all the stations used in the study area figure-3.9 shows DMC for Gonder and Dangle meteorological stations for the rest station it is available in Annex:4.From the double mass curve figure it can be seen that the stations are consistent each other.

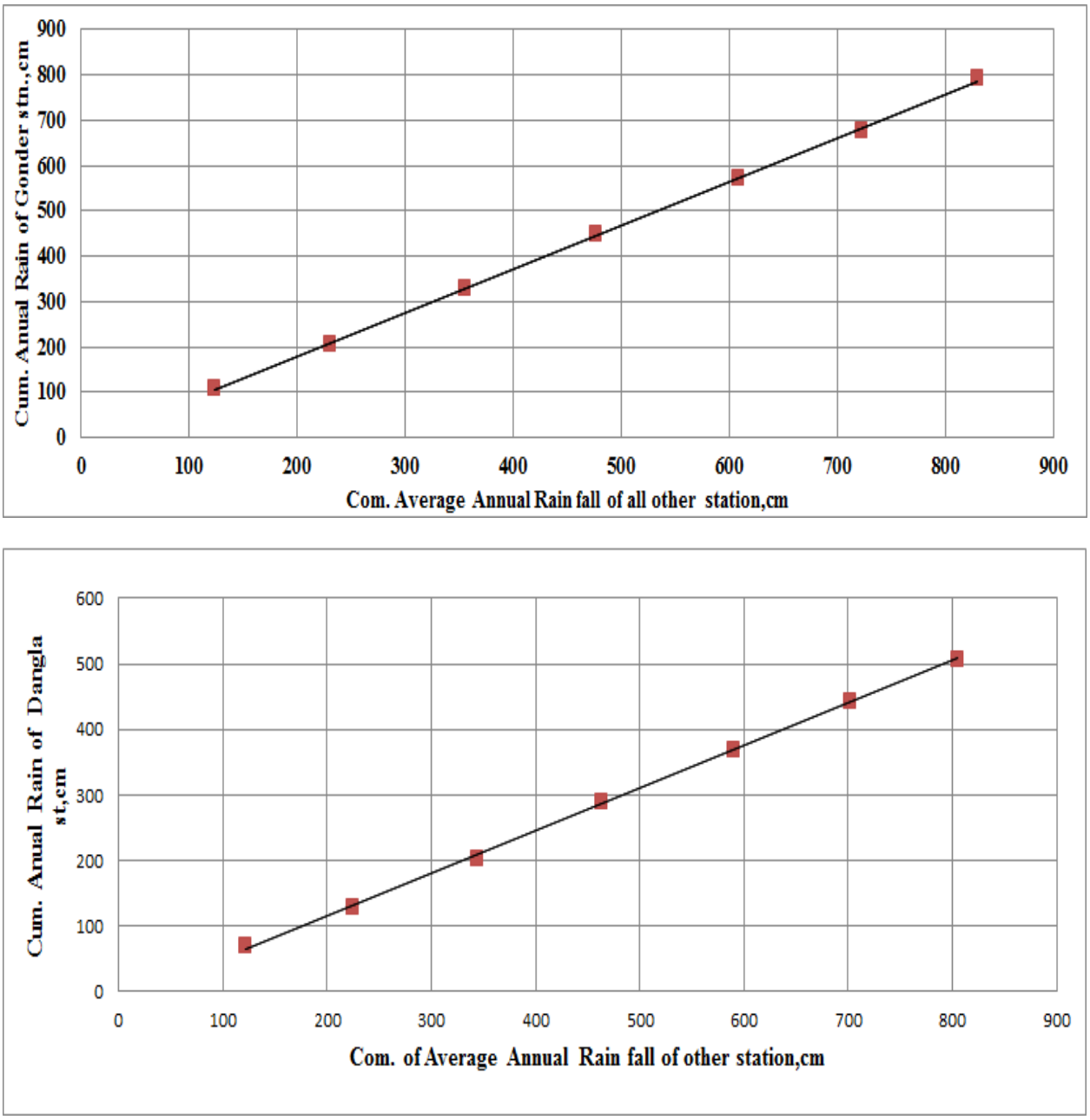

Figure 3-9: Double mass curve for Meteorological stations Gonder (Top) and Dangla (Bottom)

3.2.1.5 CORDEX-RCP climate data

In this study, results of CORDEX-Africa ensemble RCMs simulations for the historical (1951–2005) and future (2006–2100) climate projections downscaled from different GCMs under RCP2.6, RCP4.5 and RCP8.5 with spatial resolution of 50km is used .The climate data contains daily values of Precipitation, Maximum and Minimum Temperature but the other climate variables were assumed to be constant for the future time period.

I. Bias Correction for CORDEX Climate Data

For bias correction of the climate data, Linear scaling method (LS) aims to perfectly match the monthly average of corrected values with observed ones. The monthly corrected values are constructed upon the differences between observed and raw RCP data. The temperature is typically corrected with an additive and precipitation is typically corrected with a multiplier on monthly basis. First the correction for climate date was made for Historical period with that of the Observed data for the period of (2001-2010) than the correction factor is applied for future time under each climate scenarios.

Equations (3.1) and (3.2) are applied to correct future precipitation and temperature data obtained from CORDEX-RCP.

$$T_{(RCP\ future\ corr.,daily)} = T_{(RCP\ future\ raw.,daily)} + \left(T_{(obs\ mean.,daily)} - T_{(mean\ RCP\ raw.,daily)}\right)$$ ----------Eq3.1

$$P_{(RCP\ future\ corr.,daily)} = P_{(RCP\ future\ corr.,daily)} + \left(\frac{P_{(mean\ observed.,daily}}{P_{(mean\ RCP\ raw,daily}}\right)$$ ---------- Eq3.2

Due the limitation of long years of recorded data a base period of 10 years form (2001-2010) was selected to be historical period from which comparison of future impacted flow is made.

For simulation of future impacted flow in SWAT model, the future climate data was divided in to 10 years of:

I. 2031 -2040 (Recent)
II. 2051-2060(Middle)
III. 2091-2100 (Last)

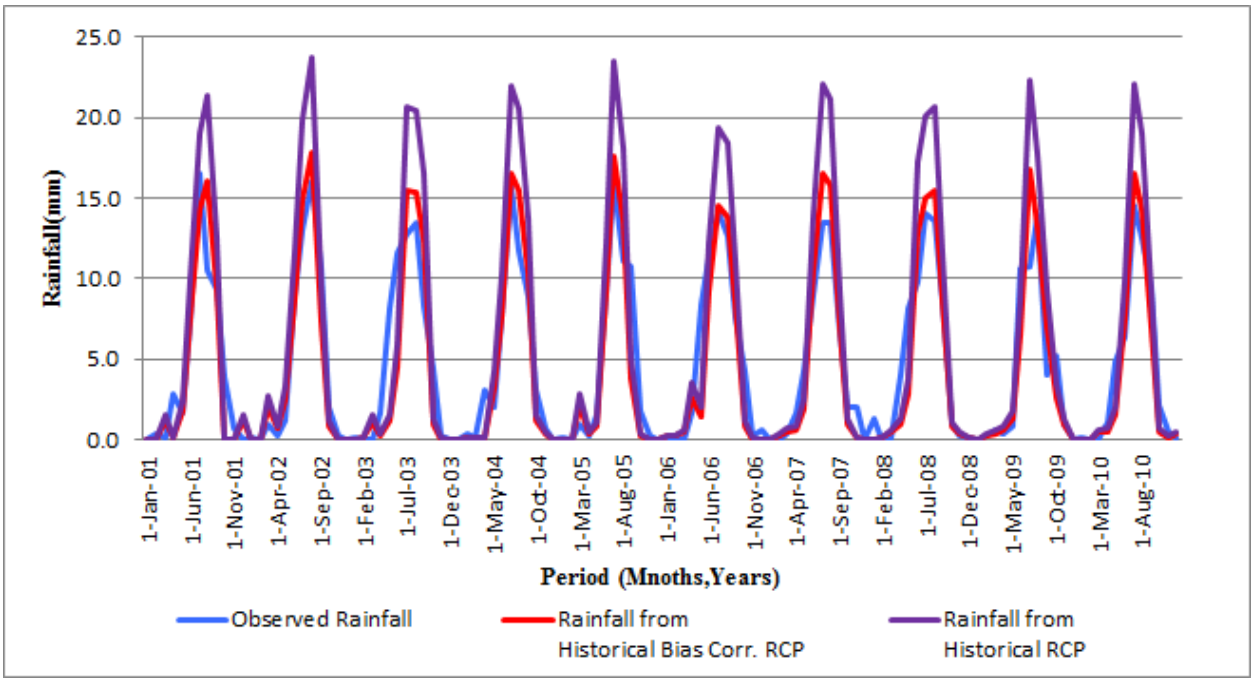

Figure 3-10 : Base Period Comparison of Monthly Average Rainfall for bias correction at D/tabor Station

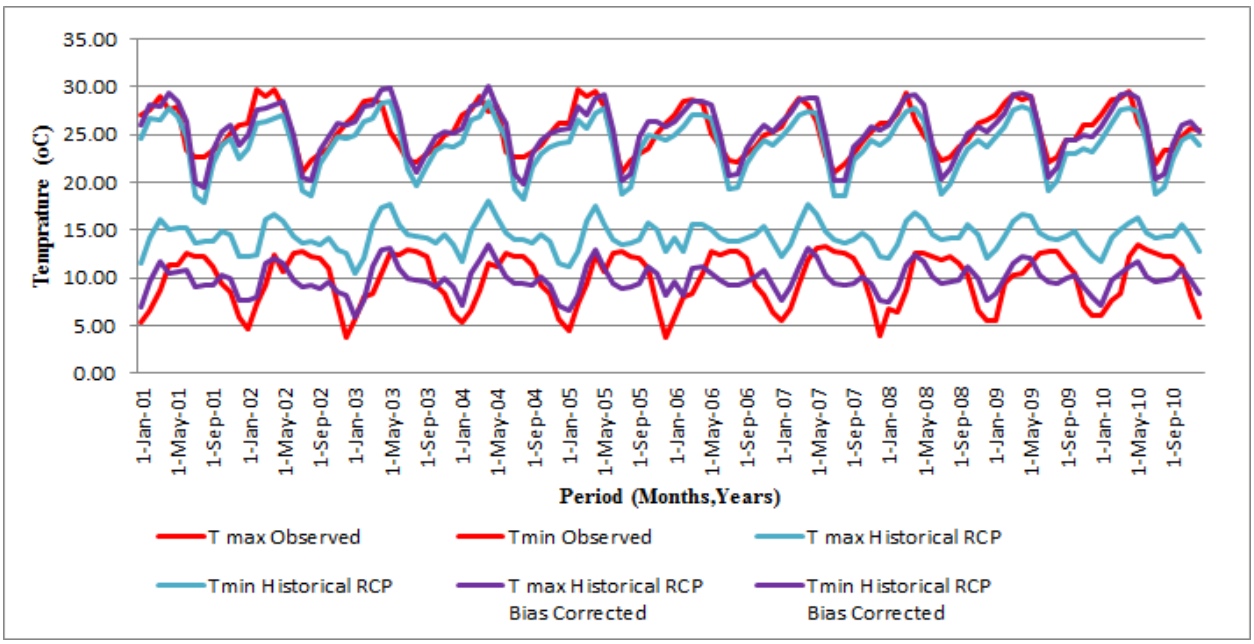

Figure 3-11Base Period Comparison of Daily Average Max. and Min. temperature in month for bias correction at D/tabor Station.

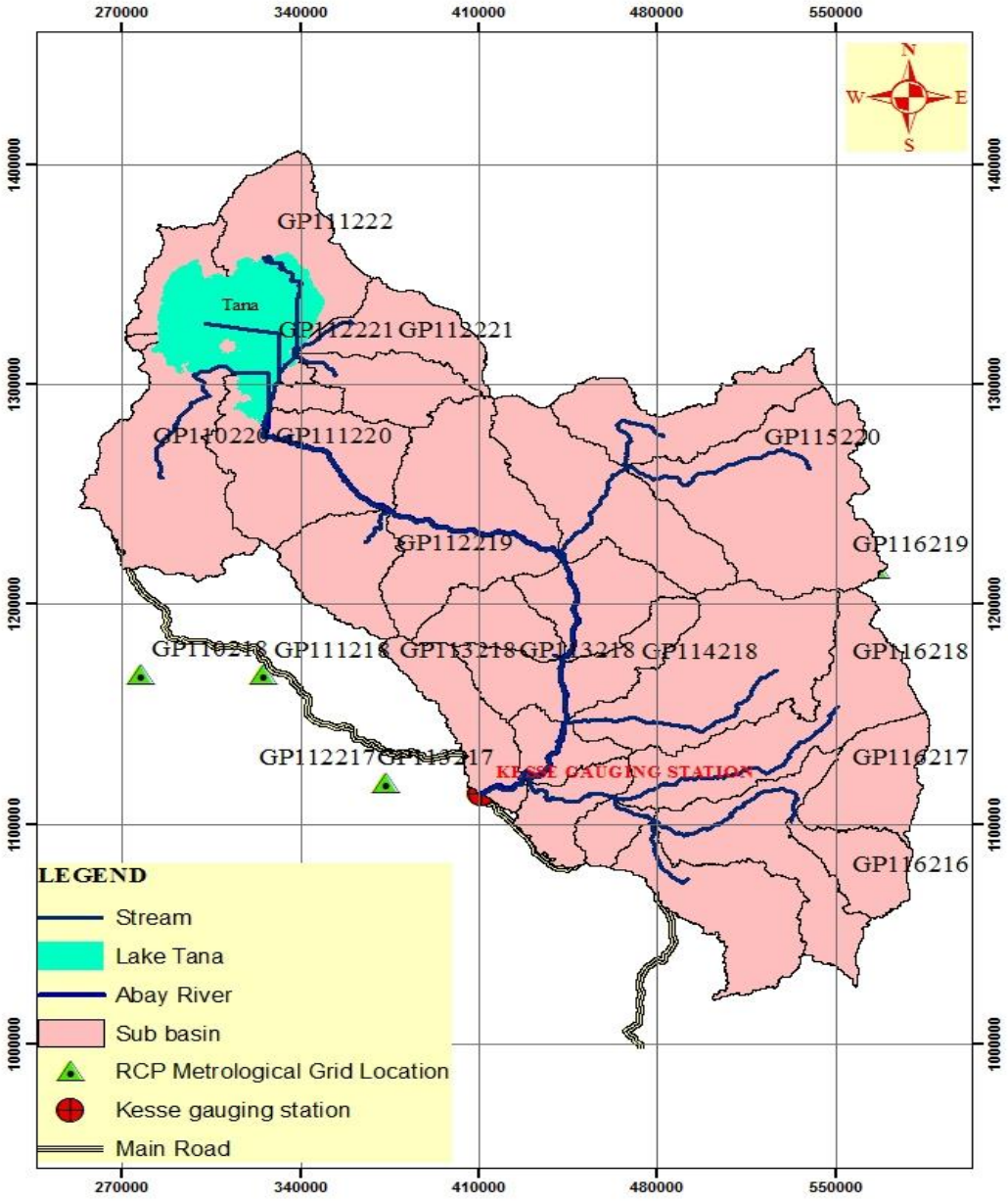

Figure 3-12: RCP grid data stations in the Research area

3.2.1.6 Spatial data

I. Digital Elevation Model (DEM)

Topography is defined by a Digital Elevation Model (DEM), which describes the elevation of any point in a given area at a specific spatial resolution as a digital file. Digital elevation model is one of the essential inputs required by SWAT to delineate the watershed in to a number of sub watershed or sub basins.

DEM is used to analyze the physical characteristics of the area such as drainage pattern of the watershed, slope, stream length, width of channel within the watershed. The raw DEM was processed & projected using Glogbal mapper16 and ARCGIS10

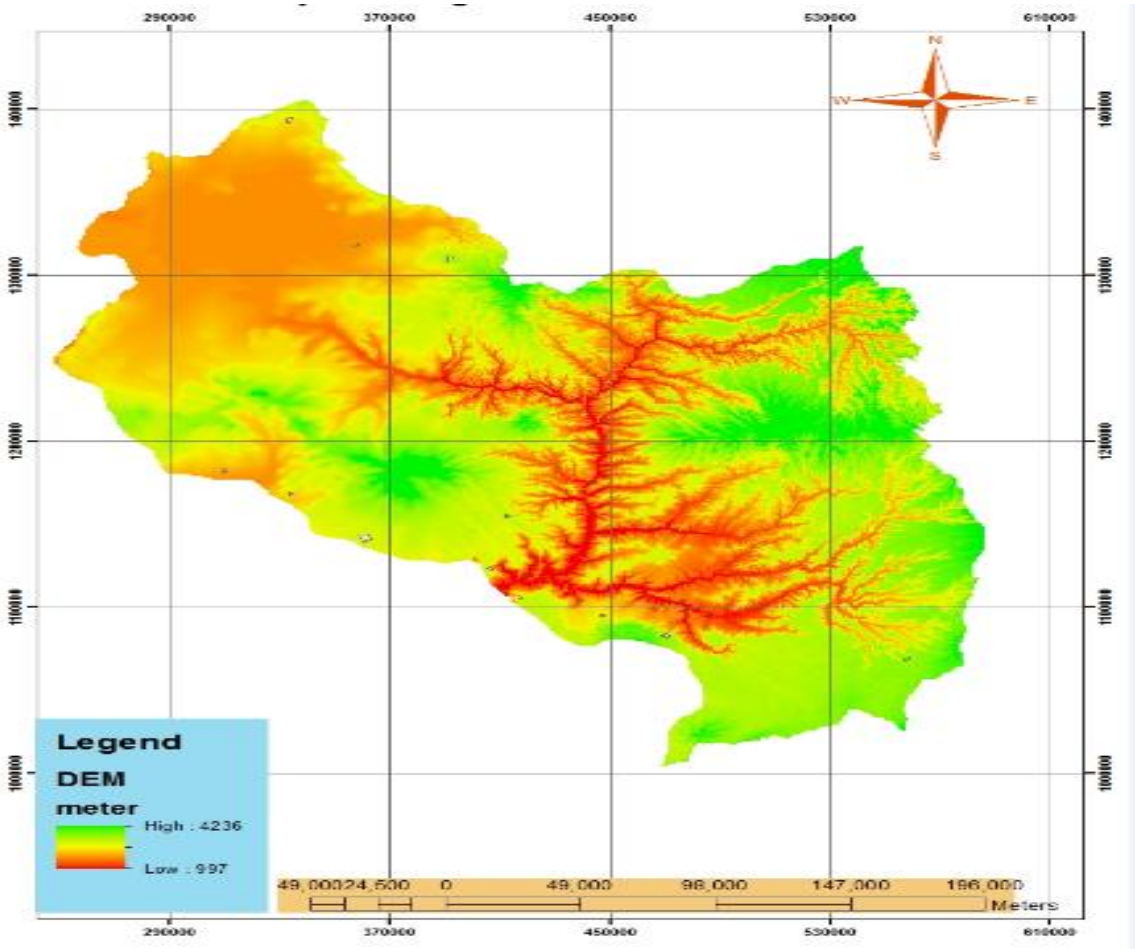

Figure 3-13: Digital Elevation Model (Meter, +MSL) for the study Area

II Land Use / Land cover Data

Land use / Land cover are the second spatial input data required by SWAT model. The land use map was obtained from the MoWIE and Blue Nile Atlas (2009). Since SWAT has predefined four letter codes for each land cover classification in such a way that the land use/Land cover classification used in the study area were assigned in SWAT database than a look up table that identifies the 4-letter SWAT code for the different categories of land use/land cover were prepared so as to relate the grid values to SWAT land cover/land use classes.

Table 3-4: Land Use classification of the study Area based on /MoWIE/and the corresponding SWAT Code

S. No.	Land use as per MoWIE	Land use as per SWAT	SWAT Code	AREA(Ha)	% of Watershed Area(100)
1	Agriculture	Agriculture Generic	AGRL	2,337,973.11	37.55
2	Agro-pastoral	Agriculture Close Grown	AGRC	2,967,670.81	47.66
3	Agro-sylvicultural	Forest Deciduous	FRSD	47,713.33	0.77
4	Marsh	Wetland	WETL	1,990.13	0.03
5	Pastoral	Pasture	PAST	510,551.84	8.2
6	Sylvicultural	Forest Evergreen	FRSE	9,464.41	0.15
7	Sylvo-pastoral	Range Brush	RNGB	40,430.55	0.65
8	Urban	Urban	URLD	4,347.68	0.07
9	Water	Water	WATR	306,228.10	4.92
Total				**6,226,369.97**	**100**

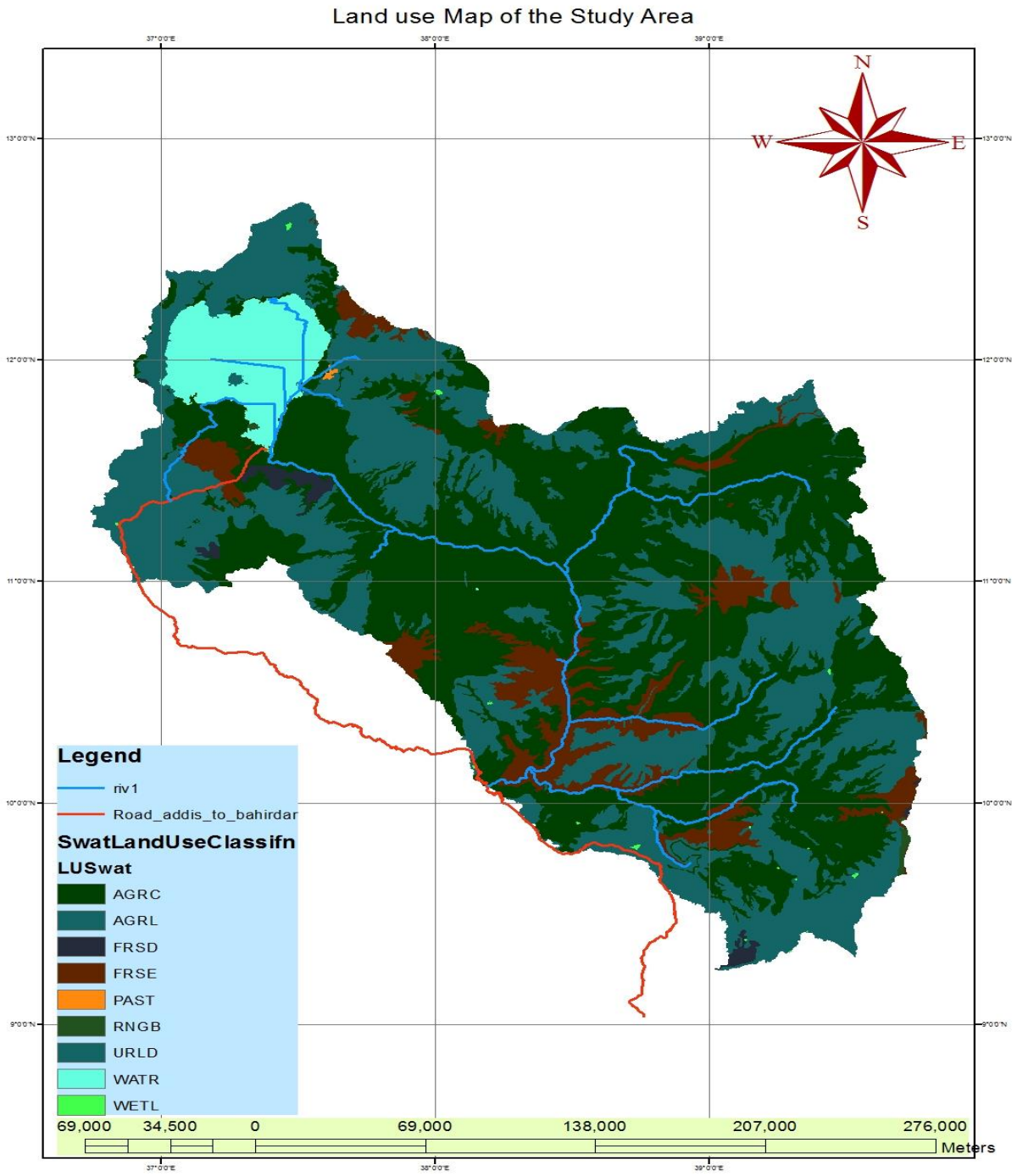

Figure 3-14 : Land use map of the Study area as per MoWIE

III Soil Data

To have the SWAT model inputs concerning catchment's soil physical and chemical properties, first the shape file format of soil type distribution through the catchment was collected from Ethiopian MoWIE GIS department. Using this shape file , soil texture, available water content, hydraulic conductivity, bulk density and organic carbon content for different layers were extracted for each Major Soils types from world Digital soil map database prepared by FAO. This world soil map was prepared by FAO and UNESCO at 1: 5 000 000 scale *(http: //www. fao.org/soils-portal/soil-survey/soil-maps-and-databases/faounesco-soil-map-of-the-world/en/).* The information provided by this map was used in combination with the Harmonized World Soil Database v1.2, a database that combines existing regional and national soil information *(http://www.fao.org/soils-portal/soil-survey/soil-maps-and-databases/harmonized-world-soil-database-v12/en/).*Finally a look up table is prepared so as to relate the grid values to SWAT soil class.

Table 3-5: Major soil type of the Research area Based on (FAO and MoWIE)

S. No.	Soil as per MowIE & FAO	Symbol	SAWT Code	AREA(Ha)	% of Watershed Area
1	Lithic Leptosols	LTLEPTOSOLS	LPq	745651.86	11.98
2	Vitric Cambisols	VTCAMBISOLS	CHz	311311.65	5.00
3	Chromic Luvisols	CHLUVISOLS	LVx	1536.35	0.02
4	Eutric Vertisols	EUVERTISOLS	VRe	166737.16	2.68
5	Humic Nitisols	HUNITISOLS	NTu	1127875.15	18.11
6	Haplic Luvisols	HPLUVISOLS	LVh	380265.70	6.11
7	Water bodies	WATER	WR	96852.26	1.56
8	Eutric leptosols	EULEPTOSOLS	LPe	2604848.46	41.84
9	Eutric Cambisols	EUCAMBISOLS	CMe	256417.20	4.12
10	Rendezic leptosols	RNLEPTOSOLS	LPr	230349.34	3.70
11	Eutric fluvisols	EUFLUVISOLS	FLe	304524.82	4.89
Total				**6,226,369.97**	**100.00**

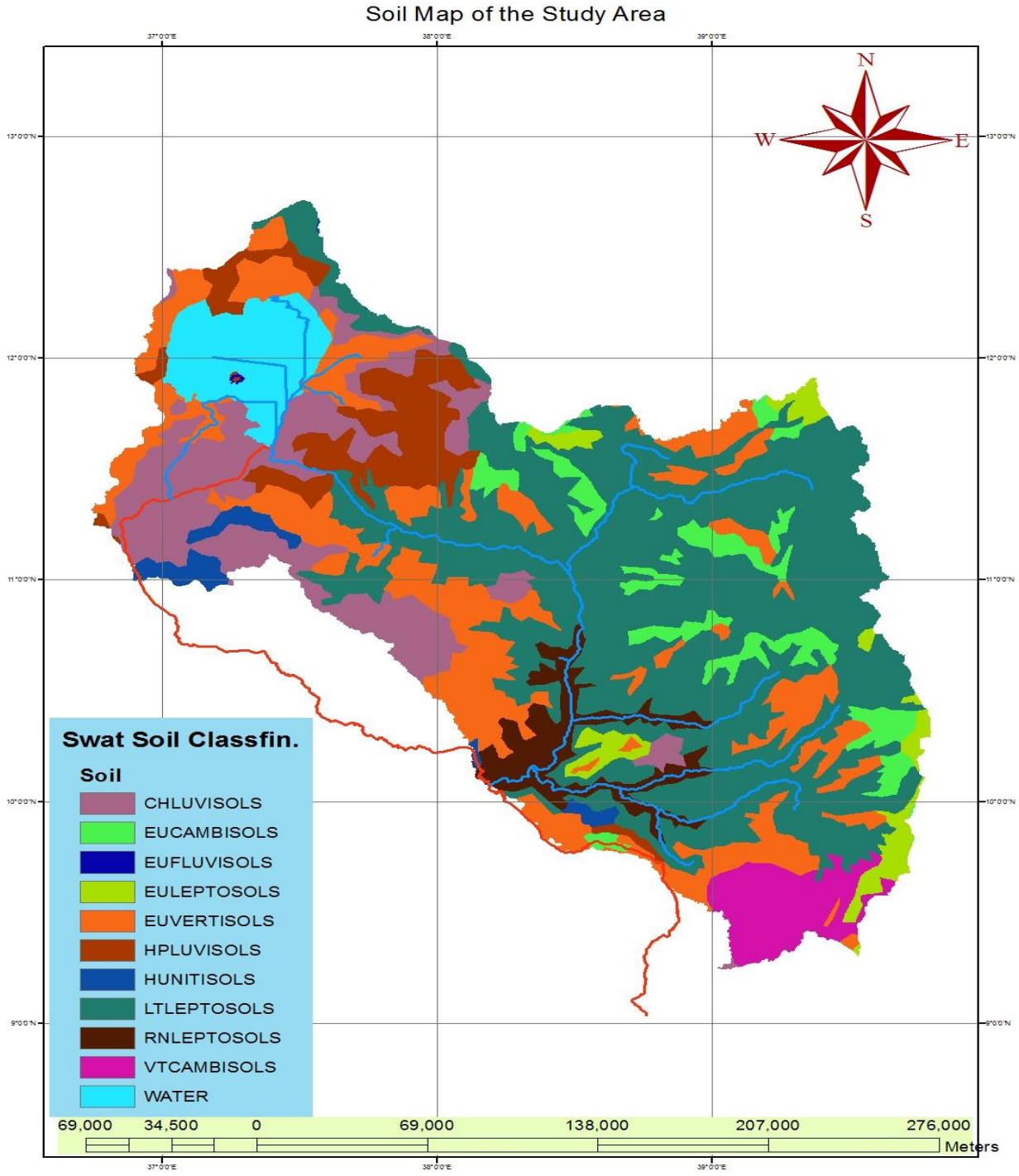

Figure 3-15: Soil Map of the Study Area as per FAO and MoWIE

3.2.2 SWAT Model Setup For The Study Area

The SWAT model was set up using the data prepared described in above section and the (ARCSWAT, 2012) interface. The interface helped to create the stream network, delineate the catchment boundary from the DEM and further subdivide the catchment into sub-basins. The land cover and soil layers were used to generate HRUs. The climatic data was also integrated spatially to assign these data as the main drivers of the model.

The general step followed to set up the model is described below:-

- ✓ The first step was to load the Digital Elevation Model in the ARCSWAT version-2012 interface.
- ✓ The stream network was generated by use of a threshold area that defines the origin of a stream. The smaller the number, the more detailed the stream network generated by the interface.
- ✓ The locations of the river gauging location for watershed delineation were added manually as sub-basin outlets (Kesse Gauging Station) this was to ensure that the model calibration was done at the exact location. Once the entire watershed outlet is selected, the sub-basins are delineated and their parameters are calculated. The delineated sub-basins are shown in Figure 4.1.
- ✓ Next, the landuse and soil maps are loaded. The lookup table for each map is also loaded in order for the interface to know which codes or names to assign to the different categories. Than slope classification is done by assigning a multiple slope option. Once the land use, soil map and slope have been loaded and reclassified, an overlay is done, resulting in landuse, soil and slope distribution within the sub-basins.
- ✓ The HRUs were then created by applying Dominant landuse, soil and slope. The number of HRUs in the sub basin is given in Table 4.1.
- ✓ Then, the climate data defined in the user weather generator for metrological stations is loaded.
- ✓ At the final step, the SWAT input files are built and the model is set to run.

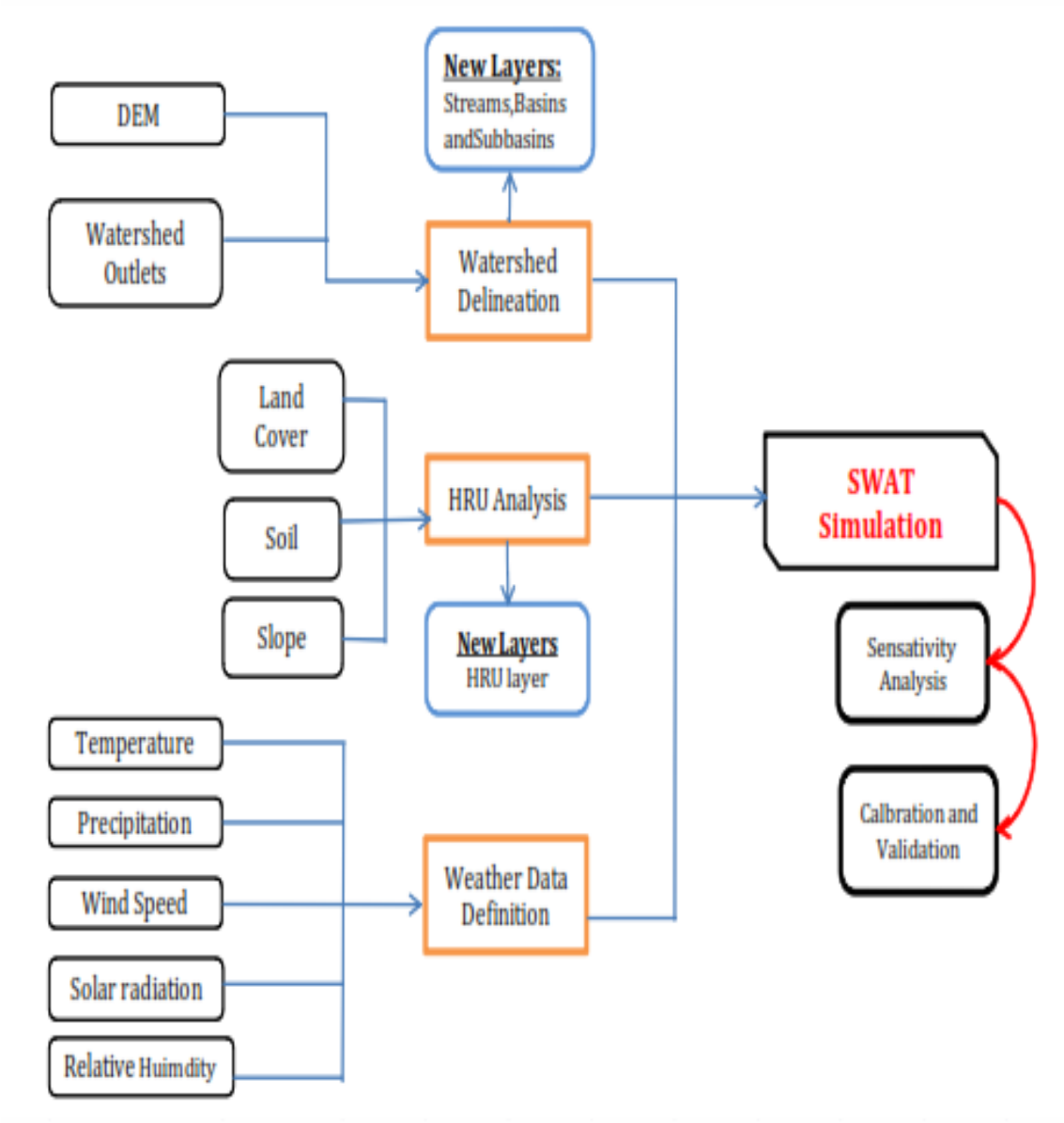

Figure 3-16: SWAT Simulation process Steps followed in this study

3.2.3 Model Calibration and Validation

3.2.3.1 Sensitivity analysis

Sensitivity analysis is a simple technique for assessing the effect of uncertainty on the system performance *(Mengistu, D.T. and Sorteberg, A, 2012)* .It is also a measure of the effect of change of one parameter on another. Sensitivity analysis was undertaken by using a built-in tool in SWAT-CUP. It uses t-test to rank the most sensitive parameter that corresponds to greater change in output response. A t-stat result provides a table of output having columns of t-stat and P-value. A t-test provides a measure of sensitivity (larger in absolute values are more sensitive) and p-values determined the significance of the sensitivity, a value close to zero has more significance. *(SWATCUP user manua*l). To improve simulation result and understand the behavior of hydrological system in the catchment, sensitivity analyses were conducted for 13 selected parameters.

3.2.3.2 Calibration

Calibration is tuning of model parameters based on checking results against observations to ensure the same response over time. This involves comparing the model results generated with the use of historic meteorological data, to recorded stream flows. In this process, model parameters varied until recorded flow patterns are accurately simulated *(SWAT user Manual)*

The ArcSWAT for ArcGIS 10 interface for SWAT 2012 is used in this study to set up the model to simulate the discharge at the outlet of the Kesse Gauging station. Calibration is achieved by SWAT calibration and uncertainty programs SWAT-CUP using Sequential Uncertainty Fitting version-2 (SUFI-2) algorithm with 1000 iterations and manual calibration.

In SUFI-2, parameter uncertainty accounts for all sources of uncertainties such as uncertainty in driving variables (e.g., rainfall), conceptual model, parameters, and measured data. The degree to which all uncertainties are accounted for is quantified by a measure referred to as the P-factor, which is the percentage of measured data bracketed by the 95% prediction uncertainty (95PPU) Another measure quantifying the strength of a calibration/uncertainty analysis is the R- factor, which is the average thickness of the 95PPU band divided by the standard deviation of the measured data .Theoretically, the value for P factor ranges between 0 and 100%, while that of R-factor ranges between 0 to infinity a P-factor-1 and R-factor 0 is a simulation that exactly correspond to the measured data

The SUFI-2 was selected due to its capability in analyzing many parameters in the model runs in iteration, the SUFI-2 measures the goodness of fit and the 95% prediction uncertainty (95PPU) between simulated and observed stream flow (*Abbaspour et al., 2015).* In addition new parameters ranges were produced which can be used in the next iteration, to re-calibrate the model until the best parameters ranges were obtained *(Abbaspour KC, 2012).*

Measured discharge data of the Abay River are collected from 2001 to 2010. Data from 2001 to 2006 is used for calibration and data from 2007 to 2010 is used for validation including three years as a warm up period (1998–2000) in order to minimize the influence of initial conditions such as soil water content.

3.2.3.3 Validation

In order to utilize the calibrated model for estimating the effectiveness of future potential management practices, the model should be tested against an independent set of measured data without further adjustments this testing of a model with an independent set of data set is commonly referred to as model validation.*(Santhi et al., 2001).*

After finding the best parameter during calibration period these best parameters ranges were then applied to validate the stream flow from 2007 to 2010. The statistical criteria (R2 and E_{NS}) used during the calibration procedure were also checked here to make sure that the simulated volume is still within the accuracy limits.

3.2.3.4 Model performance evaluation

The Performance evaluation parameters used to check the performance of SWAT model are: the coefficient of determination (R^2), Nash-Sutcliffe efficiency (E_{NS}) and Percent Bias (PBIAS), the P-factor and R-factor .R^2 describes the degree of co-linearity between simulated and measured data, i.e. the proportion of the variance. R^2 ranges from 0 to 1, with higher values indicating less error variance and typically values greater than 0.6 are considered acceptable.

Nash-Sutcliffe efficiency (E_{NS}) simulation efficiency measure how well trends in the measured data are reproduced by the simulated results over a specified time period and for a specified time step *(Santhi et al. 2001).*

E_{NS} displays how fine the observed plot fits the simulated plot. E_{NS} ranges from $-\infty$ to 1with higher values indicating a less error and typically, values greater than 0.5 are considered acceptable *(Santhi et al., 2001).*

It is calculated as follows:

$$E_{NS} = \frac{\left[\sum_{i=1}^{n} (q_{oi} - q_{si})\right]^2}{\sum_{i=0}^{n} (q_{si} - q_{s,mean})^2 \sum_{i=0}^{n} (q_{oi} - q_{o,mean})^2} \text{----------Eq3.3}$$

$$R^2 = \frac{\left[\sum_{i=1}^{n} (q_{si} - q_{s,mean})((q_{oi} - q_{o,mean})\right]^2}{\sum_{i=0}^{n} (q_{si} - q_{s,mean})^2 \sum_{i=0}^{n} (q_{oi} - q_{o,mean})^2} \text{----------Eq3.4}$$

Where:

q_{si} is the simulated stream flow

q_{oi} is the measured stream flow

$q_{s,mean}$ is the average simulated stream flow

$q_{o,mean}$ is the average measured stream flow

Percent Bias (PBIAS) measures the average tendency of the simulated data to be larger or smaller than their observed counterparts, In other words, it characterizes the percent mean deviation between observed and simulated flows. PBIAS can be positive or negative, positive means underestimation and negative means overestimation, typically, values of -25 < PBIAS < +25% are considered acceptable.(Santhi et al. ,2001).

$$PBIASE = 100 * \frac{\left[\sum_{i=1}^{n} q_{Si} - \sum_{i=1}^{n} q_{Oi}\right]}{\sum_{i=1}^{n} q_{Oi}} \text{----------3.5}$$

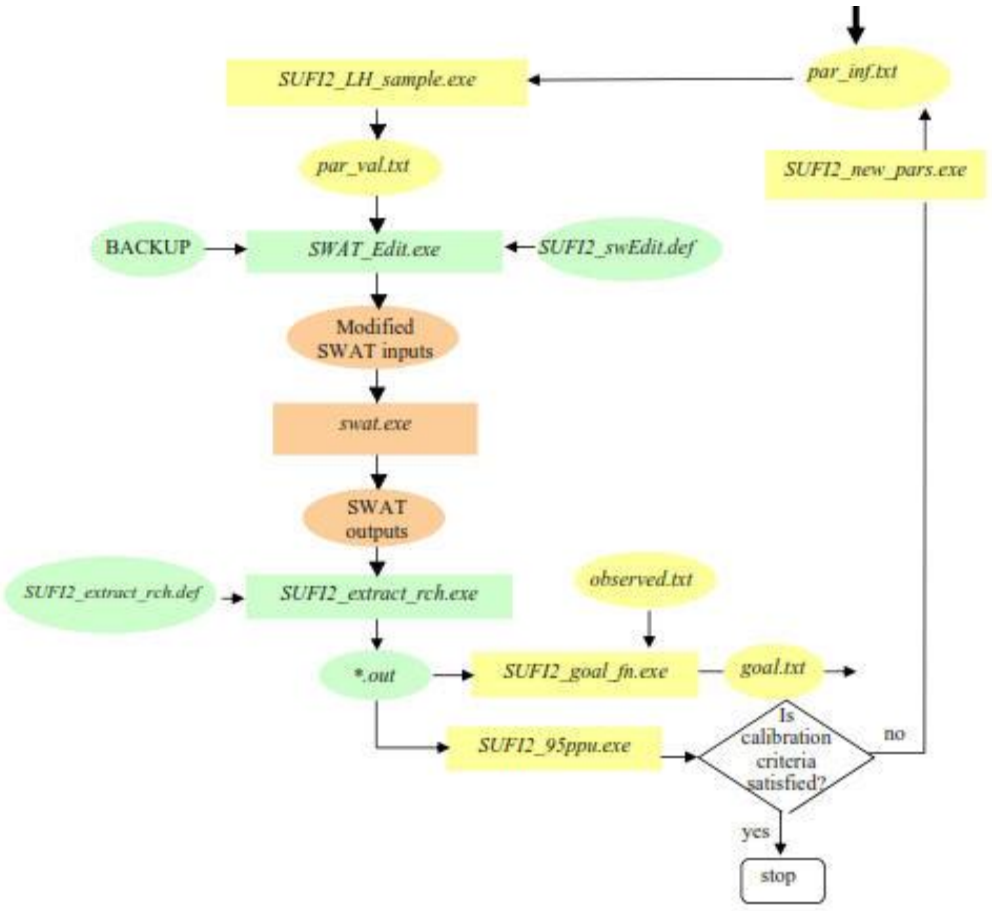

Figure 3-17: SWATCUP-SUFI2 process for calibration and validation (SWAT-CUP user manual)

3.2.4 Impact Of Climate Change On Stream flow

After finalizing the calibration and validation process for the observed climate data the model was run for the historical period (2001-2010) and resulted a good performance measure for the data derived from an ensemble of downscaled climate data based on the Coordinated Regional climate Downscaling Experiment over African domain (CORDEX-Africa) with Coupled Model Intercomparison Project Phase 5 (CMIP5) simulations under Representative Concentration Pathways viz. RCP2.6, RCP4.5 and RCP8.5 climate scenarios. The input climate data (daily rainfall, minimum and maximum temperature) under each RCP scenarios were used for future simulation. The impact of climate change was analyzed taking the historical simulated flow from (2001-2010) as the baseline against which the future flow is compared for three future periods of 10 years: early 21st (2031-2040), mid-21st (2051-2060) and late 21st 2091-2100.

In simulating the future flow other climate variables such as wind speed, solar radiation, and relative humidity were assumed to be constant throughout the future simulation periods. Even though it is definite that in the future land use changes will also take place, this was also assumed to be constant as the objective of this study is only to get indicative results with respect to the change in the climate variables (Rainfall and Temperature) keeping all other factors constant. Finally the impact of climate change on the average flows of monthly, seasonal and annual stream flow and Maximum and minimum annual daily Flow was analyzed relative to base period flows.

.

CHAPTER FOUR

4. RESULT AND DISCUSSION

4.1 SWAT HYDROLOGICAL MODEL RESULTS

4.1.1 Watershed Delineation

Using Arc-SWAT, Upper Abay basin was delineated using Digital Elevation Model (DEM) data. From the topographic report a total area of 62,253sq km with 27 sub basins were generated by taking an outlet at 'KESE' Gauging station located in Abay River.

4.1.2 Determination Of Hydrologic Response Units

The catchment delineation was followed by the determination of HRUs; From the 27 sub basins 129 hydrological response units were further generated depending on distinct soil, land and slope types regardless of their spatial positioning. The figure 4-1 and 4-2 below show the delineated catchment and HRU delineated and Table 4.1 shows the topographic report of the catchment. From the topographic report, also found out that the elevation of the catchment, ranges between 997m-4236m and the mean elevation was found to be 2255m

Table 4-1: Delineated catchments with their HRU's and area coverage

S.NO	Name	Elevation Ranges			Delineated area , number of Sub-basin and HRU's		
		Max	Min	Mean	Area,Km^2	Number of Sub-basin	Number of HRU's
1	Abay basin upstream of KESE Station	4236	997	2255	62,263.70	27	129

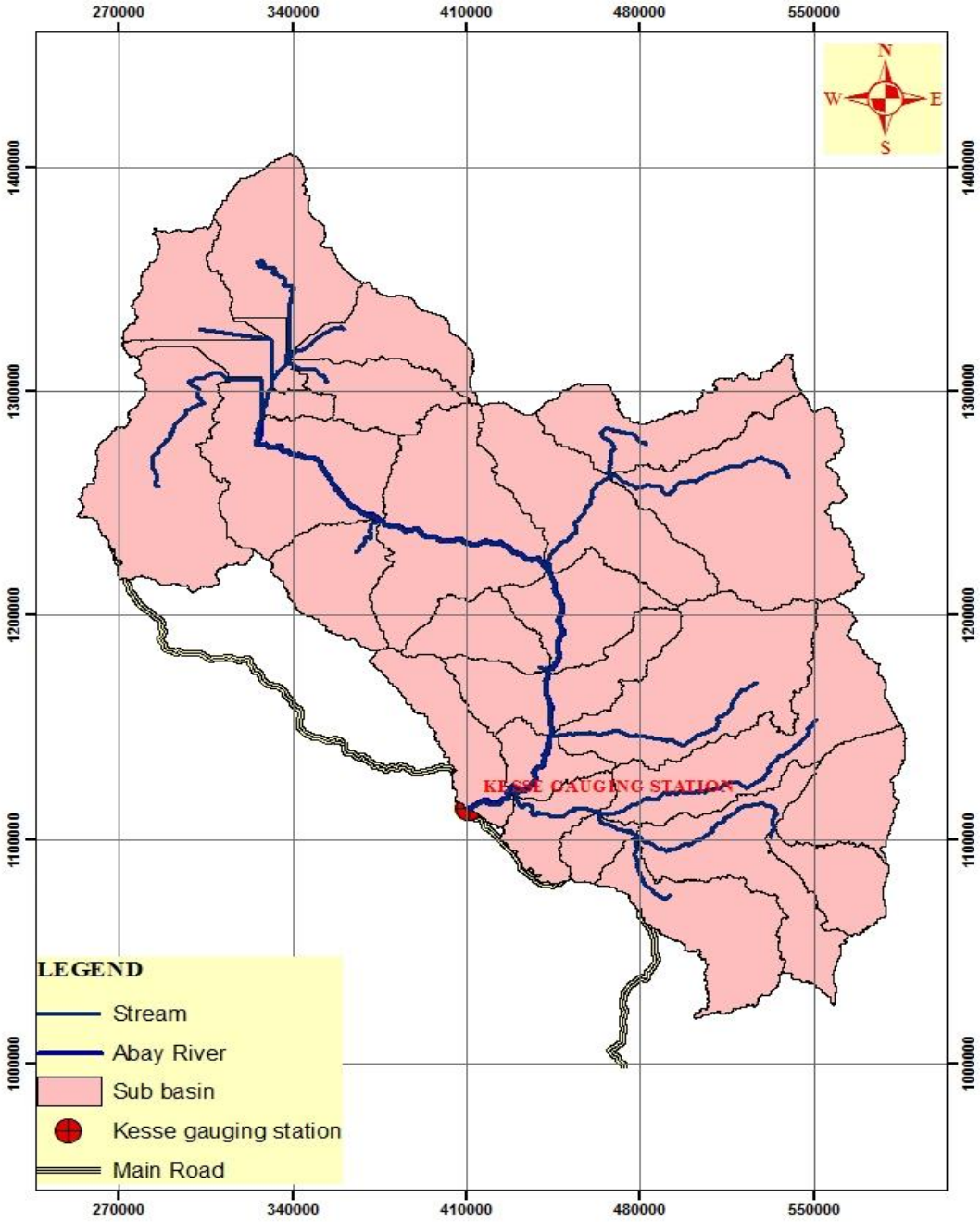

Figure 4-1: Sub-basin Delineated for the study Area by SWAT model

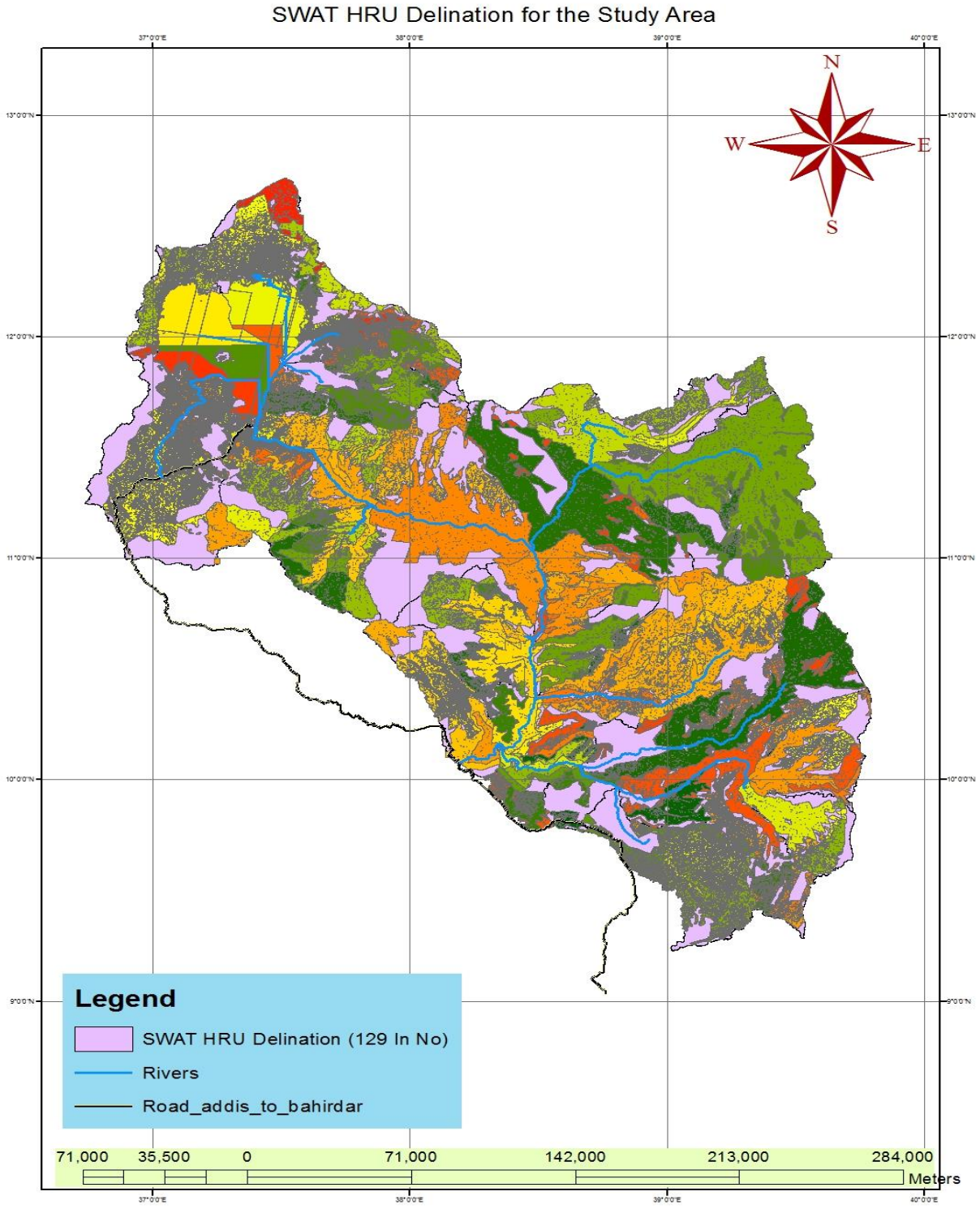

Figure 4-2: HRU Delineated for the study Area by SWAT model

4.1.3 Performance Evaluation Of SWAT Hydrologic Model

4.1.3.1 Sensitivity analysis

For sensitivity analysis, 27 parameters were considered out of which 13 were found to be relatively more sensitive. The t-stat offers a measure of sensitivity, the largest absolute value represents higher sensitivity and p-value determined the significance of sensitivity a value close to zero has more significance. Sensitivity rank is shown is shown in Table 4.2. REVAPMN is the least important parameter because of the very high p-value and very low t-value. CN2 is the most important influencing parameter on stream flow with very low p-value and very high t-value.

Table 4-2: Sensitivity analysis for selected parameter

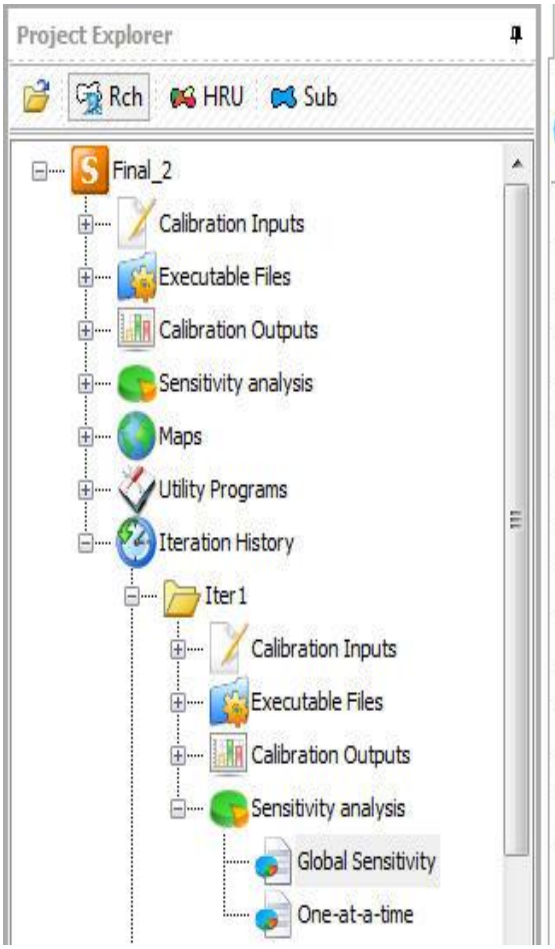

Iter1 - Global Sensitivity | Iter1 - Par_inf.txt | Iter2 - 9

Iter1 - Global Sensitivity

Global sensitivity analysis can be performed after an iteration.

Parameter Name	t-Stat	P-Value
9:R__SOL_AWC(..).sol	-0.059728388	0.952396514
12:R__SLSUBBSN.hru	-1.223824651	0.221611362
3:V__GW_DELAY.gw	-1.762825420	0.078558393
13:V__REVAPMN.gw	-1.771007375	0.077186179
7:V__CH_N2.rte	-2.094057808	0.036772269
10:R__SOL_K(..).sol	-2.310264325	0.021291501
8:V__CH_K2.rte	-2.368224724	0.018264028
11:A__HRU_SLP.hru	2.605553429	0.009453901
6:V__ESCO.hru	3.026852026	0.002602313
5:A__GW_REVAP.gw	-6.264649398	0.000000001
2:V__ALPHA_BF.gw	19.696410888	0.000000000
4:V__GWQMN.gw	-25.804364104	0.000000000
1:R__CN2.mgt	74.221456818	0.000000000

4.1.3.2 Flow Calibration and Validation

After the completion of sensitivity analysis flow calibration was performed using observed flow gauged at the outlet of the watershed (Kesse station) for a period of six years from January 1 st, 2001 to December 31st, 2006 and a warm up period of three years January 1st, 1998 to December 31 1st, 2000 and validated from January 1st, 2007 to December 31st, 2010.

Table 4-3: Initial and final adjusted parameter values

RANK	Parameter Name	Unit	Fitted Value (Factor)	Initial Values	Final Adjusted Values	Method of Parameter Adjustment
1	R_CN2		0.02	68.1	74.2	R: Multiply Initial Value by (1+Factor)
2	V__ALPHA_BF	Days	0.24	0.0	0.2	V: Replace Parameter by Values
3	V__GW_DELAY	Days	252.33	31.0	252.3	A: add Values to Initial Parameter
4	V__GWQMN	mm	30.00	0.0	30.0	
5	A__GW_REVAP		0.09	0.02	0.11	
6	V__ESCO		0.38	0.95	0.38	
7	V__CH_N2		0.11	0.13	0.11	
8	V__CH_K2	mm/Hr.	103.69	0	103.7	
9	R__SOL_AWC	mmWATER/mmSoil	0.09	88.1	96.0	
10	R__SOL_K	mm/Hr.	0.22	93.72	114.6	
11	A__HRU_SLP	m/m	0.05	0.12	0.17	
12	R__SLSUBBSN	m	0.56	36.51	56.95	
13	V__REVAPMN	mm	1.23	1	1.23	

I. Monthly Calibration and Validation Result

Table-4.4 shows model performance parameters (R^2, E_{NS}, p-factor, r-factor and PBIAS) calculated using the observed and simulated discharge for calibration (2001-2006) and validation (2007–2010) period at Kesse gauging station for Monthly bases. Accordingly the results fulfilled the requirements suggested by *Santhi et al. (2001)* for R^2 >0.6 and E_{NS}> 0.5.

Table 4-4: Statistical analysis result for Monthly calibration and validation

No	Name	Calibration (2001-2006)					Validation (2007-2010)				
		p-factor	r-factor	R^2	E_{NS}	PBIASE	p-factor	r-factor	R^2	E_{NS}	PBIASE
1	Kesse Gauging Station	0.88	0.71	0.91	0.9	10.3	0.72	0.78	0.76	0.74	10.8

Comparison between observed and simulated flows, for monthly calibration and validation are presented in figure 4.3.The shape of observed flow were well captured by the shapes of the simulated flow. Nevertheless, some high peaks were not matched well and low flows were over estimated by the model during the validation period. The over estimation might be due to the scarcity of climate gauging station in the study area, parameter selected for calibration and the data quality of some gauging station

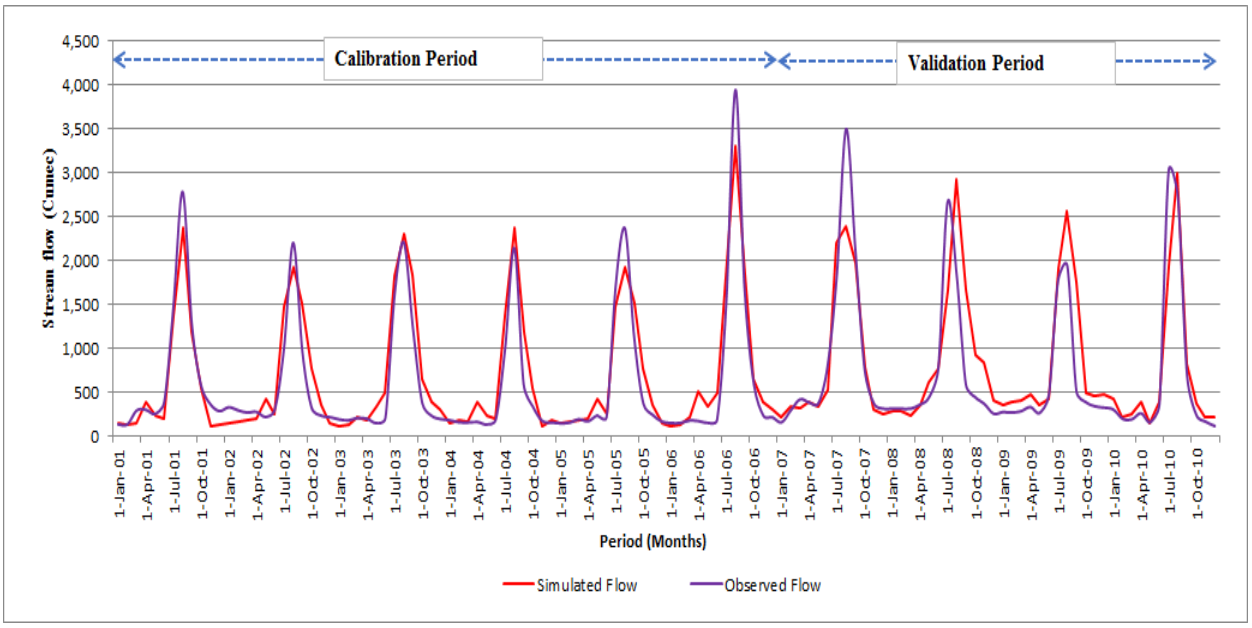

Figure 4-3: Calibration and validation result of average daily simulated and observed flow in months at the out left of the watershed (Kesse Gauging Stn.) for the period of 2001-2010).

II. Daily Calibration and Validation result

The daily base simulated discharge for calibration (2001-2006) and validation (2007–2010) period at Kesse gauging station despite lower performance parameters (R^2, E_{NS}, and PBIAS) than the monthly base, the model performed very good to good during the calibration and validation period respectively .The result obtained fulfilled the requirements suggested by *Santhi et al. (2001)* for R^2 >0.6 and E_{NS}> 0.5.

Table 4-5: Statistical analysis result for daily calibration and validation

No	Name	Calibration (2001-2006)					Validation (2007-2010)				
		p-factor	r-factor	R^2	E_{NS}	PBIASE	p-factor	r-factor	R^2	E_{NS}	PBIASE
1	Kesse Gauging Station	0.74	0.81	0.84	0.8	14.2	0.7	0.78	0.72	0.69	17.5

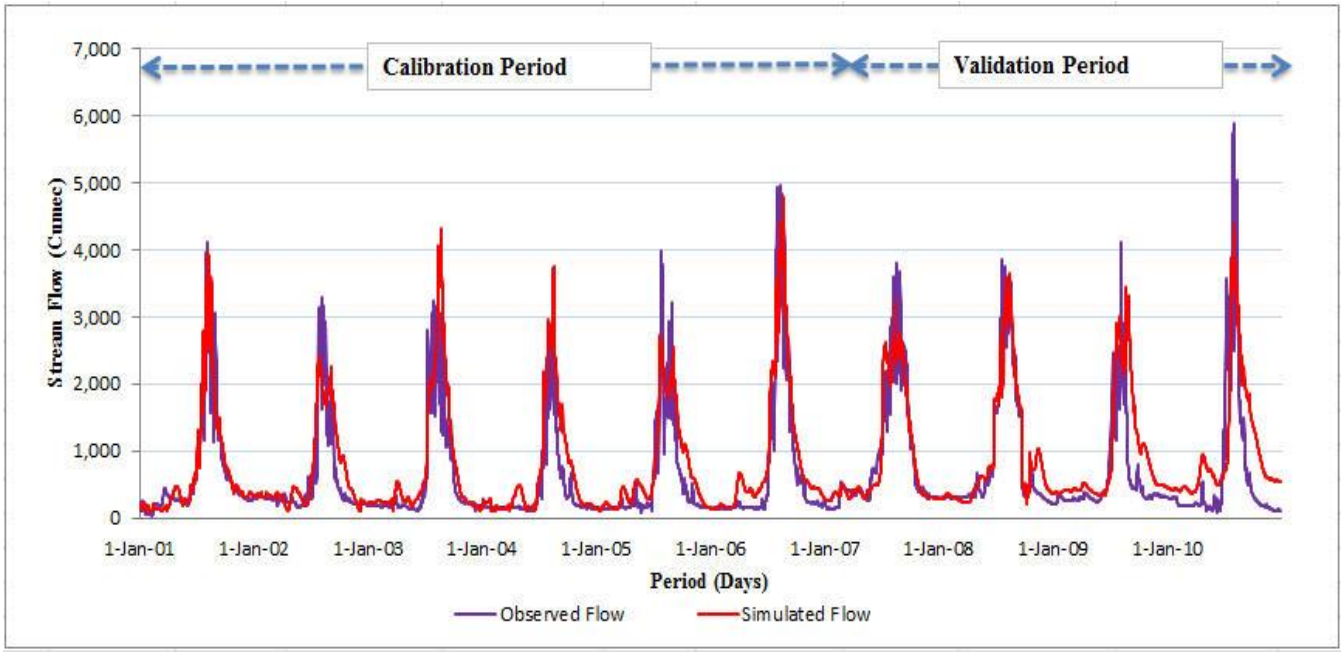

Figure 4-4: Calibration and Validation result of daily simulated and observed flow at the outlet of the watershed (Kesse Gauging Stn.) for the period of 2001-2010)

4.2 STATISTICAL RESULTS OF RCP CLIMATE PROJECTIONS

4.2.1 Base Period analysis for rainfall and Potential evaporation

I. Rainfall

The monthly average bias corrected RCP Rainfall data for the study area and the frequency of events has similar behavior as the observed Rainfall for the base period with a correlation coefficient of 0.9 with observed data

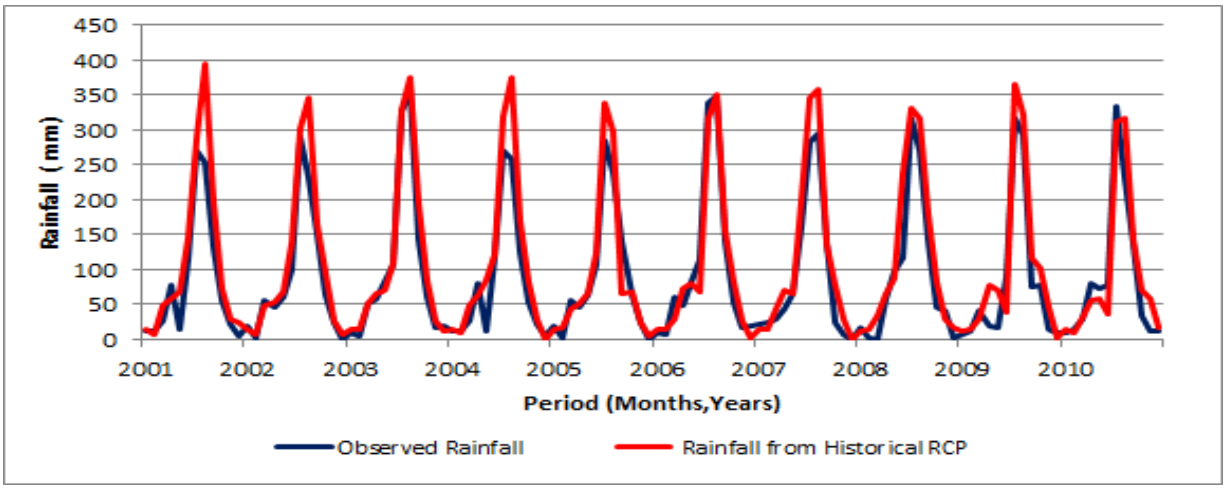

Figure 4-5: Daily Average Observed Rainfall and Rainfall form Historical RCP data in Months for (2001-2010)

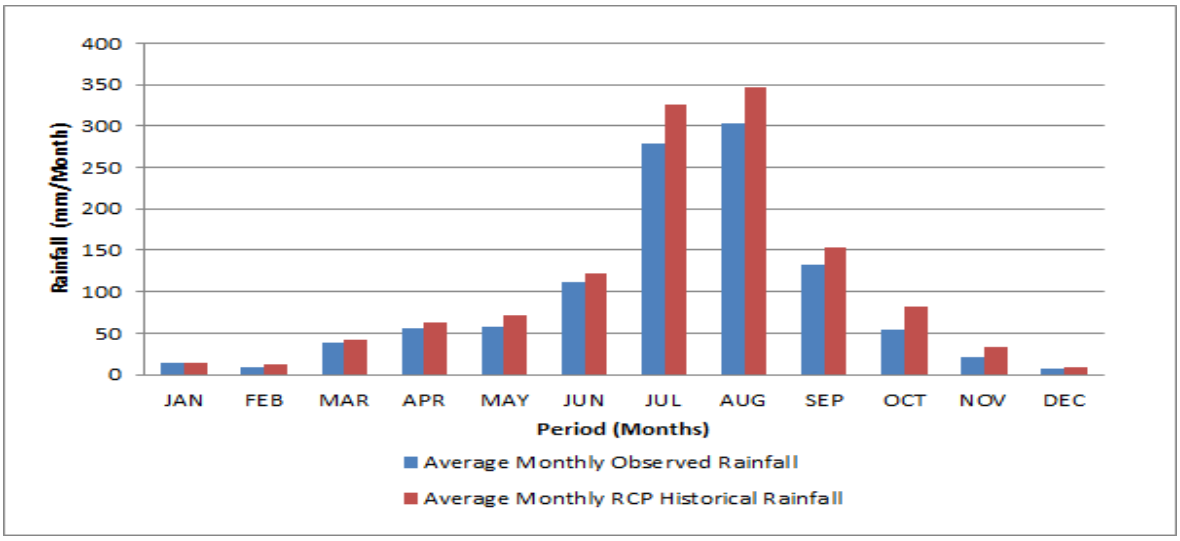

Figure 4-6: Observed and Historical RCP mean monthly rainfall for a period of 2001-2010)

II. Potential Evapotranspiration

The Potential Evapotranspiration at base period has correlation coefficient of 0.93 with observed data as shown in the figure 4-7 below

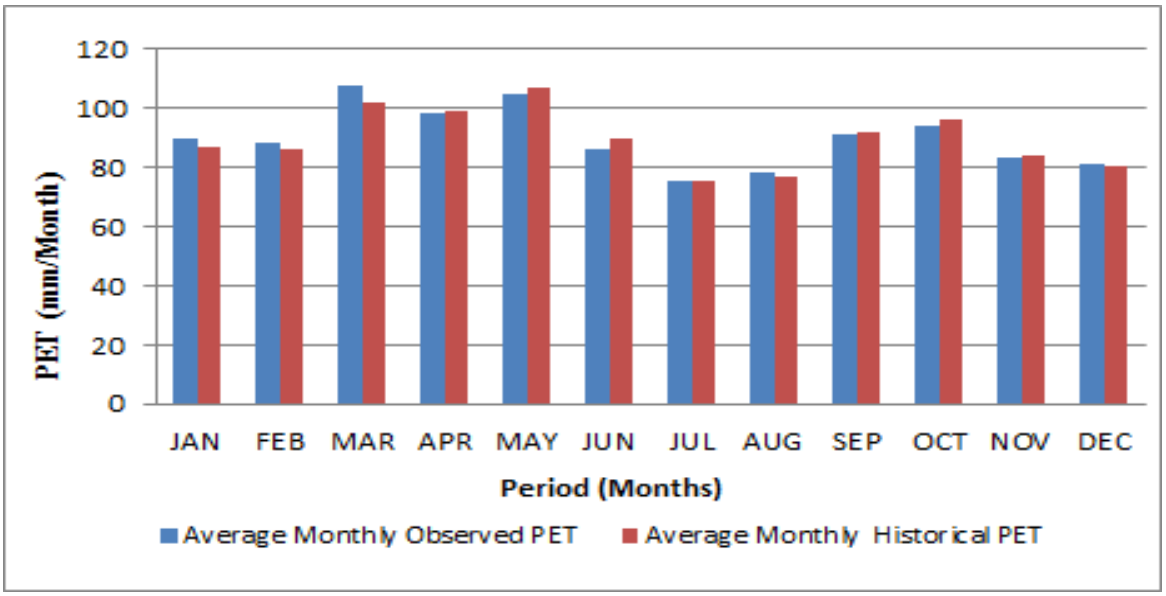

Figure 4-7: Average monthly observed and Historical RCP potential Evapotranspiration at base period for the study area from (2001-2010)

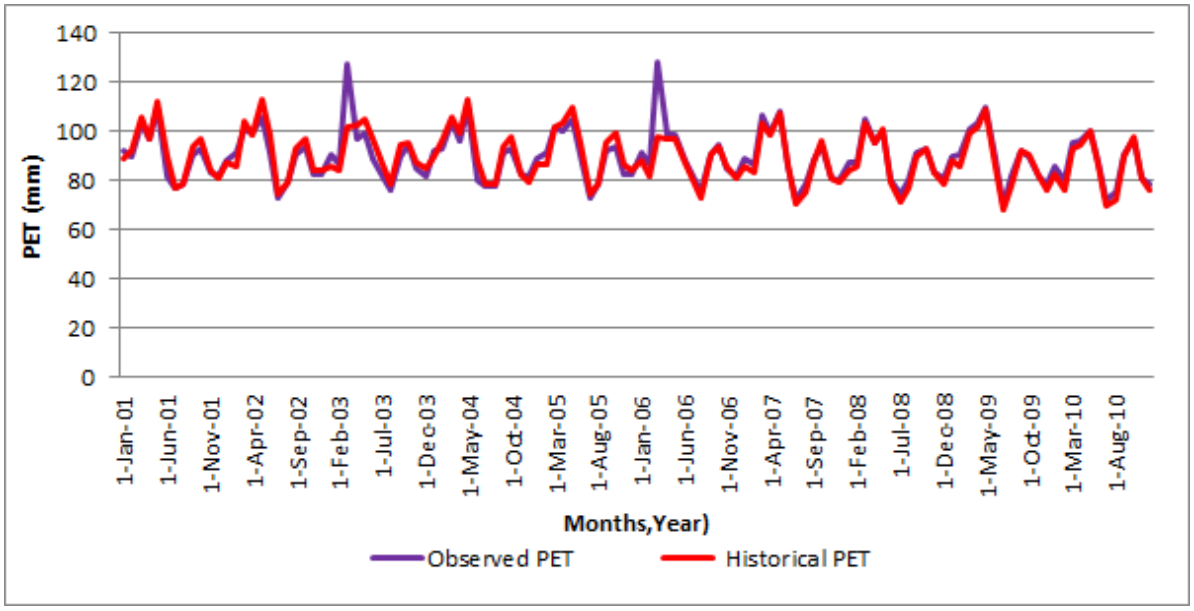

Figure 4-8: Daily Average observed and Historical RCP potential Evapotranspiration in months for (2001-2010)

4.2.2 Projected Future Climate Variables Generated From RCP Scenarios

The future scenarios were developed by dividing the future time series into three equal periods of 10 years: 2030s (2031-2040), 2050s (2051-2060) and 2090s (2091-2100). The period from 2001-2010 was taken as a base period.

RCP2.6 (Minimum Emission Scenario)

I. Rainfall

The Rainfall obtained from RCP grid data for each meteorological stations used in the study area were bias corrected before using it in SWAT hydrological model in such a way Rainfall for the study area is calculated for each RCP climate date under each future time series and finally a comparison is made with respect to the base period. Accordingly for RCP2.6 scenario the seasonal change of Rainfall when compared to the base period shows an increase in all season for all future time series with maximum change in Bega (ONDJ) with (+46.9%) in 2090s and minimum increase in Kirmet (JJAS) with (+6.2%) in 2030s

Table 4-6: Percentage of change of seasonal Rainfall from the base period rainfall for RCP2.6

S.NO	Watershed	Seasons	Rainfall from RCP2.6 (2031-2040)	Rainfall from RCP2.6 (2051-2060)	Rainfall from RCP2.6 (2091-2100)
			% Change	% Change	% Change
1	Study Area	FMAM	11.9	22.2	36.9
		JJAS	6.2	9.9	13.6
		ONDJ	28.6	36.3	46.9
		ANNUAL	9.4	14.6	20.7

The annual rainfall also shows an increasing trend in all the future time series compared to the base period with maximum increase (+20.7%) in the 2090s .The monthly average rainfall in the future time series of 2030s, 2050s and 2090s also shows in an increment relative to the base period with maximum increase in the month of December with (+95.89%) in 2090s and minimum change in June with (+3.8%) in 2030s.

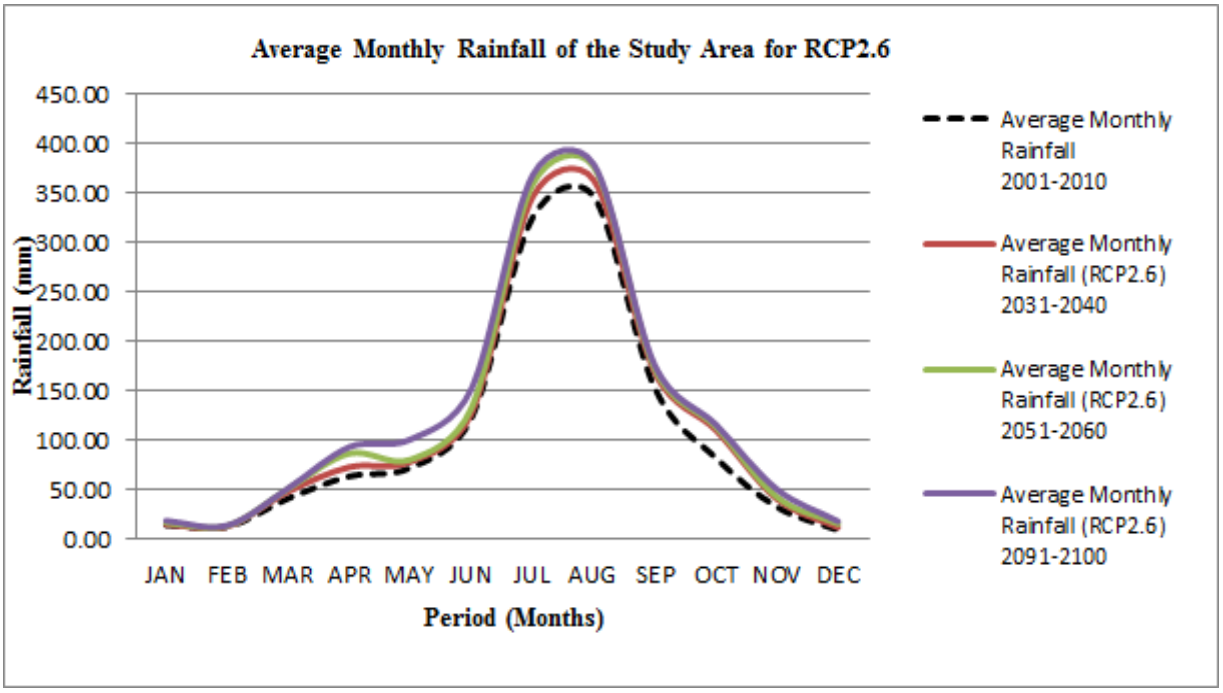

Figure 4-9 : Monthly average rainfall for base period and future time series of the study Area for RCP 2.6

II. Evapotranspiration

The future Evapotranspiration obtained from RCP2.6 shows an increasing trend in all seasons and months in the future time series for 2030s, 2050s and 2090s compared with the base period: 2001-2010. Maximum change PET is observed in Belg (FMAM) with (+5.39%) during the mid-period (2050s) and minimum change is observed in Bega (ONDJ) season with (+2.84%) during 2050s.

Table 4-7: Percentage of change of seasonal PET from the period PET for RCP2.6

S.NO	Watershed	Seasons	PET from RCP2.6 (2031-2040)	PET from RCP2.6 (2051-2060)	PET from RCP2.6 (2091-2100)
			% Change	% Change	% Change
1	Study Area	FMAM	3.98	5.39	3.98
		JJAS	4.29	3.27	3.43
		ONDJ	3.05	2.84	3.26
		ANNUAL	3.78	3.91	3.58

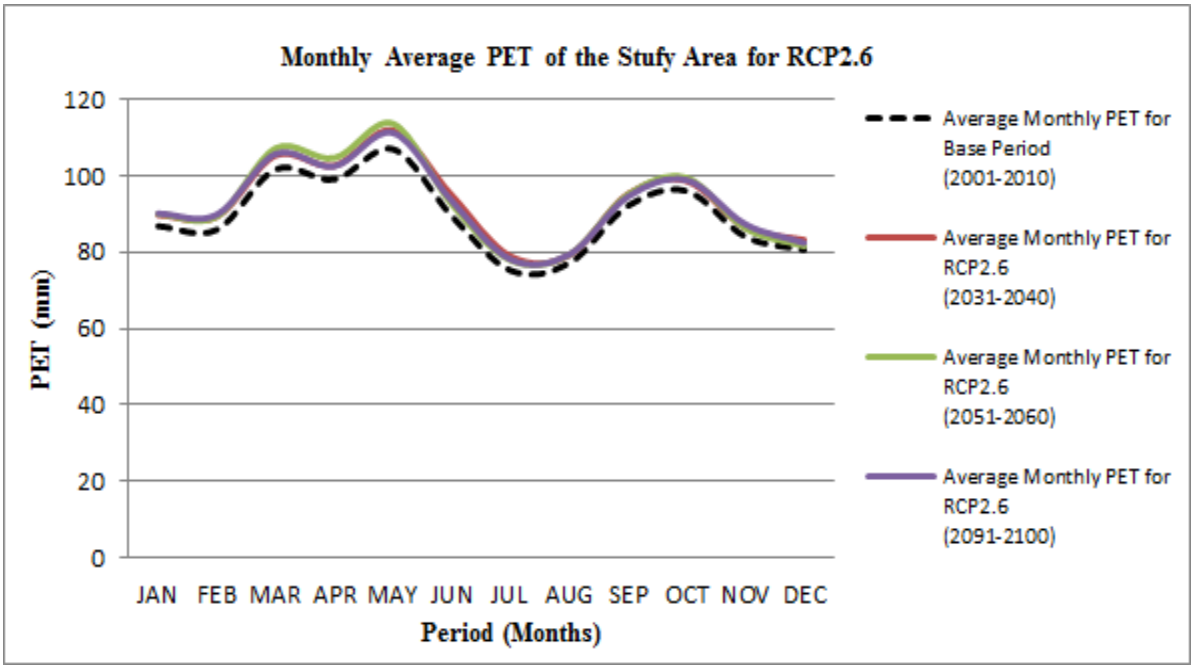

Figure 4-10: Base periods and future time series of monthly average Potential Evapotranspiration of the study area for RCP2.6

RCP4.5 (Medium to high Emission Scenario)

I. Rainfall

The Rainfall for the future time series under RCP4.5 scenario is described as follows:

For the 1st future time series like that of RCP2.6 the mean seasonal , annual and monthly precipitation shows an increasing trend in all the three future time series when compared with the base period. Maximum increase is expected during low flow time Bega (ONDJ) season with (+45.7%) in 2090s and a minimum increase is expected in high flow time Kiremt (JJAS) season with (+8.1%) in 2030s.

The monthly average rainfall in the future time series under RCP4.5 shows an increment during 2030s, 2050s and 2090s future time. Maximum increase rainfall is observed in the month of March with (+145.52%) in 2090s and minimum change is observed in July with (+0.31%) in 2030s.

Table 4-8: Percentage of change of seasonal Rainfall from the base period rainfall for RCP4.5

S.NO	Watershed	Seasons	Rainfall from RCP4.5 (2031-2040)	Rainfall from RCP4.5 (2051-2060)	Rainfall from RCP4.5 (2091-2100)
			% Change	% Change	% Change
1	Study Area	FMAM	18.8	28.6	34.0
		JJAS	8.1	11.8	20.3
		ONDJ	9.8	24.2	45.7
		ANNUAL	9.9	15.6	25.1

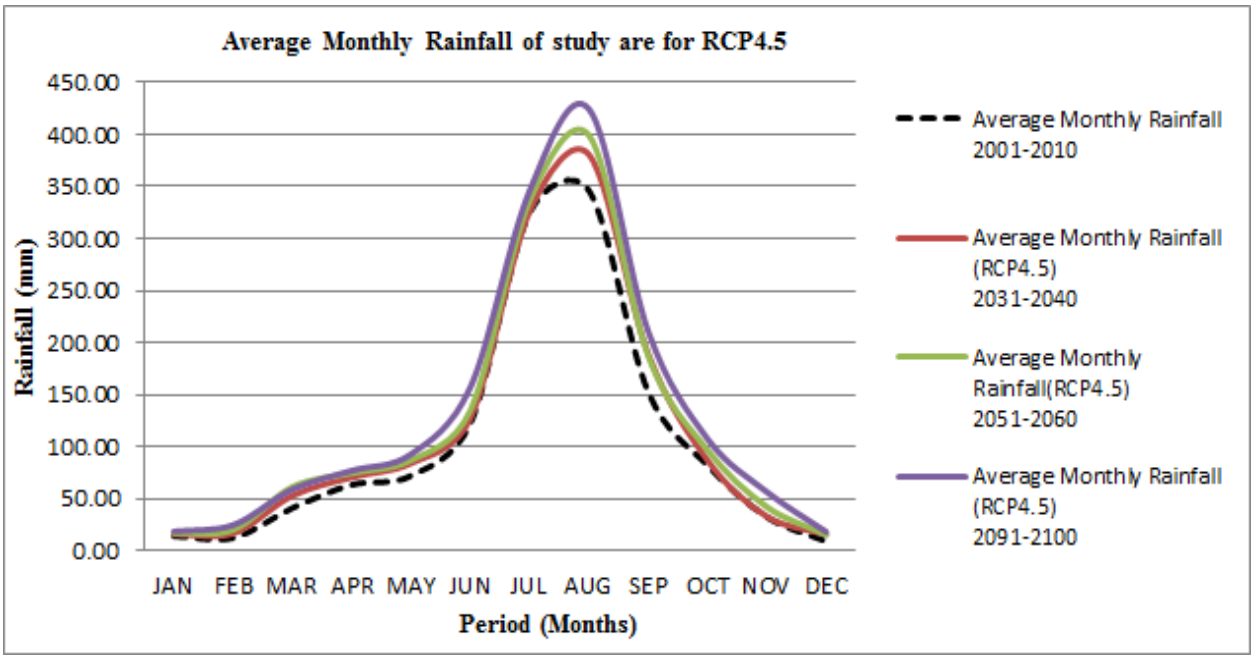

Figure 4-11: Monthly average rainfall of the base period and future time series of the study Area for RCP4.5

II. Potential Evapotranspiration

The future Evapotranspiration obtained from RCP4.5 climate scenario results an increasing trend in 2030s, 2050s and 2090s comparing with the base period:2001-2010.

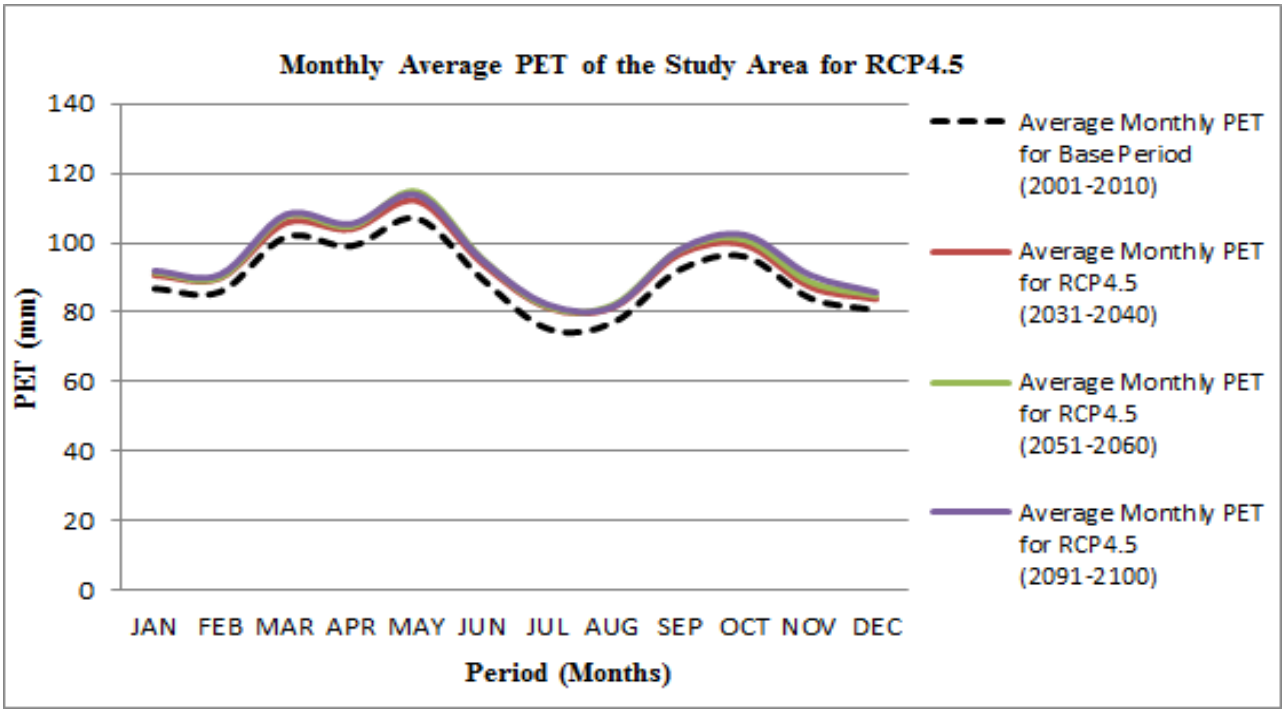

Figure 4-12: Base periods and future time series of monthly average Potential Evapotranspiration of the study area for RCP4.5

Table 4-9: Percentage of change of seasonal PET from the base period for RCP4.5

S.NO	Watershed	Seasons	PET from RCP4.5 (2031-2040)	PET from RCP4.5 (2051-2060)	PET from RCP4.5 (2091-2100)
			% Change	% Change	% Change
1	Study Area	FMAM	4.56	5.95	6.24
		JJAS	5.85	6.87	6.83
		ONDJ	3.91	5.30	6.68
		ANNUAL	4.75	6.02	6.56

As it can be seen form the table above for RCP4.5 scenario the maximum increase in PET is observed in 2050s during the Kirmet (JJAS) season with (+6.87%) and minimum increase in Bega (ONDJ) season with (+3.92%) in 2030s.

RCP8.5 (high Emission Scenario)

I. Rainfall

The average annual, seasonal and monthly rainfall pattern of for the future time series for RCP 8.5 scenario is described as follows:-

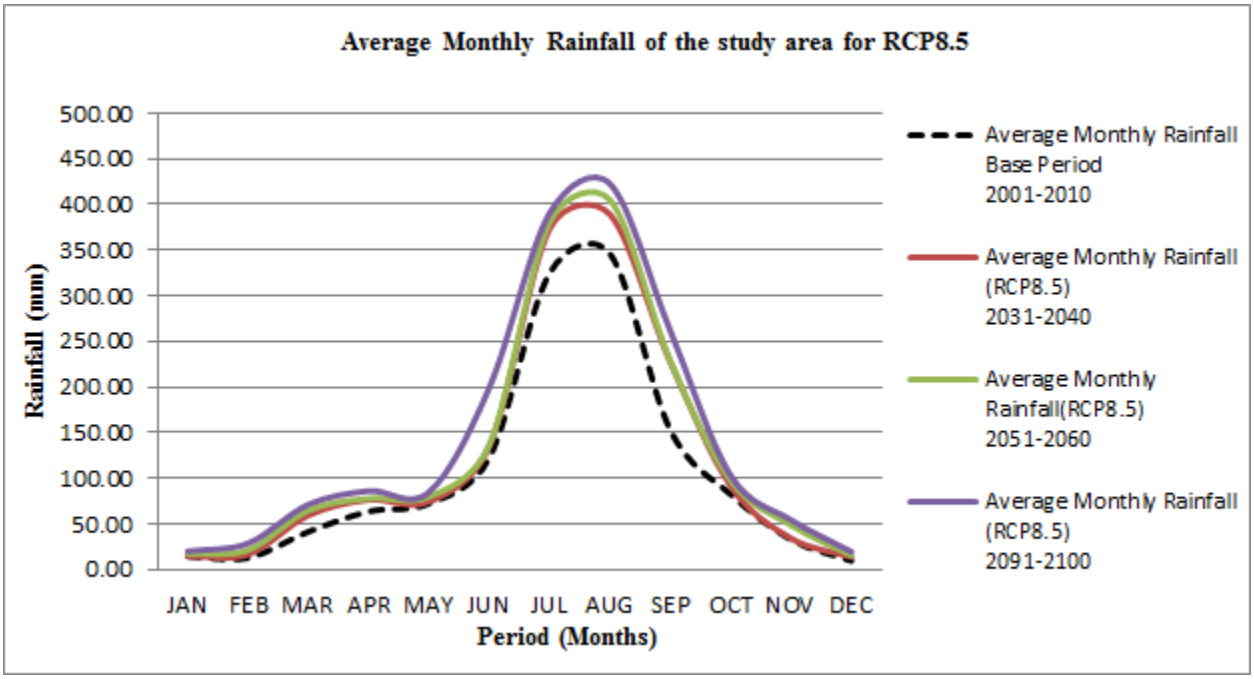

Figure 4-13: Monthly average rainfall of the base period and future time series of the study Area for RCP8.5.

Table 4-10: Percentage of change of annual and seasonal Rainfall from the base period rainfall for RCP8.5

S.NO	Watershed	Seasons	Rainfall from RCP8.5 (2031-2040)	Rainfall from RCP8.5 (2051-2060)	Rainfall from RCP8.5 (2091-2100)
			% Change	% Change	% Change
1	Study Area	FMAM	19.3	28.3	42.6
		JJAS	18.9	21.7	34.7
		ONDJ	11.0	28.6	42.0
		ANNUAL	18.1	23.4	36.6

The 3rd climate scenario RCP8 considered in simulating future flow shows an increase in Precipitation and Potential evapotranspiration relative to the base period. The average annual

rainfall may increases by (+18.1%), (+23.4%) and (+36.6%) for 2030s, 2050s and 2090s respectively which is higher than the preceding two scenarios RCP2.6 and 4.5.

The monthly average rainfall in the future time series for RCP8.5 shows an increasing trend observed in all the month with maximum of increment in rainfall during the month of March with (+243.1%) in 2090s

II .Potential Evapotranspiration

The future Evapotranspiration result obtained from RCP8.5 climate scenario like that of the other RCP scenario results an increasing trend in the future time series for all the three periods from 2030s, 2050s and 2090s compared with the base period: 2001-2010. The increase in PET is also much higher than that of the above two scenarios (RCP 2.6 &RCP 4.5)

Table 4-11: Percentage of change of annual and seasonal PET with respect to base period for RCP8.5

S.NO	Watershed	Seasons	PET from RCP8.5 (2031-2040)	PET from RCP8.5 (2051-2060)	PET from RCP8.5 (2091-2100)
			% Change	% Change	% Change
1	Study Area	FMAM	4.16	8.59	18.41
		JJAS	5.04	9.04	19.14
		ONDJ	3.58	7.99	17.02
		ANNUAL	4.25	8.53	18.18

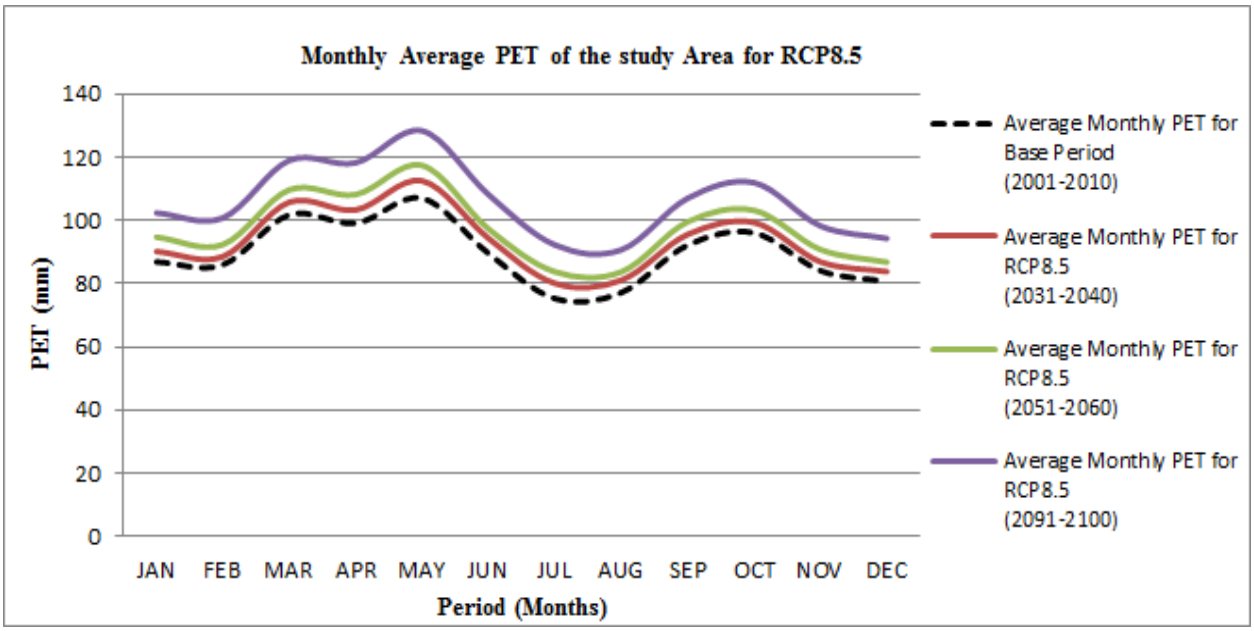

Figure 4-14: Base periods and future time series monthly average Potential Evapotranspiration of the study area for RCP8.5

4.2.3 Summery Of Projected Climate Variables

Generally the projected Precipitation and Potential Evapotranspiration showed an increasing trend in 2030s, 2050s and 2090s over the basin for all RCP Scenarios. The Figure 4.15 and 4.16 below shows the result of the projected mean monthly and annual change for Precipitation and Potential Evapotranspiration from the base period.

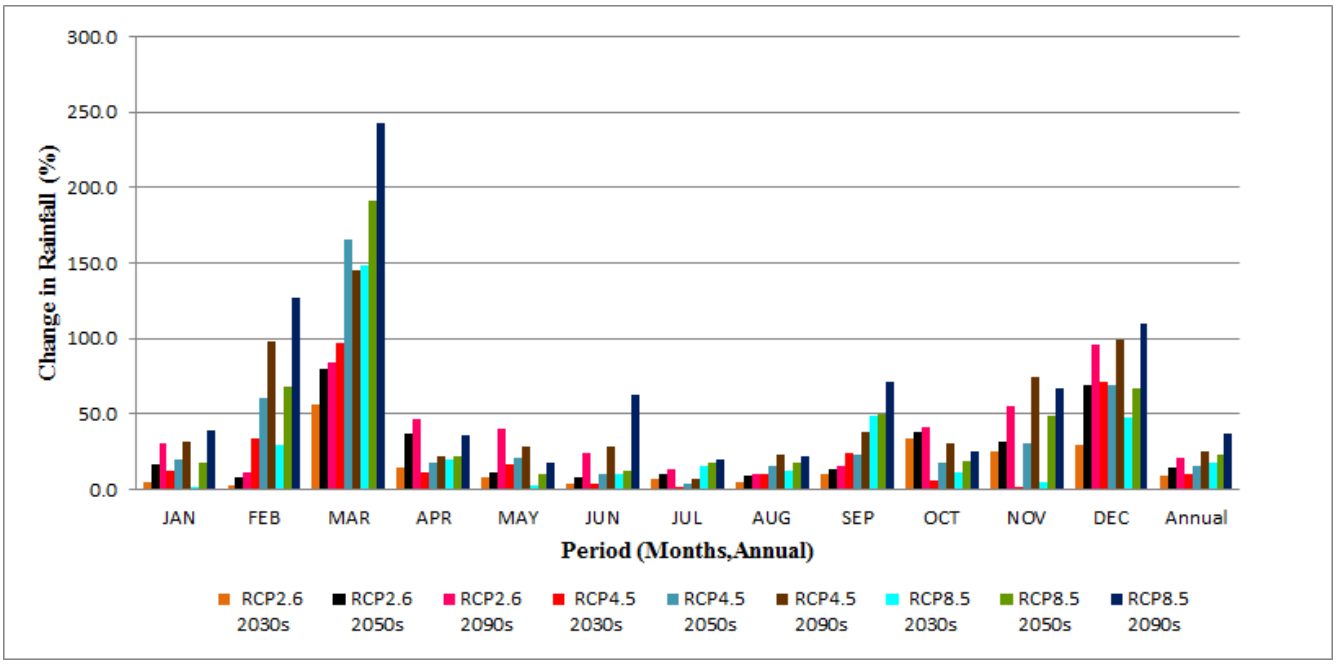

Figure 4-15: Mean monthly and Annual Rainfall change of the Study Area for all RCP scenarios and projected period

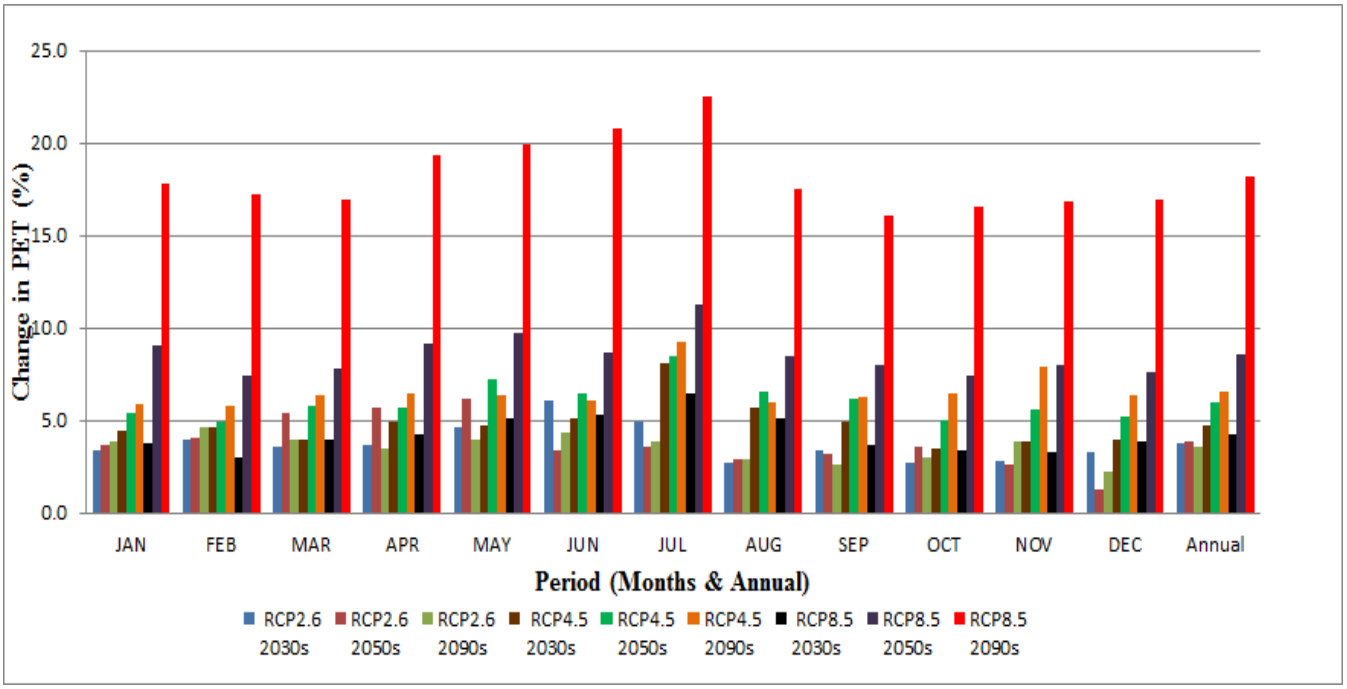

Figure 4-16: Mean monthly and Annual PET change of the Study Area for all RCP scenarios and projected period

4.3 IMPACT OF CLIMATE CHANGE ON WATER RESOURCE AVAILABILITY

Stream flow is mainly dependent on the amount of Rain falling on its watershed area and the actual Evapotranspiration amount released into the atmosphere *(Conway et al., 1993)* hence, changes in precipitation and temperature can significantly influence river flow patterns. The effect of climate change on Abay River flow at Kesse Gauging station was analyzed on a monthly, seasonal and annual basis. The results of the analysis were discussed in the following section:-

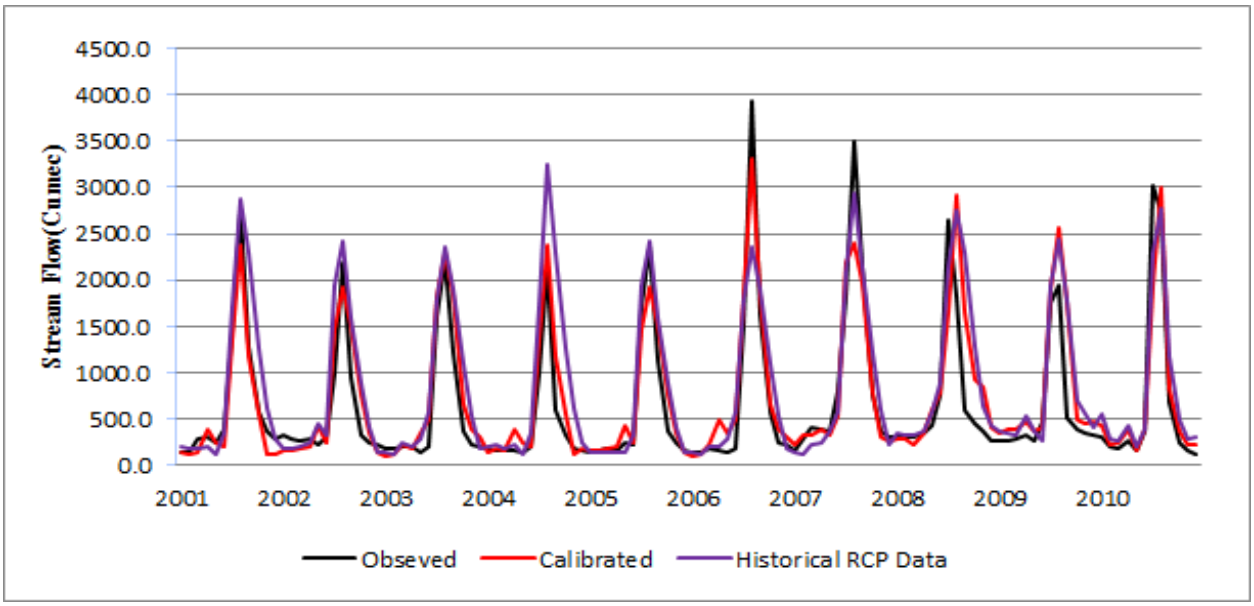

Figure 4-17: Average Daily Stream Flow in months for Observed, Calibrated and Historical RCP

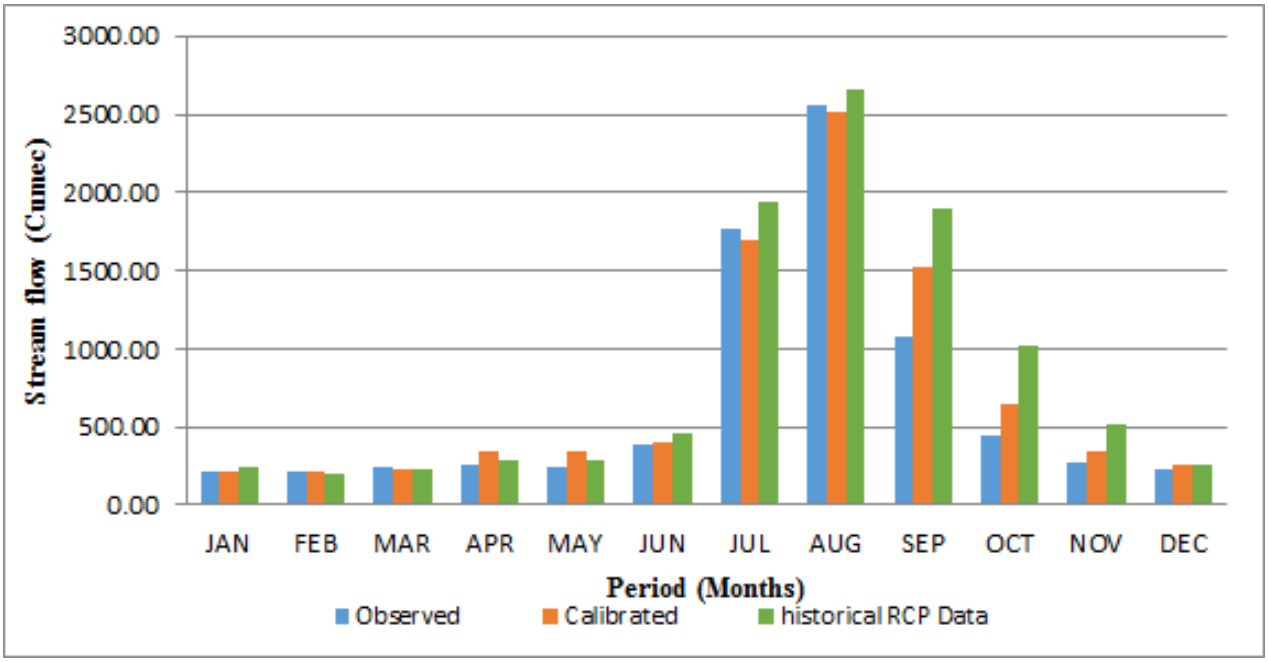

Figure 4-18: Average monthly observed, Calibrated and stream from RCP Historical Data

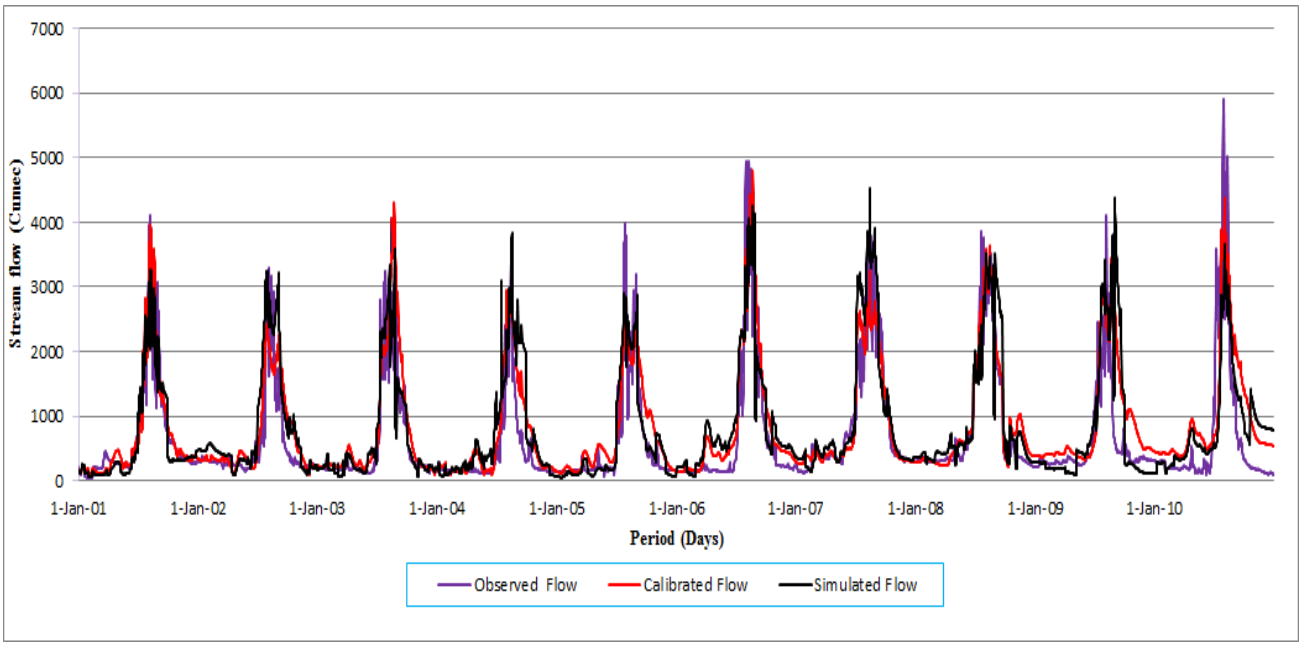

Figure 4-19: Daily observed, Calibrated and stream from RCP Historical Data

4.3.1 Impact of Climate Change On Monthly, Seasonal, Extreme And Annual Flow

The impact of climate change was analyzed taking the 2001-2010 simulated river flow as the baseline against which the future flows for the 2030s, 2050s and 2090s were compared .The result of the analysis for all the RCP Scenarios are presented as follows:-

4.3.1.1 Flow analysis result for RCP 2.6 (Low Emission Scenario)

Daily and Monthly flow analysis result for RCP2.6

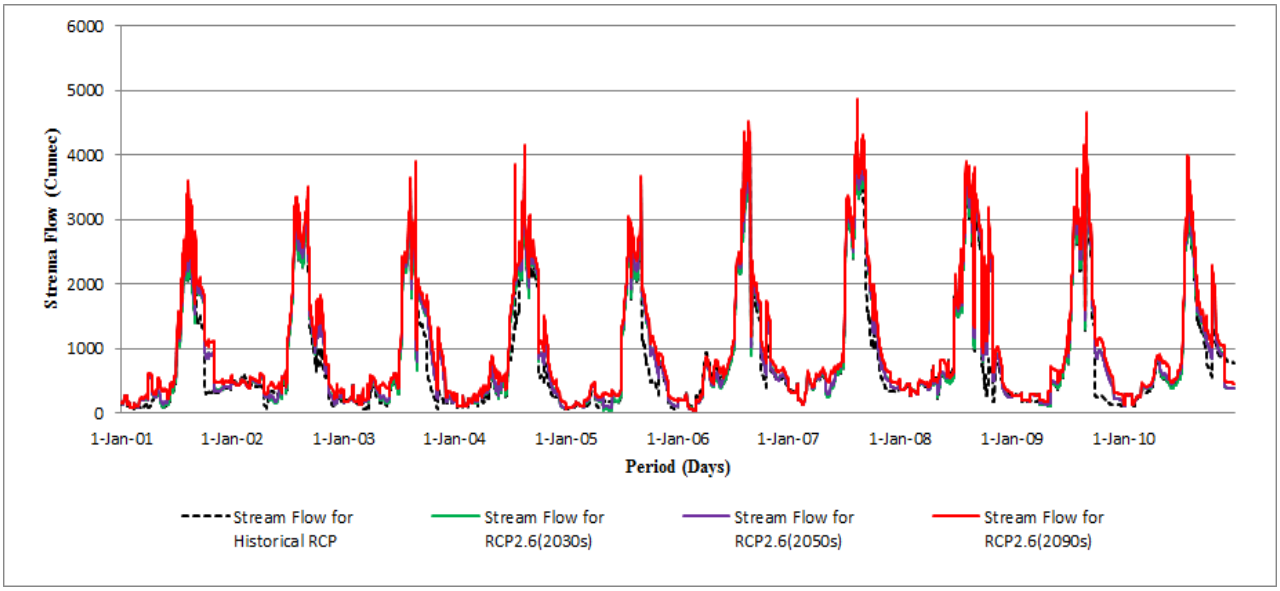

Figure 4-20: Daily stream flow for Abay River at Kesse for Historical RCP and RCP2.6 climate data

The mean monthly flow volume shows an increasing trend for all the months except for July which shows a decrease by (-0.22%) for the period of 2030s.All the other months shows an increase in mean monthly flow for all future time series with maximum increase in May with (+95.51%) in 2090s. The overall trend shows that the monthly future flow volume in the in Abay River exhibits an increasing trend for RCP2.6 which may reach up to (+16.06%) in 2030s, (+19.85%) in 2050s and (+35.70%) in 2090s

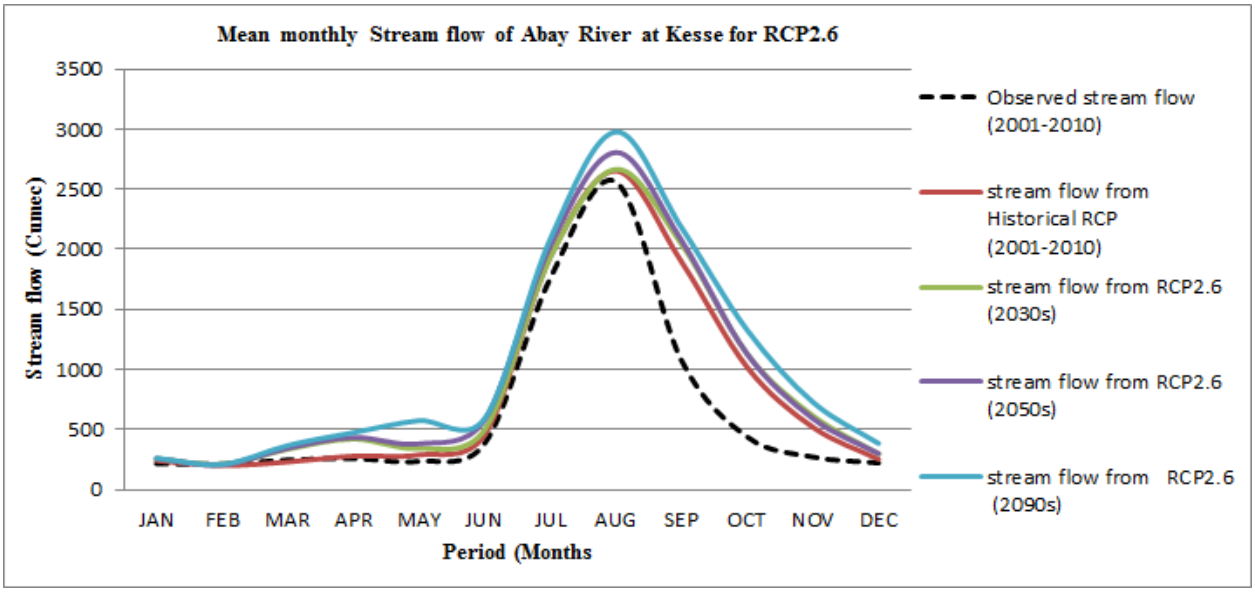

Figure 4-21: Average monthly observed Stream flow; 2001-2010, average monthly Stream flow Historical: 2001-2010, average monthly Stream flow: 2030s, average monthly Stream flow: 2050s and average monthly Stream flow: 2090s of the study area for RCP 2.6.

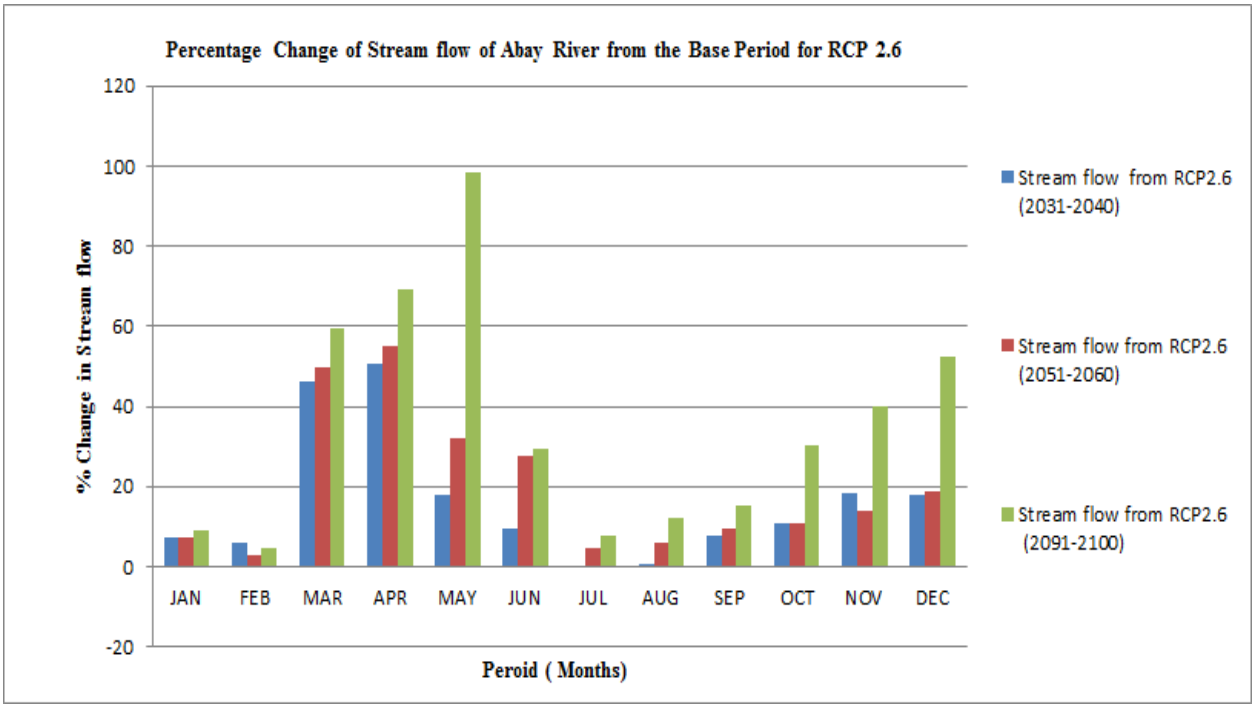

Figure 4-22: Monthly Percentage change in flow volume of Abay River from the base period for RCP2.6

Seasonal and annual flow analysis result for RCP 2.6

The impacts of climate change on the seasonal and annual flow volume were also presented so as to foresee its consequence on the socio-economic condition of the area. There are three seasons in the study area: Kiremt (rainy and cropping season), Belg (small rain season) and Bega (dry season). Figure 4.23 and Table 4.12 below reveals the implication of climate change on the River flow in these seasons.

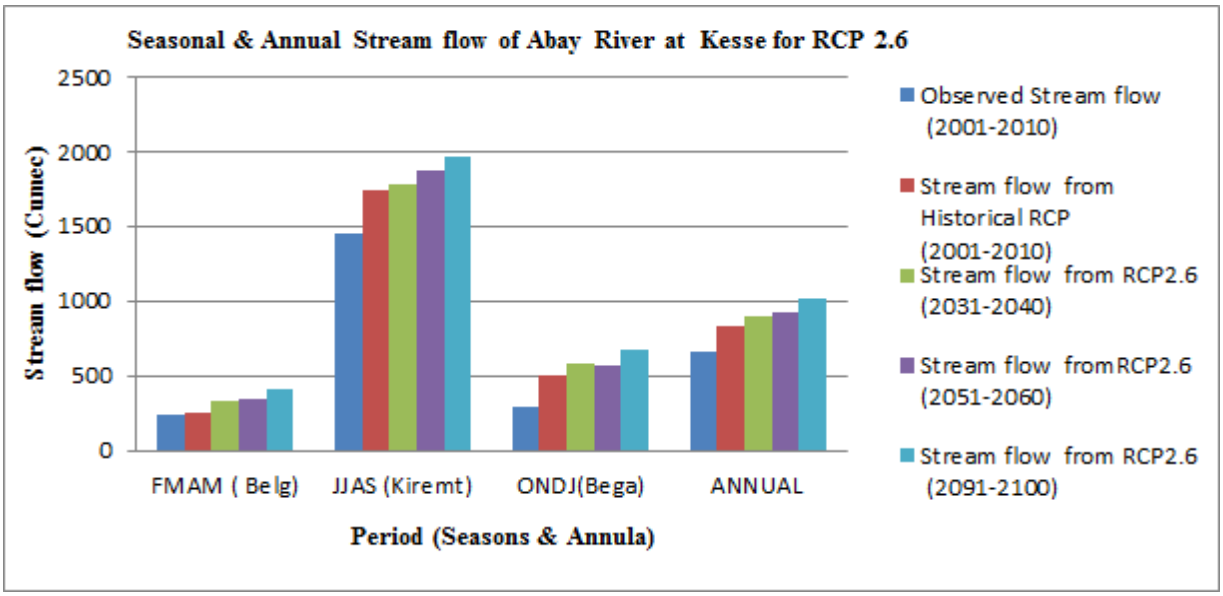

Figure 4-23: Average seasonal and annual flow volume of Abay River at Kesse for RCP2.6

Maximum change in seasonal flow was observed in small rainy season (Belg) with (+62.55%) and Dry season (Bega) with (+33.12%). Kirmet Season shows relatively low increment with (+12.89%) compared with the base period. For 2090s future period, Belg (FMAM) and Bega(ONDJ) seasons are expected to show the larger share in increased flow volume than that of Kiremt season. The other results are explained in the table below.

Table 4-12: Percentage of change of seasonal Stream flow from the base period for RCP2.6

S.NO	Watershed	Seasons	Stream flow RCP from 2.6 (2031-2040)	Stream flow RCP from 2.6 (2051-2060)	Stream flow RCP from 2.6 (2091-2100)
			% change	% change	% change
1	Study Area	FMAM	31.1	36.7	62.6
		JJAS	2.9	7.9	12.9
		ONDJ	13.3	12.2	33.1
		ANNUAL	7.8	11.7	22.0

As we can see from the above figures and table there may be an annual increase in runoff flow in all the three future time with (+7.8%) in 2030s, (+11.77%) in 2050s and (+22.0%) in 2090s.

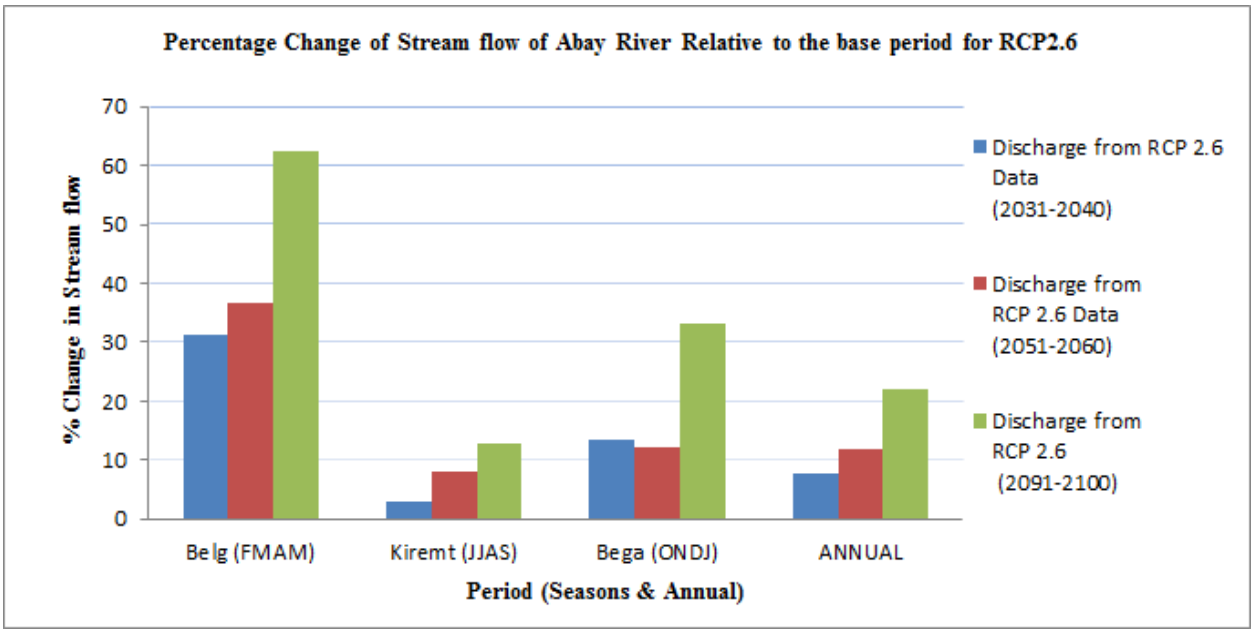

Figure 4-24: Percentage change in seasonal and annual flow volume of Abay River from the period for RCP2.6

Table 4-13: Percentage of change of rainy month‘s runoff from the base period for RCP2.6

S.NO	WATERSHED	MONTHS	Stream flow from RCP 2.6 (2031-2040)	Stream flow from RCP 2.6 (2051-2060)	Stream flow from RCP 2.6 (2091-2100)
			% change	% change	% change
1	STUDY AREA	JUNE	9.46	27.51	29.53
		JULY	-0.22	4.71	7.65
		AUGUST	0.49	5.80	12.24
		SEPTEMBER	7.83	9.44	15.13

4.3.1.2 Flow analysis result for RCP 4.5(Medium to High Emission scenario)

Daily and Monthly flow analysis result for RCP4.5

The future flow was also analyzed for RCP4.5 scenario (medium to high emission scenario) and the result is discussed as follows:

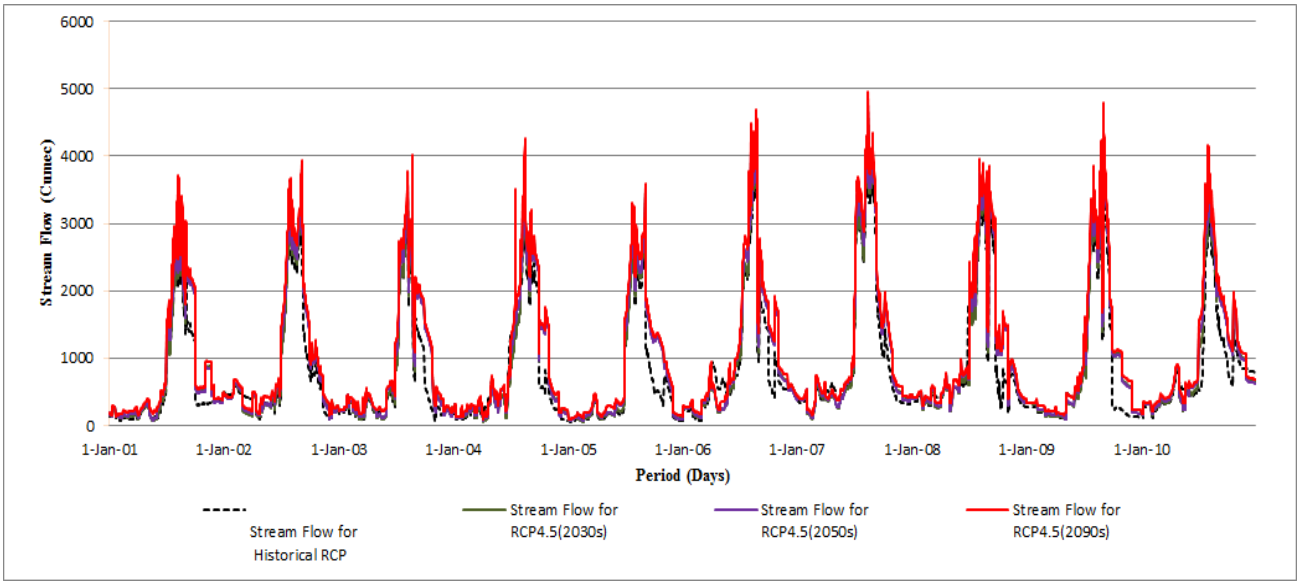

Figure 4-25: Daily stream flow of Abay River at Kesse for Historical RCP and RCP4.5 climate data

From the figure 4.26 below we can see that for RCP4.5 scenario the flow volume shows an increasing trend except for the month of May which shows a slight decrease with (-6.5%) and (-2.52%), by 2030s and 2050s respectively. All the remaining months shows an increasing flow in all the future period with maximum of (+52%) in March for 2090s and minimum increase in July with (+0.18%) for 2030s when compared against the base period.

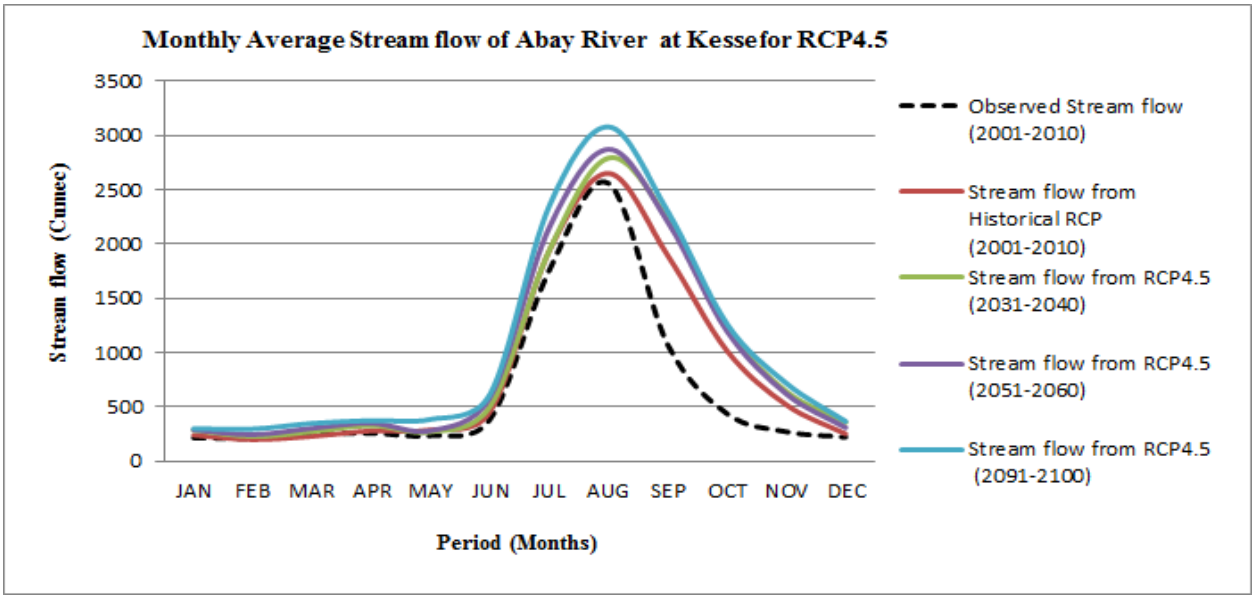

Figure 4-26: Average monthly observed Stream flow; 2001-2010, average monthly Stream flow Historical: 2001-2010, average monthly Stream flow: 2030s and average monthly Stream flow: 2050s and average monthly Stream flow: 2090s of the study area for RCP4.5

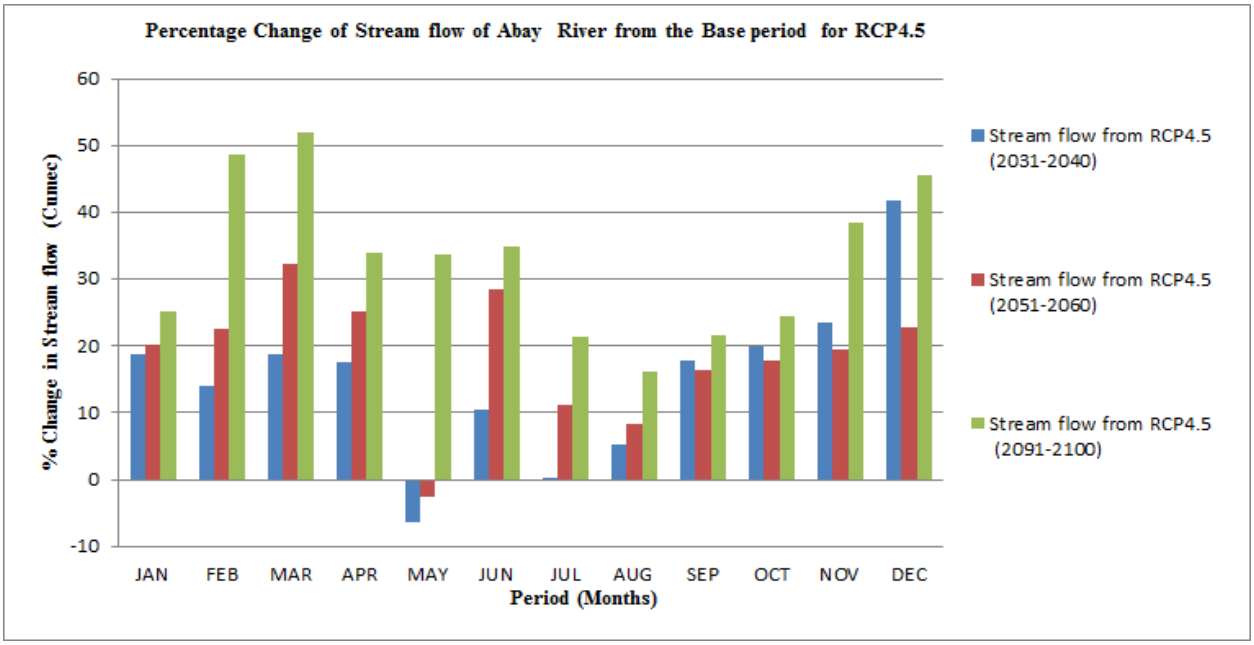

Figure 4-27: Monthly Percentage change in flow volume of Abay River from the baseline for RCP4.5

Table 4-14: Percentage of change of rainy month's runoff from the base period for RCP4.5

S.NO	Watershed	Months	Stream flow from RCP4.5 (2031-2040)	Stream flow from RCP4.5 (2051-2060)	Stream flow fromRCP4.5 (2091-2100)
			% Change	% Change	%Change
1	Study Area	JUNE	10.54	28.56	34.82
		JULY	0.18	11.08	21.36
		AUGUST	5.34	8.37	16.17
		SEPTEMBER	17.88	16.37	21.49

Seasonal and annual flow analysis result for RCP 4.5

Table 4-15: Percentage change of seasonal and annual Stream flow from the base period for RCP4.5

S.NO	Watershed	Months	Stream flow from RCP4.5 (2031-2040)	Stream flow from RCP4.5 (2051-2060)	Stream flow from RCP4.5 (2091-2100)
			% Change	% Change	%Change
1	Study Area	FMAM	10.1	18.3	40.9
		JJAS	7.7	12.6	20.3
		ONDJ	23.5	19.1	30.7
		ANNUAL	11.1	14.5	24.5

For RCP4.5 climate data the future flow volume shows an increase in all the seasons compared to the base period with maximum increasing in flow volume of (+40.9%) for FMAM (Belg) season in 2090s and minimum increase of (+7.7%) in JJAS (Kiremt) season in 2030s. The annual flow for RCP4.5 scenario also shows an increasing flow volume with (+11.1%) in 2030s, (+14.5%) in 2050s and (+24.5%) in 2090s.

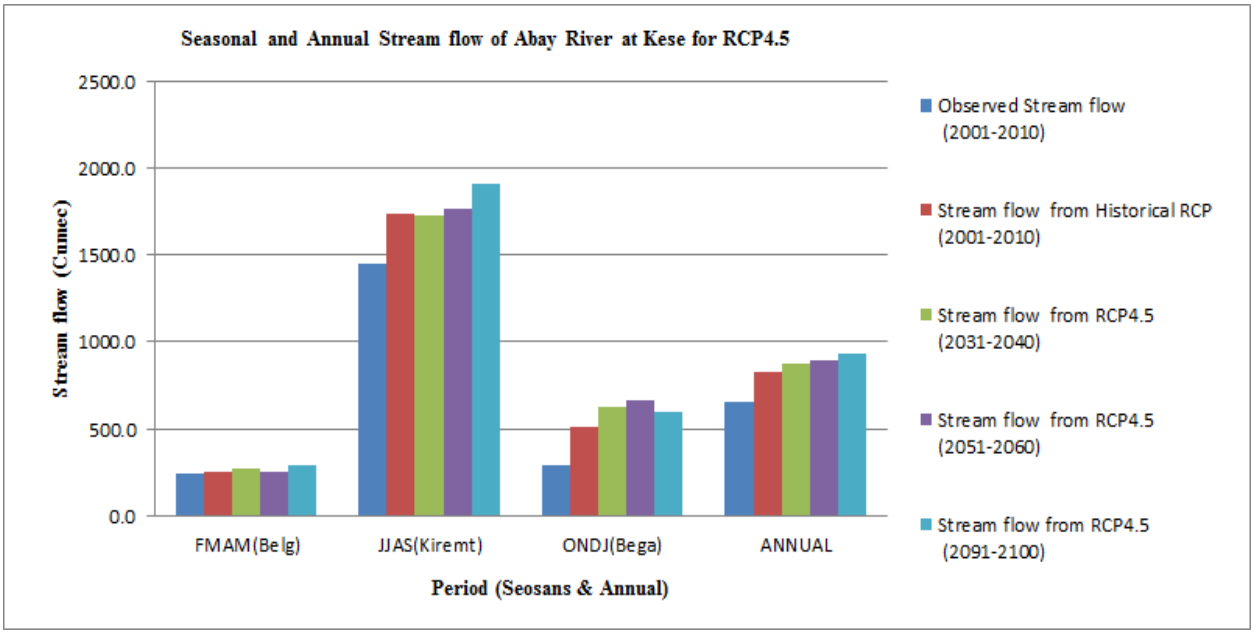

Figure 4-28: Average seasonal and annual flow volume of Abay River at Kesse for RCP 4.5

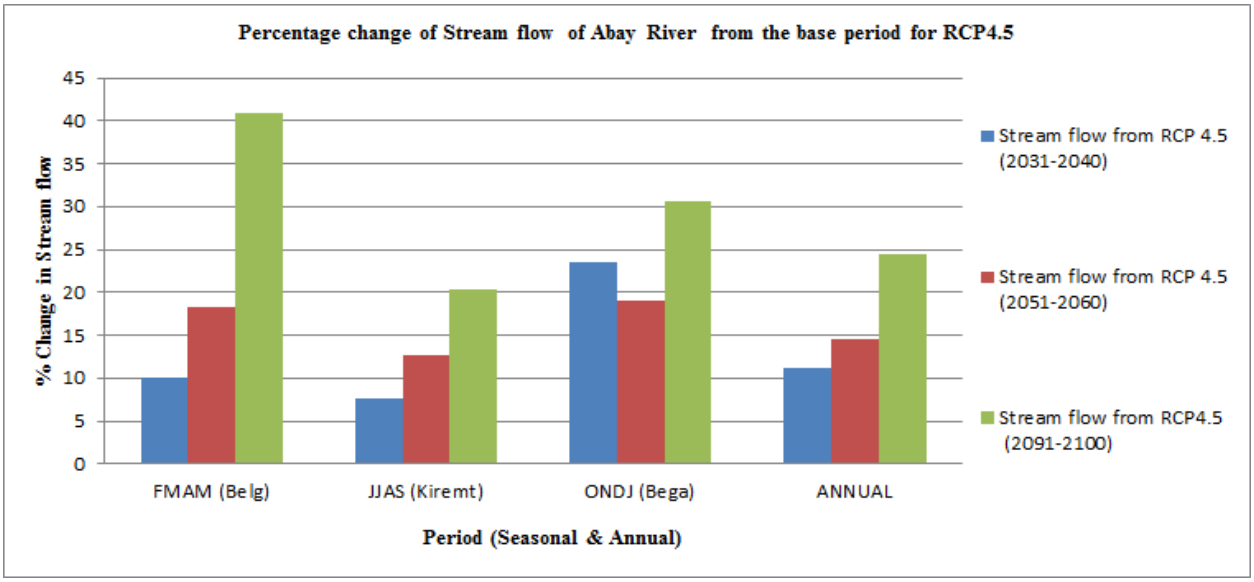

Figure 4-29: Percentage change in Seasonal and annual change of Stream flow of Abay River from the base period for RCP4.5

4.3.1.3 Flow analysis result for RCP 8.5 (high Emission Scenario)

Daily and Monthly flow analysis result for RCP8.5

The 3rd scenario of climate data used in the study is RCP8.5 (High Emission scenario) and the result of the analysis is descried as follows:

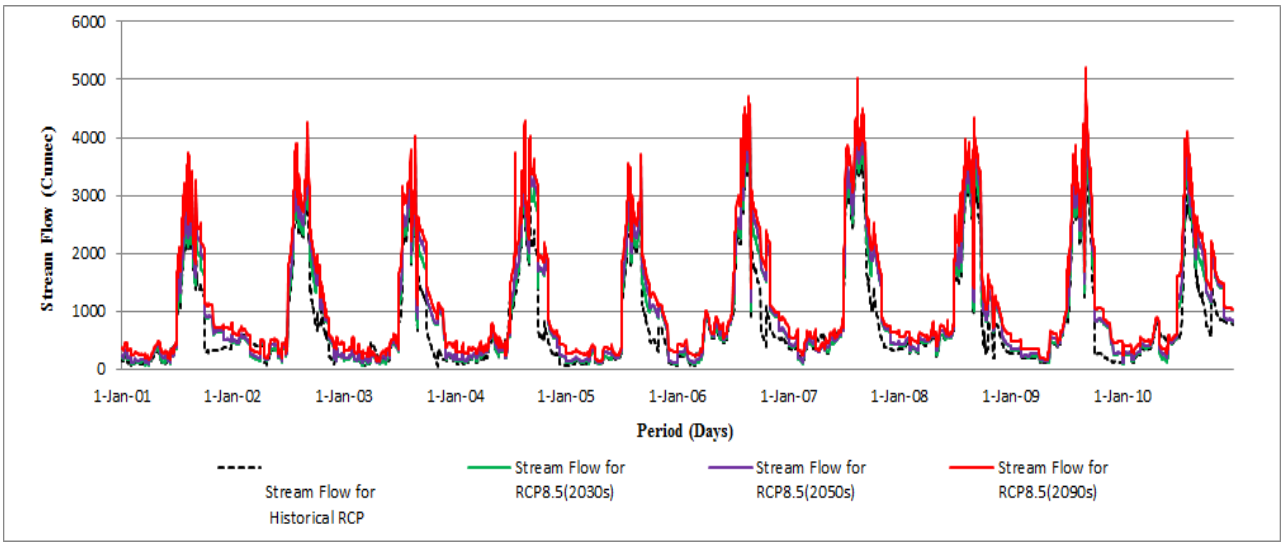

Figure4-30: Daily stream flow of Abay River at Kesse for Historical RCP and RCP8.5 climate data

Like that of the previous two RCP Scenarios the monthly flow volume for RCP8.5 shows increasing trend in all the future time series but the increase in this case much higher than the

from the previous two scenarios (RCP4.5 &RCP2.6) .Maximum increase in the month of December with (+138.6%) in 2090s and a minimum increase in August with (+2.36%) in 2030s.

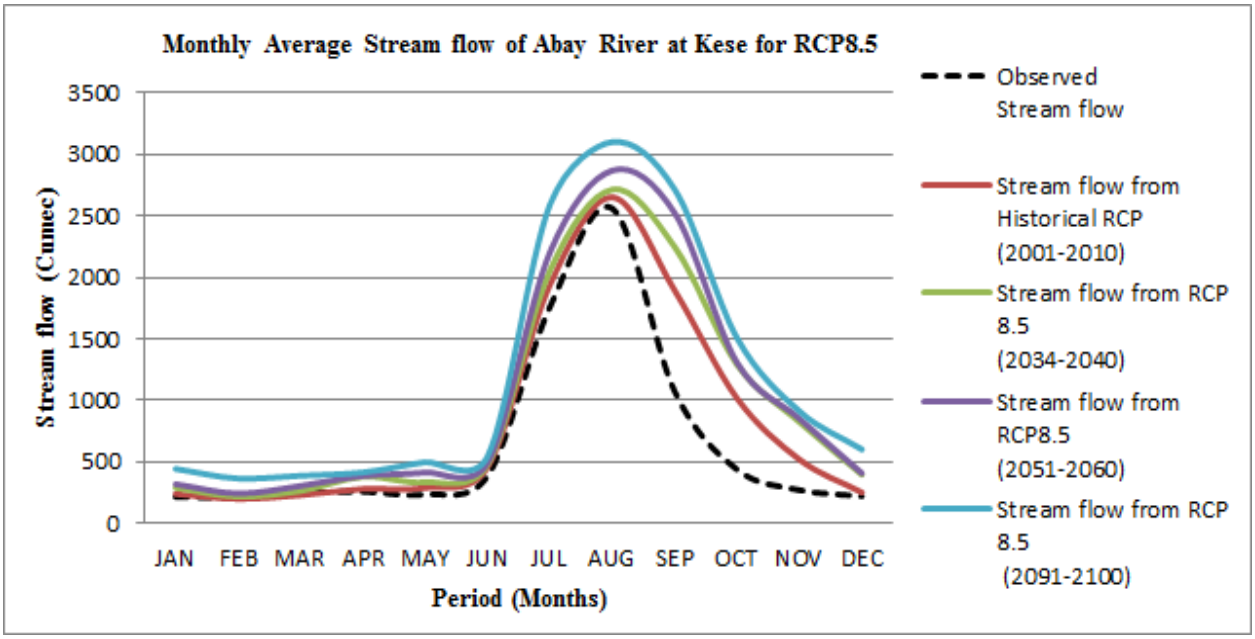

Figure 4-31: Monthly Average observed Stream flow; 2001-2010, monthly average Stream flow Historical: 2001-2010, Monthly average Stream flow: 2030s, Monthly average Stream flow: 2050s & monthly average Stream flow 2090s of the study area for RCP8.5.

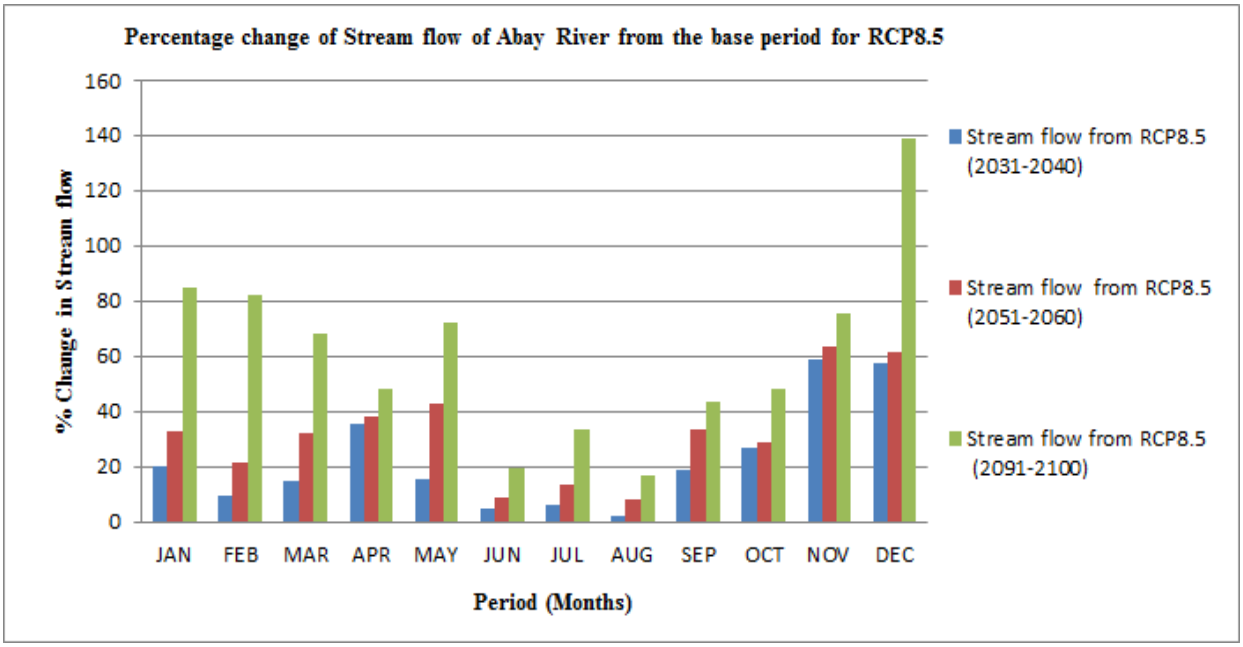

Figure 4-32: Monthly Percentage changes in flow volume of Abay River from the base period for RCP8.5

Table 4-16: Percentage of change of rainy month's Stream flow from the base period for RCP8.5

S.NO	Watershed	Months	Stream flow from RCP 8.5 (2031-2040)	Stream flow from RCP 8.5 (2051-2060)	Stream flow from RCP 8.5 (2091-2100)
			% Change	% Change	%Change
1	Study Area	JUNE	4.76	8.50	19.16
		JULY	5.93	13.71	33.65
		AUGUST	2.36	8.19	16.91
		SEPTEMBER	18.72	33.27	43.43

Seasonal and annual flow analysis result for RCP8.5

Table 4-17: Percentage of change of Seasonal and Annual Runoff from the base period for RCP8.5

S.NO	Watershed	Months	Stream flow from RCP8.5 (2031-2040)	Stream flow from RCP8.5 (2051-2060)	Stream flow from RCP8.5 (2091-2100)
			% Change	% Change	%Change
1	Study Area	FMAM	19.7	34.9	66.6
		JJAS	7.98	16.59	28.97
		ONDJ	38.06	42.22	70.76
		ANNUAL	15.28	23.64	41.24

The seasonal and annual flow analysis result reveals that there is an increase in flow volume in all future time period with maximum increase in Bega (FMAM) with (+70.8%) and minimum increase in Kiremt (JJAS) with (+7.9%) for 2090s and 2030s future time respectively.

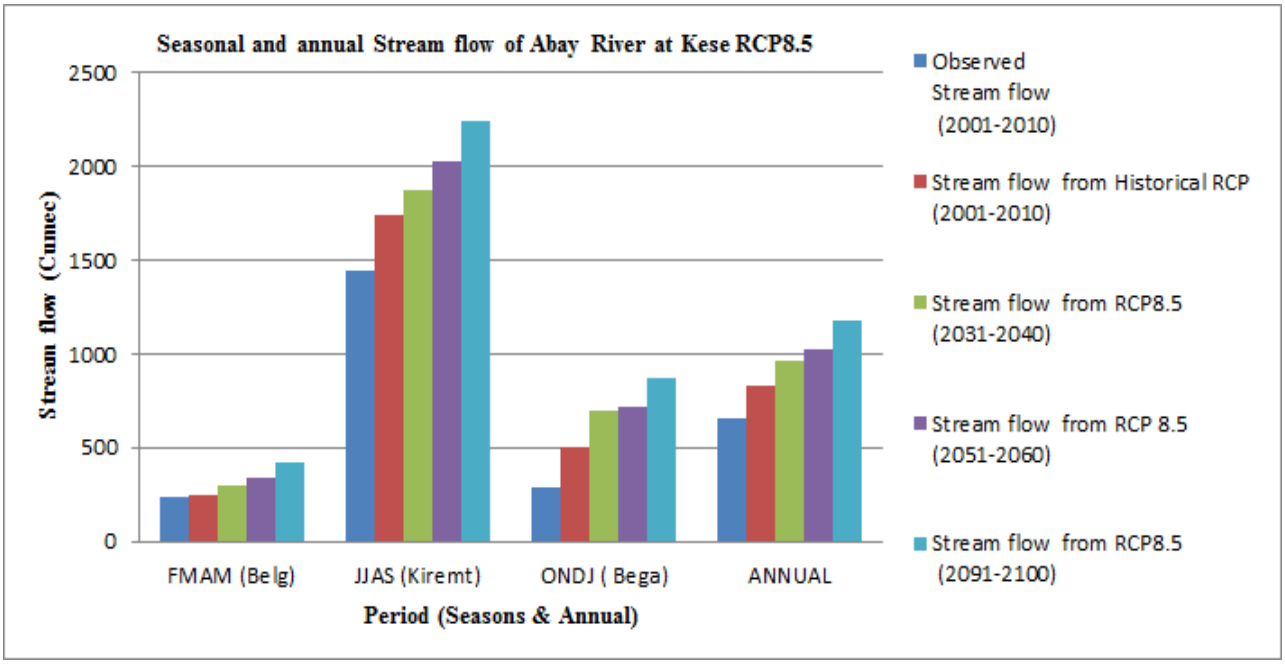

Figure 4-33: Average seasonal and annual flow volume of Abay River at Kesse for RCP8.5

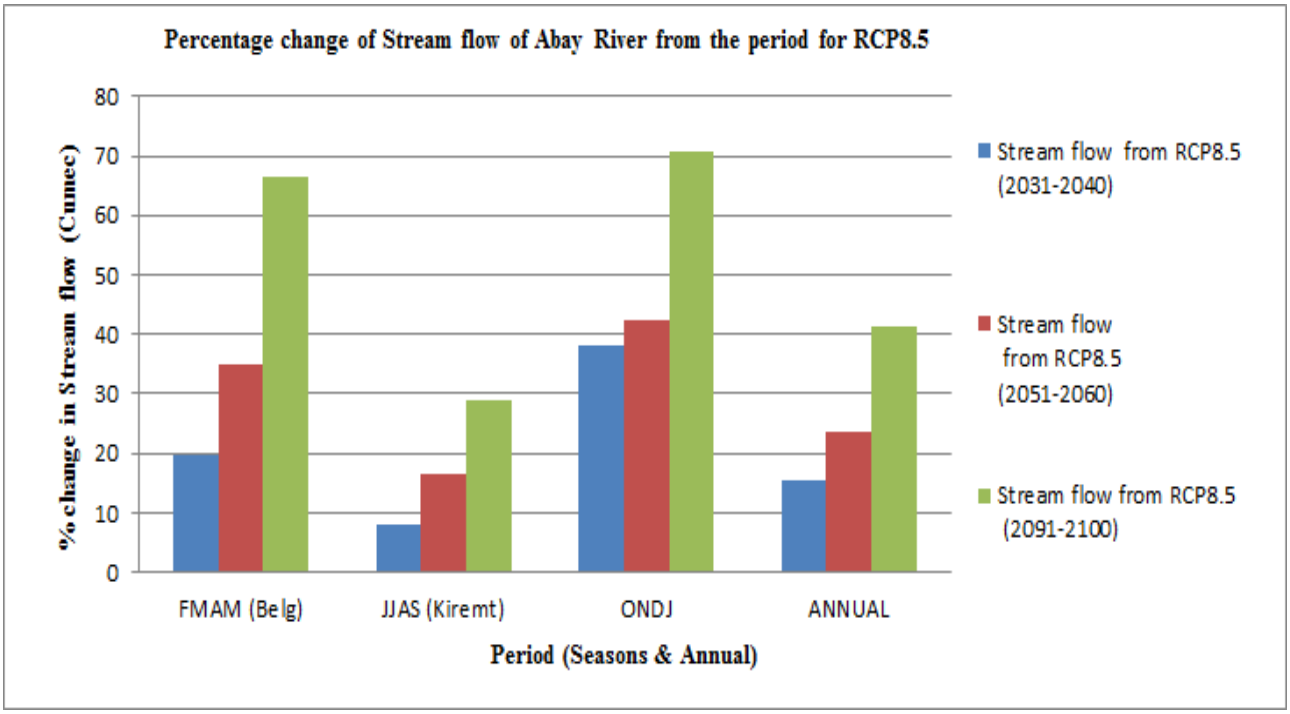

Figure 4-34: Percentage change in seasonal and annual flow volume of Abay River from the base period for RCP8.5

4.3.2 Summary of Results for Impact of Climate Change on Stream flow for all RCPs

Generally from the analysis result, all the climate scenarios (RCP2.6, RCP4.5 and RCP8.5) under three future time period: 2030s, 2050s and 2090s showed an increasing trend in mean annual flow The monthly stream flow change also shows an increasing trend in all the months under all RCP scenarios with the exception of a decreasing trend in the month of June for RCP2.6 during 2030s with a value of (-0.2%) and monthly reduction in stream flow is also expected in the month of May for RCP4.5 during 2030s and 2050s with a value of (-6.5%) and (-2.5%) respectively. Figure 4.35 below shows the percentage of change of annual and monthly stream flow for all climate scenarios and the three future time period.

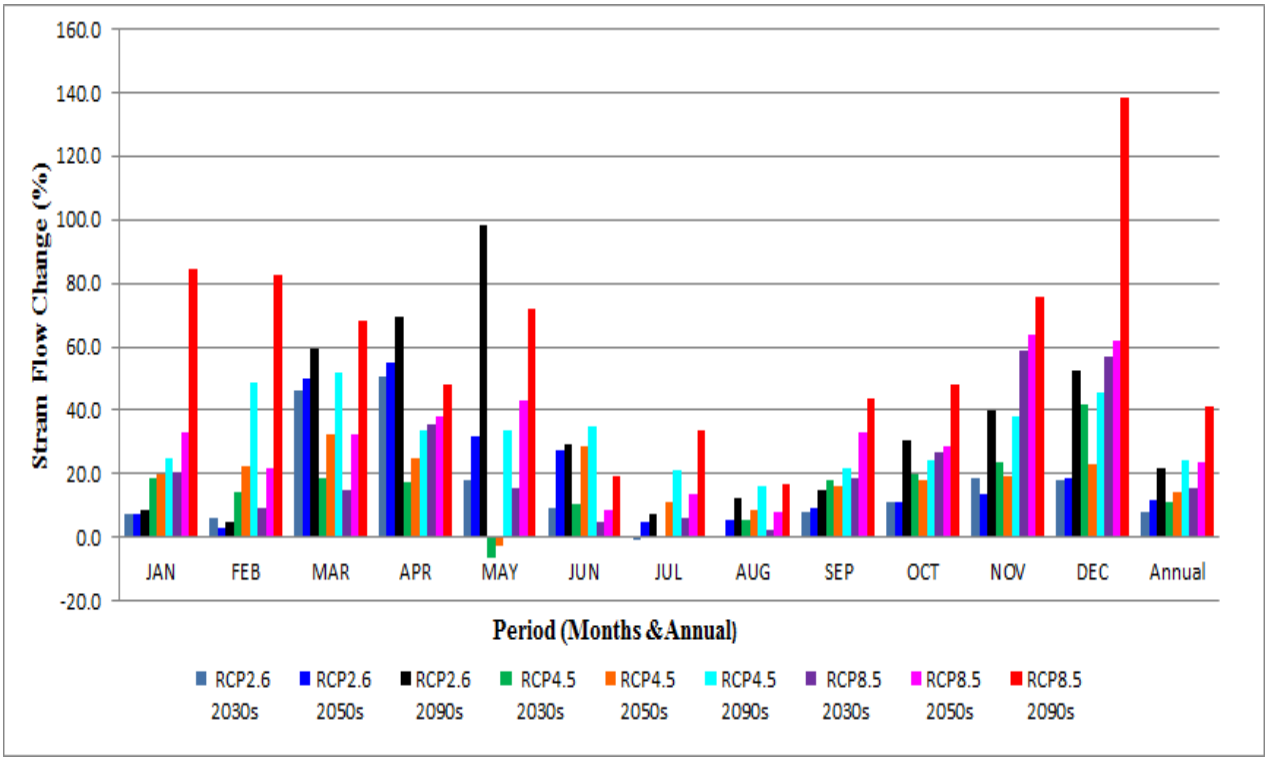

Figure 4-35: Mean monthly and annual stream flow changes under all RCP and Projected period

4.3.3 Extreme flow analysis Result for All RCPs

4.3.3.1 Annual Daily maximum Stream flow analysis

The annual maximum flow series (peak flow pattern) shows an increasing trend when compared to the annual peak stream flow occurred during the base period.

The annual peak flow pattern for early future time (2030s) shows an increasing trend for all RCP scenarios except for RCP2.6 in 2036 which shows a decreasing trend with (-1.4%) from the Base Period of the same duration. Maximum increase is expected in 2035 for RCP2.6 with (+21.9%), (+21.5%) for RCP 4.5 and (+16.4%) in 2032s for RCP8.5 increment when compared with the base period. The annual peak flow pattern for mid future period 2050s shows an increasing trend for all RCP scenarios with maximum increase with (+24.9%) in 2052 for RCP8.5.For the far future period (2090s) the increase in the annual peak flow is more than the increase than the two preceding two future (2030s and 2060s) and maximum increase is observed in 2092 with a value of (+30.8%) from the base period.

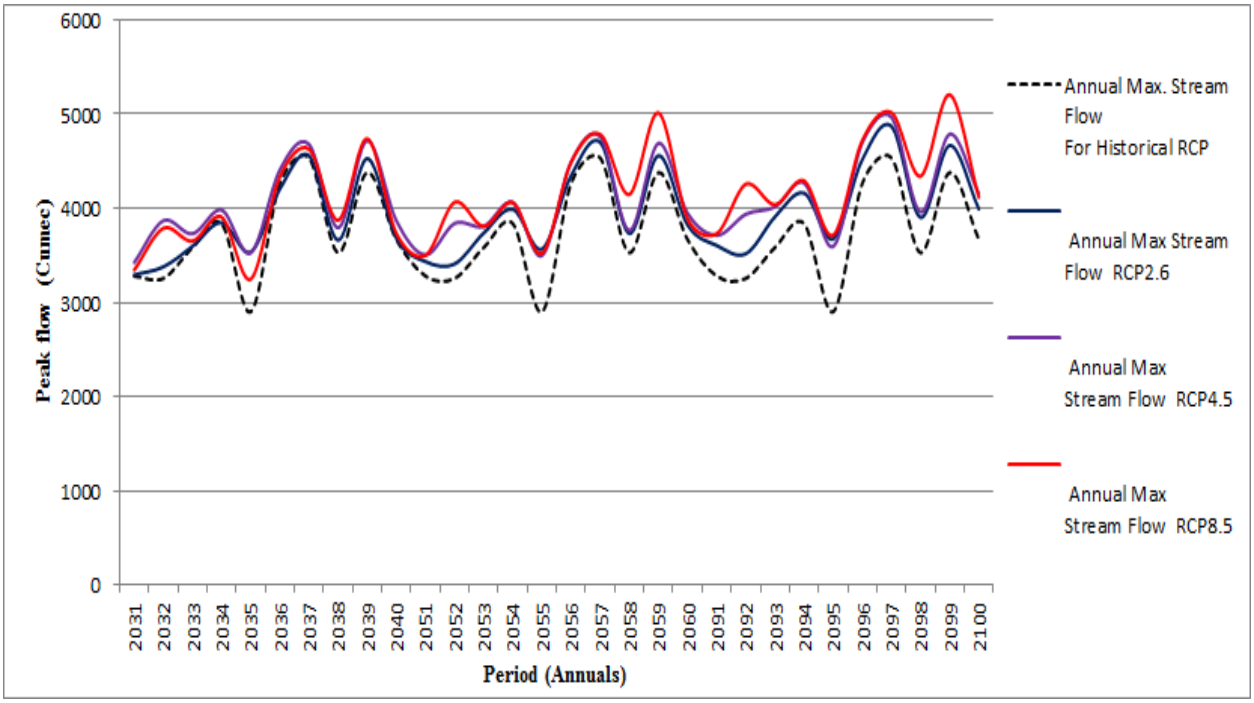

Figure 4-36: Annual Daily maximum flow for all RCPs

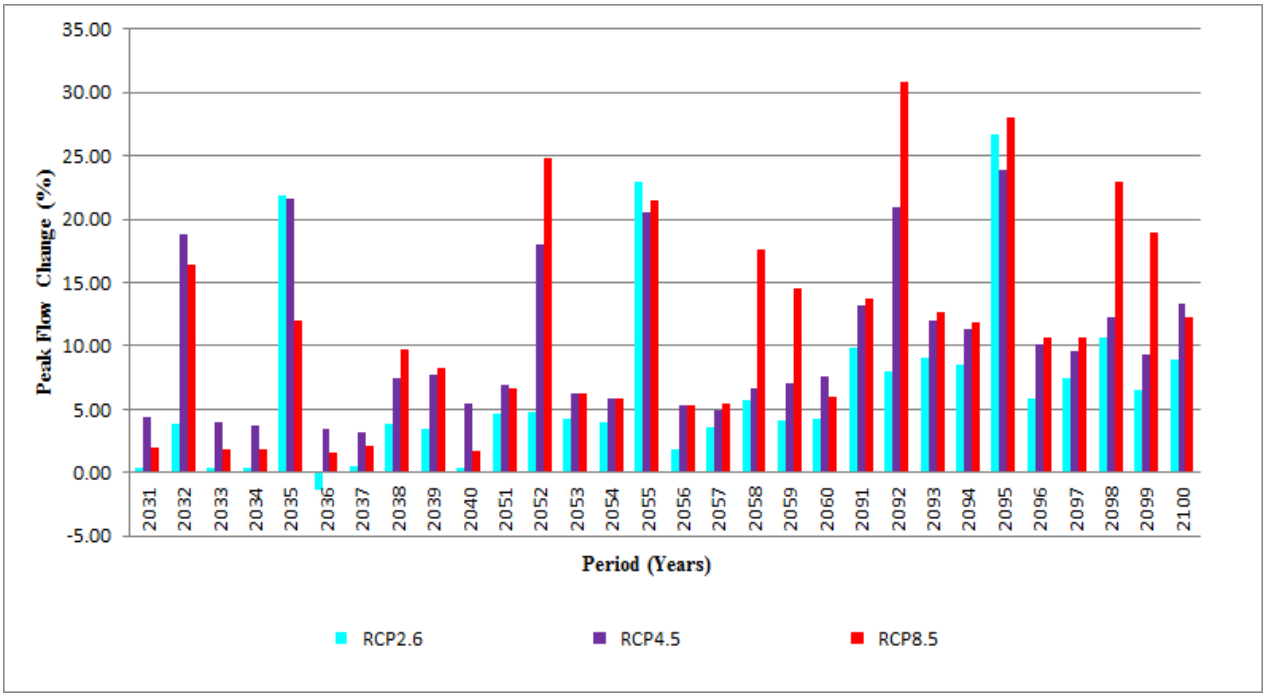

Figure 4-37: Percentage change of annual daily maximum flow from the base period for all RCPs

4.3.3.2 Annual Daily Low Stream flow analysis

The annual low flow pattern shows both increasing and decreasing trend from the period. For RCP2.6 Maximum increment in low flow is expected in 2092 with (+145.7%) and maximum decrease with (-54.04%) in 2056 for. RCP4.5 Maximum increment in low flow is expected in 2093 with (+155.5%) and maximum decrease with (-36.4%) in 2034 for. RCP8.5 Maximum increment in low flow is expected in 2094 with (+281.2%) and maximum decrease with (-33.5%) in 2037

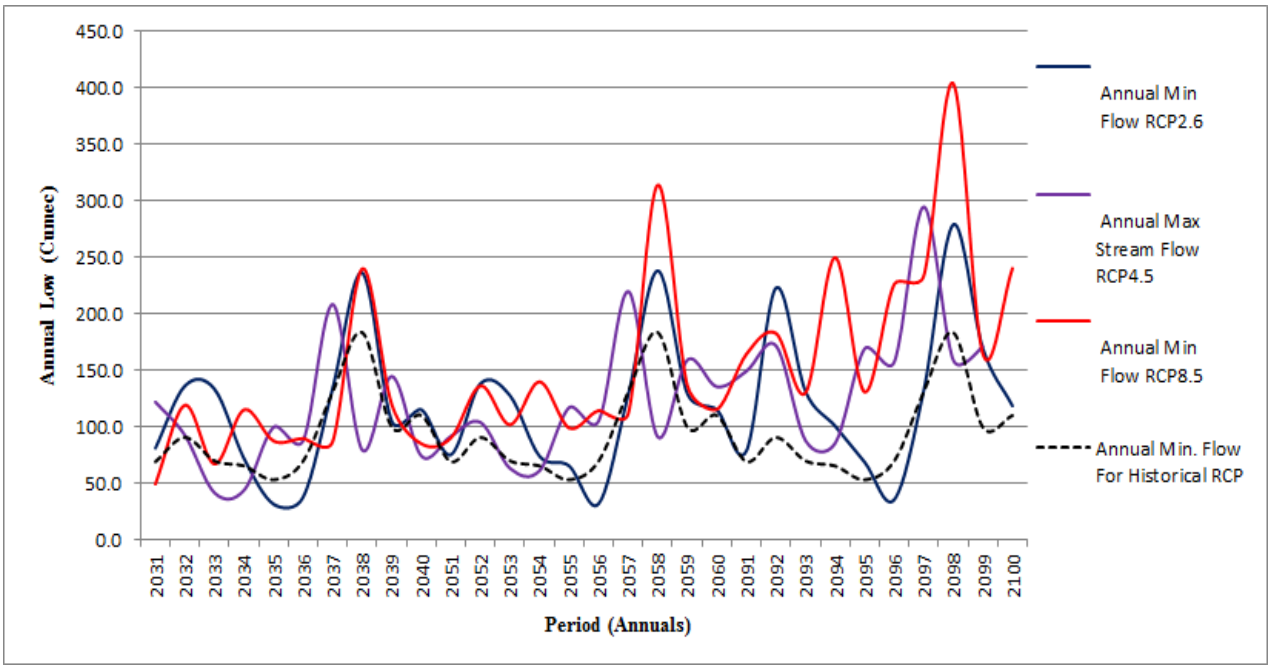

Figure 4-38: Annual Daily minimum flow for All RCP

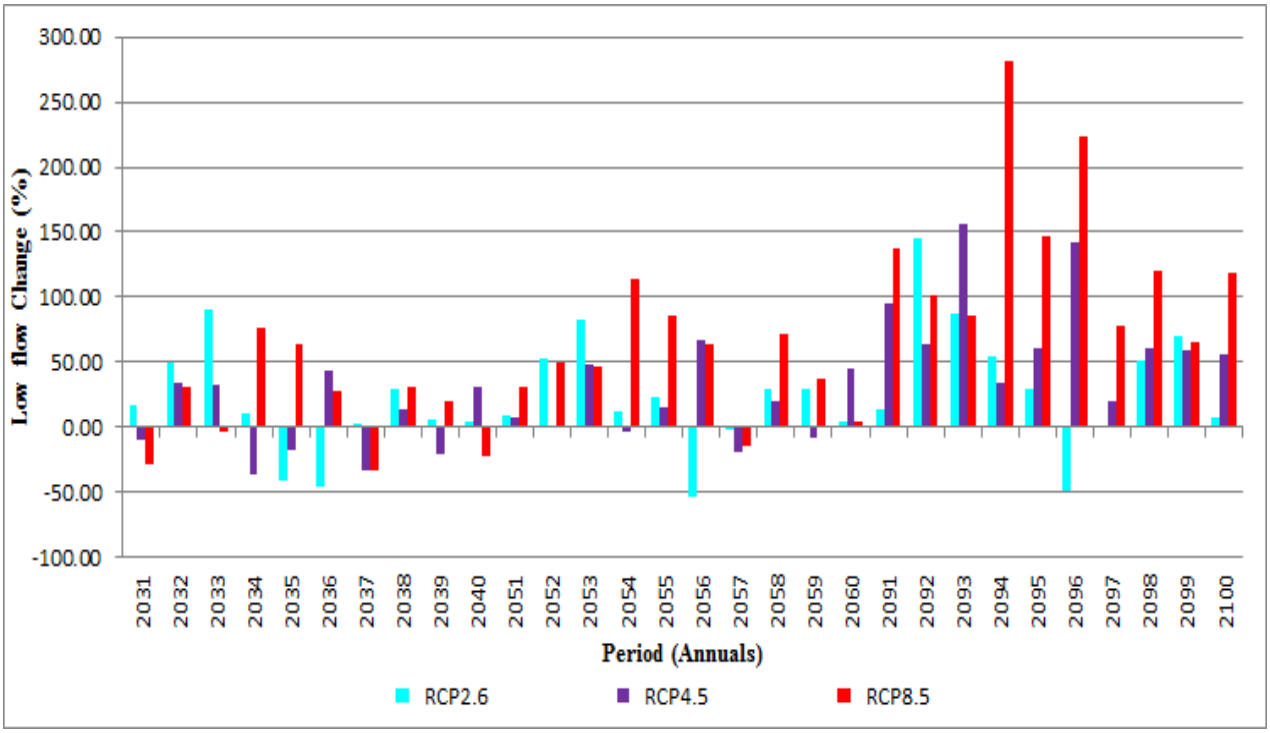

Figure 4-39: Percentage change of annual daily minimum flow from the base period for all RCPs

4.4 SENSITIVITY OF FUTURE STREAM FLOW TO CLIMATE CHANGE

The sensitivity of stream flow can be interpreted as negatively or positively change rate of water resource (water availability) to a change of climate Variables *(Byung Sik Kim.et., al., 2012).* The change in the future simulated stream flow was compared against the change in future Rainfall and Potential Evapotranspiration in order examine for which climate variables (PCP or PET) is more significant for the change in the future simulated flow. Accordingly the following section discuss the result of annual and Seasonal change in simulated flow for change in PCP and PET for each future time series under each RCP scenario compared against the base period .The result revealed that the future simulated flow is significantly more sensitive to a change in Rainfall than to Potential Evapotranspiration under all RCP scenarios.

Table 4-18: Summary of Annual Change of stream flow, Rainfall and PET from the base period for RCP2.6

TIME	FLOW_2030S	PCP_2030s	PET_2030s
RCP2.6(2031-2040)	7.8	12.7	3.78
TIME	**FLOW_2060S**	**PCP_2060s**	**PET_2060s**
RCP2.6 (2051-2060)	11.7	19.6	3.91
TIME	**FLOW_2090S**	**PCP_2090s**	**PET_2090s**
RCP2.6(2091-2100)	22.0	27.7	3.58

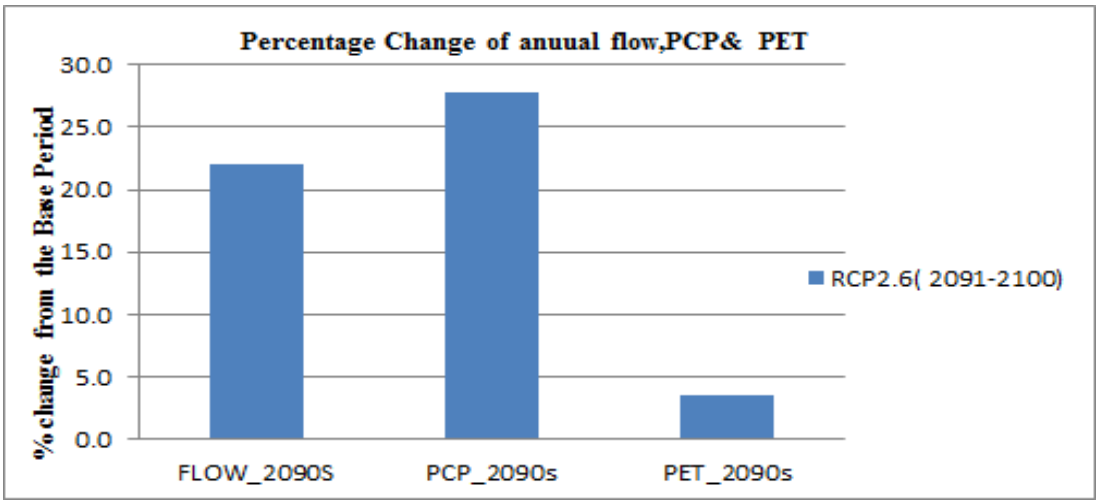

Figure 4-40: Percentage change of Annual Flow, PCP and PET with Respect to the base period for RCP2.6 (2091-2100)

Table 4-19: Summary of Annual Change of stream flow, Rainfall and PET from base period for RCP8.5

TIME	FLOW_2030S	PCP_2030s	PET_2030s
RCP8.5 (2031-2040)	15.3	24.3	4.25
TIME	**FLOW_2060S**	**PCP_2060s**	**PET_2060s**
RCP8.5 (2051-2060)	23.6	31.38	8.53
TIME	**FLOW_2090S**	**PCP_2090s**	**PET_2090s**
RCP8.5 (2091-2100)	41.2	49.1	18.18

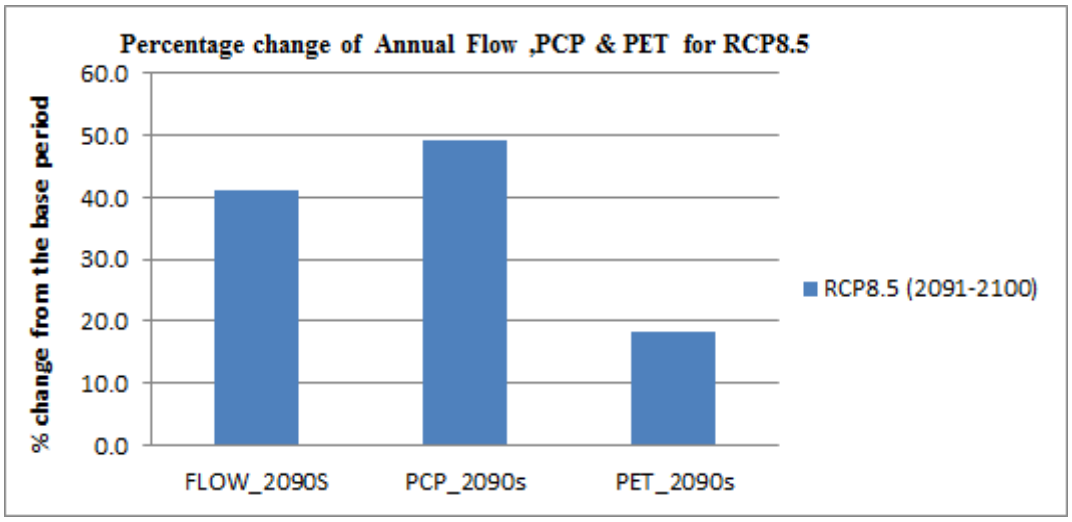

Figure 4-41: Percentage change of Annual Flow, PCP and PET with Respect to the base period for RCP8.5 (2091-2100)

From the result it can be seen that the catchment, seems likely to be seriously dominated by the impact of the Rainfall changes than potential Evapotranspiration. The rest of the result is found in the Annex: 6

\

4.5 SIGNIFICANCE AND UNCERTAINTIES OF CLIMATE CHANGE IMPACT ON FUTURE FLOW

This study on the impact of climate change on water availability of the selected Abay catchment (Upper Abay basin) involved a series of models and model outputs, which are based on simplified assumptions. Hence, it is unquestionable that the uncertainties presented in each of the models and model outputs kept on cumulating while progressing towards the final output.

The types of uncertainties existed throughout the whole process can be associated with the data quality of observed data, RCM models used to generate CORDEX-RCP Data, the Bias Correction adopted, the hydrologic modeling applied and the parameter selected for sensitivity analysis can be one source of uncertainty in the process of simulation.

The assumptions involved in the hydrologic model simulations are also a portion of the uncertainty. As described in the previous section, the determination of the impacted flow was only based on the precipitation and temperature changes in the future. The other climatic variables as wind speed, solar radiation, and relative humidity were assumed to be constant throughout the future simulation periods. Even though it is definite that in the future land use changes will also take place, this is also assumed to be constant. Hence, these assumptions can definitely lead to a certain level of additional uncertainty. As a result, it is clear that all types of uncertainties mentioned above are propagated on the future predicted flow volume and influence the model predictive capability for the future period.

Thus, considering the assumptions and methods used in this study, the result shows that the future flow volume of Abay River is affected by the climate change impact.

Accordingly, for RCP2.6 as it is showed in figure 4.33 below, the future flow for Abay River is significantly affected by climate change in all the months except for the month June, July and August which shows insignificant as the future predicted flows are within the uncertainty bands.

It is also shown in figure 4.34 below; the future predicted flow is significantly affected by climate change for Belg and Bega seasons and annually especially during 2060s and 2090s. For Krimet (JJAS) season the climate change may be insignificant as the impacted future flow is within the uncertainty band.

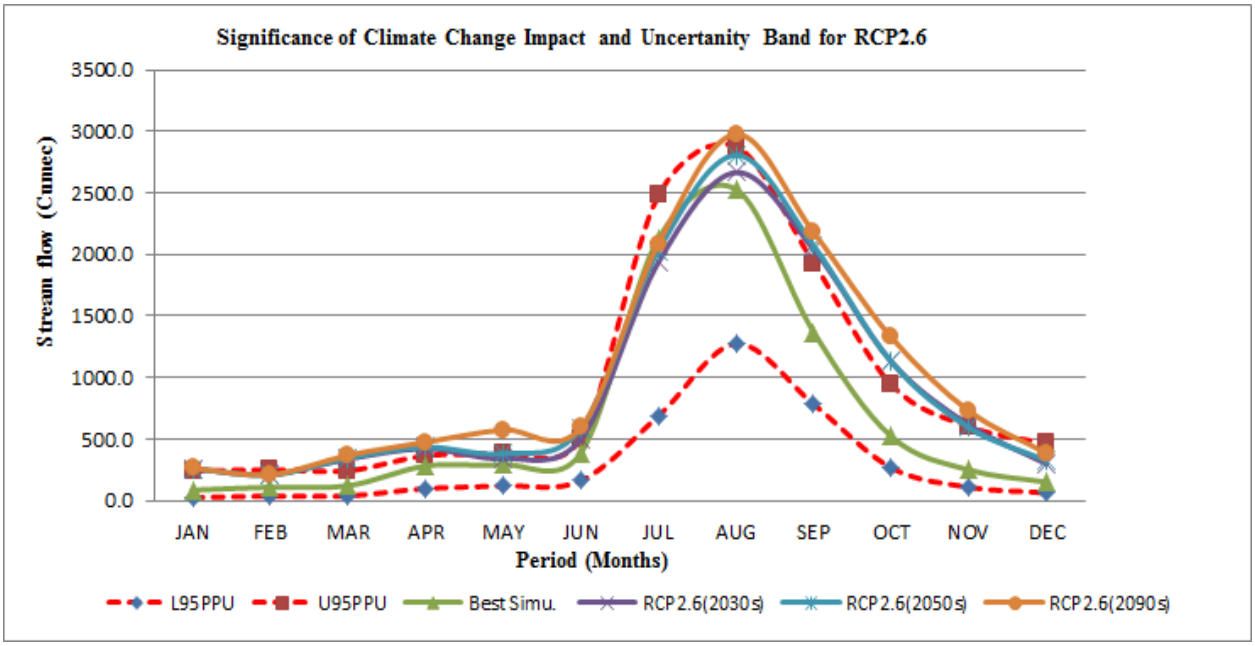

Figure 4-42: Average monthly future flow and uncertainty Band for RCP 2.6 Scenario

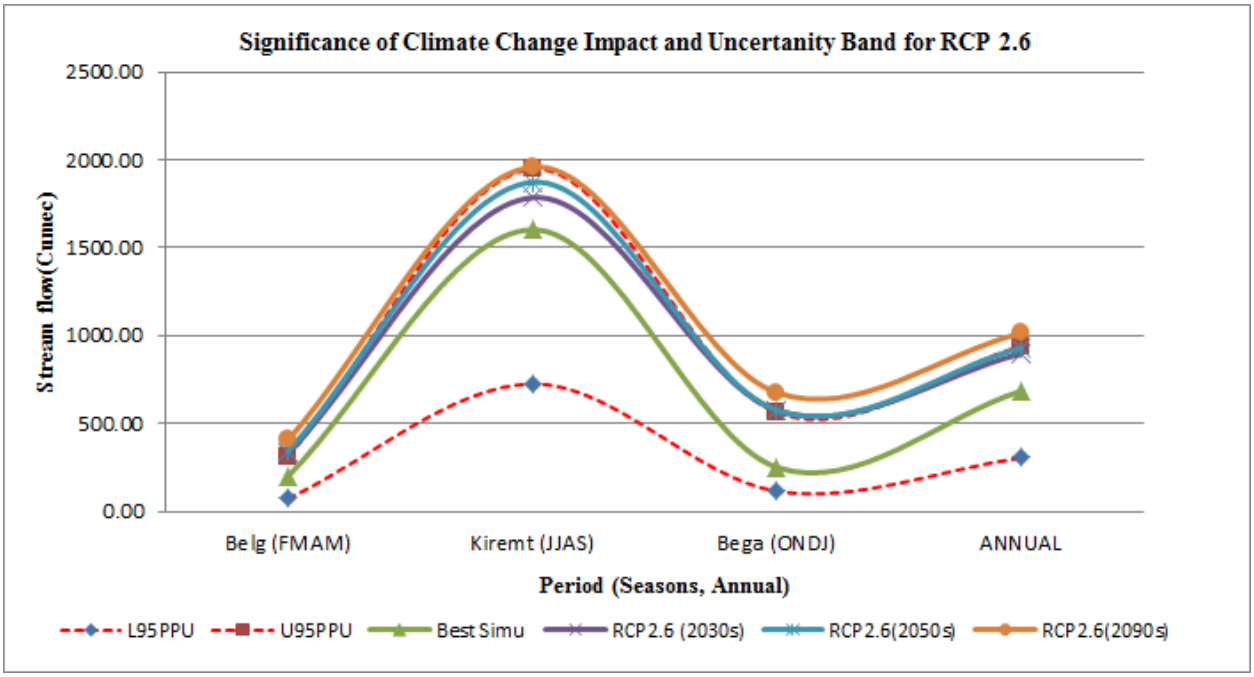

Figure 4-43: Average seasonal and annual future flow and uncertainty Band for RCP2.6 Scenario

For RCP4.5 considering the assumptions and methods used in this study, the result shows that the future flow volume of Abay River will be significantly affected by the climate change impacts in most of the months as the impacted future flow is out of the uncertainty band in all future time series. The impacted flow is insignificant for 2030s, 2060s and 2090s for the month of July and December, for the month August the impacted flow is insignificant for 2030s and 2060s and significant over 2090s.

In general the future flow of Abay River for RCP4.5 climate scenario is affected by climate change in all future time period for Bega season and annually. For Belg and kirmet season the impacted future flow is significantly affected by climate change during 2090s and insignificant over the period of 2030s and 2060s.

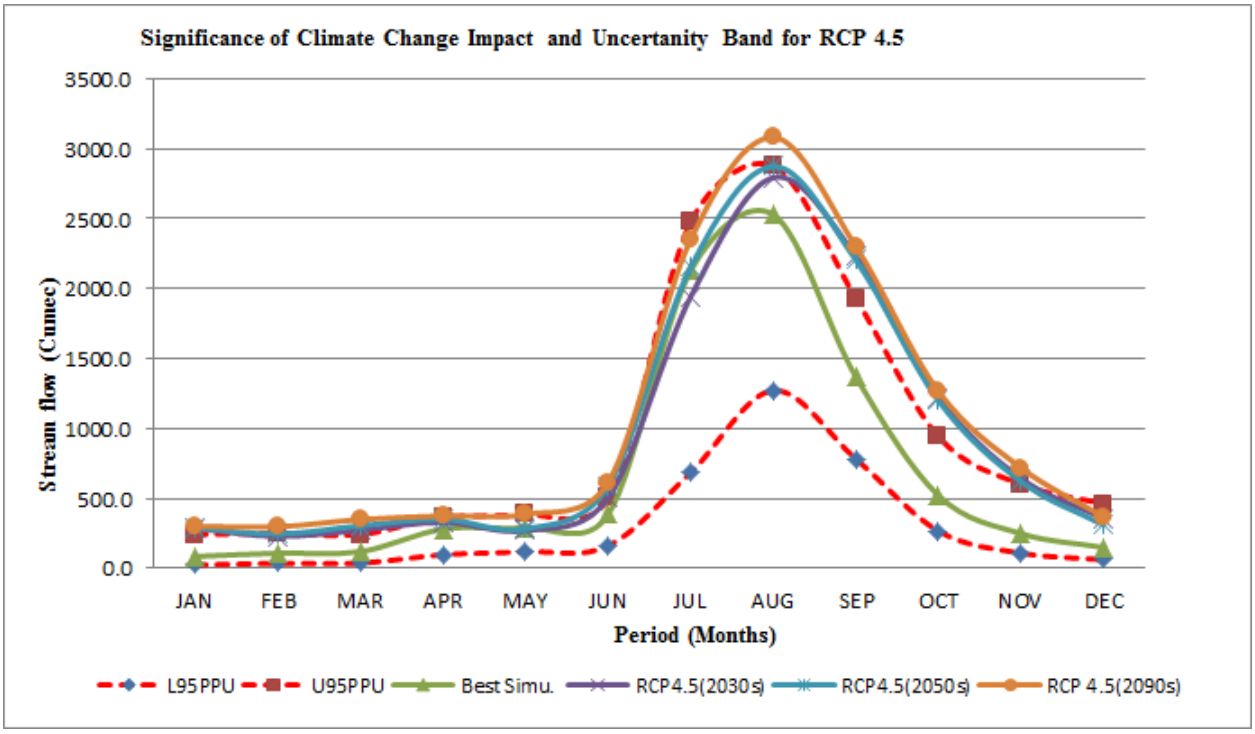

Figure 4-44: Average monthly future flow and uncertainty Band for RCP4.5 Scenario

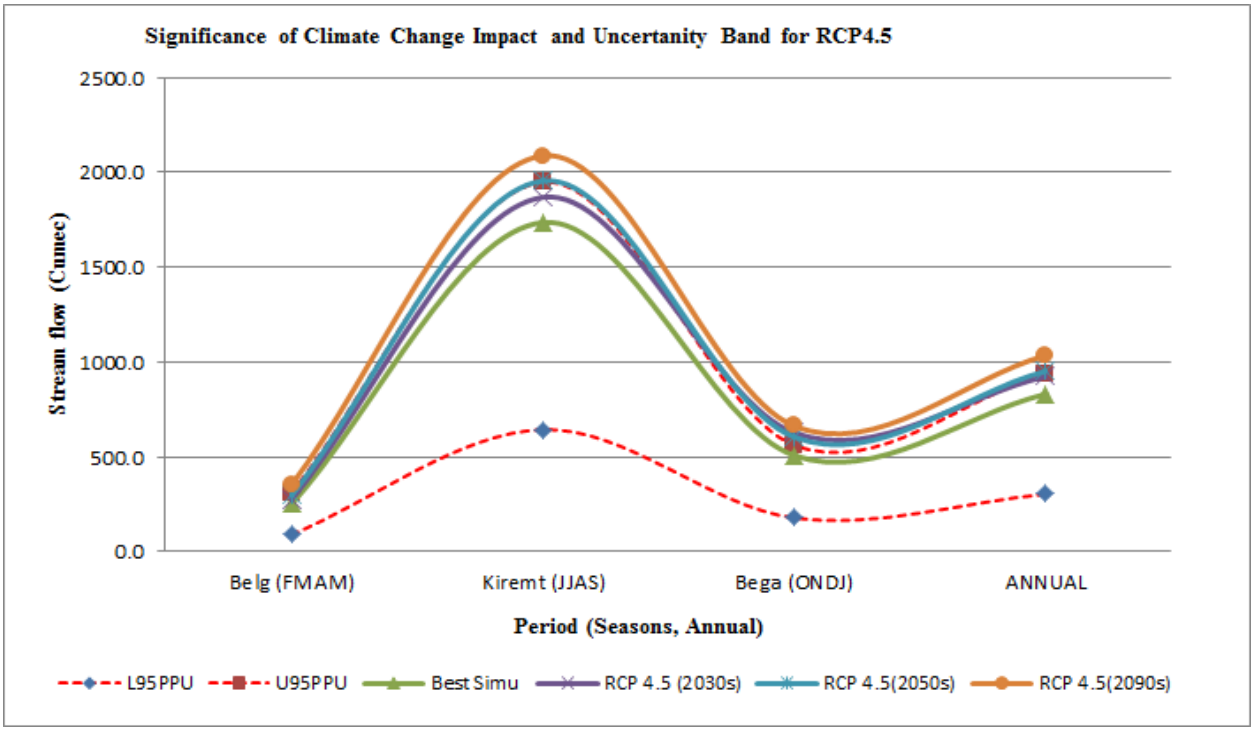

Figure 4-45: Average seasonal and annual future flow and uncertainty Band for RCP4.5 Scenario

Considering the assumptions and methods used in this study, for RCP8.5 scenario the climate change significantly affect the future flow during all the months of 2090s .But for 2030s and 2060s the future impacted flow is insignificant during the month of June, July, August and December and significant over the rust of the months.

The impacted flow is significantly affected by the climate change for all the seasons during 2090s. For 2030s and 2060s, seasons of Kiremt, Bega and Annual flow shows significantly affected by climate change but climate change has insignificant effect on Belg season during 2030s and 2060s.

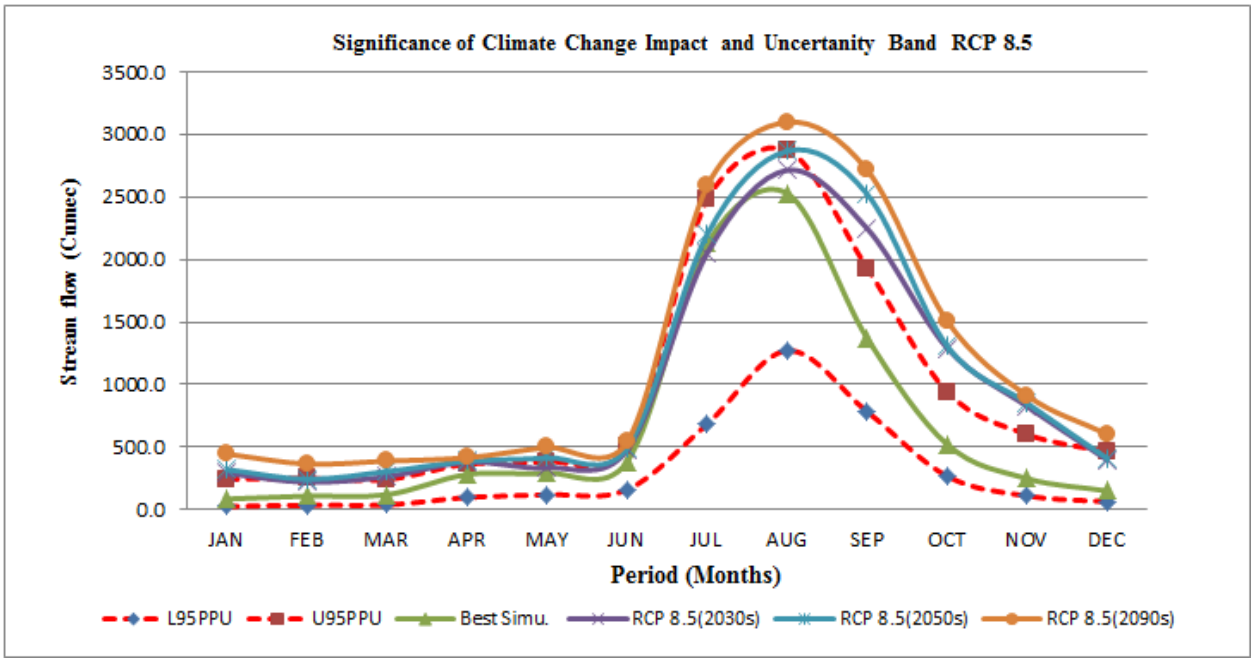

Figure 4-46: Average monthly future flow and uncertainty band for RCP 8.5 Scenario

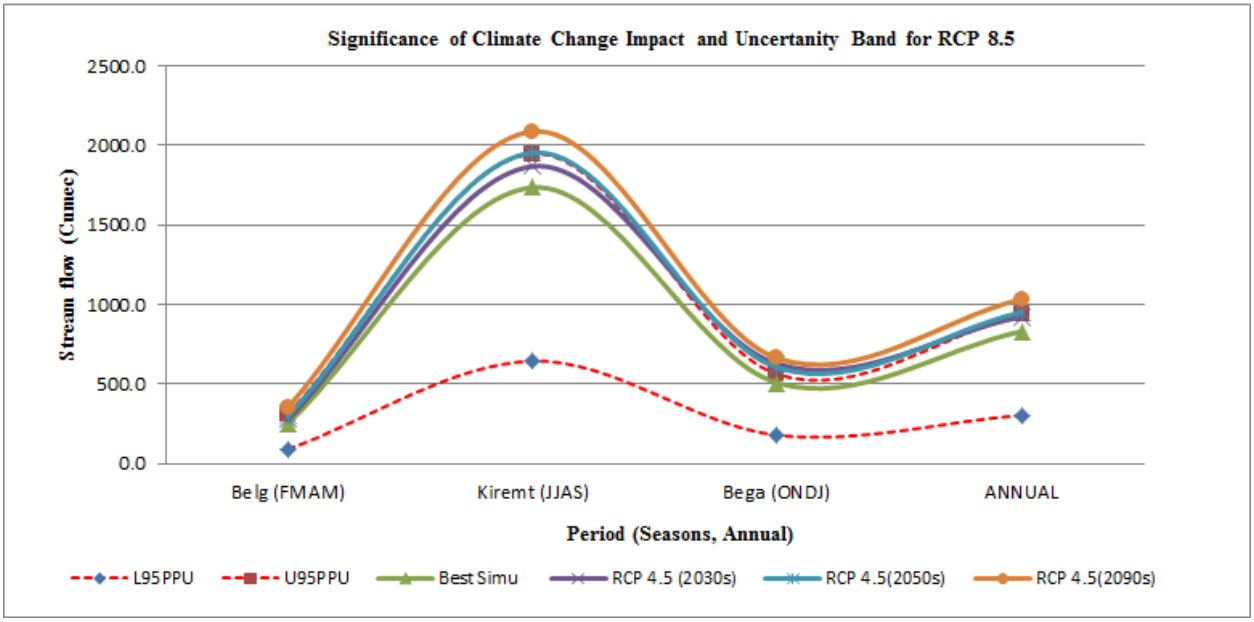

Figure 4-47: Average seasonal and annual future flow and uncertainty Band for RCP8.5 Scenario

4.6 COMPARISON OF THIS THESIS RESULT WITH THE PREVIOUS RESEARCHES

Many research works have been done on climate change in Abay basin using different climate scenarios approach; most of the studies previously conducted were based on an old emission scenario called 'SRES'. Studies are being conducted in the area using the newly released RCP climate data on .In the following session the results of previous studies were compared with the result of this thesis:

1. *Laifang Li et, al., 2015* conducted a research on Ethiopian Kiremt (JJAS) season precipitation based on CMIP5: The study pointed out that Kiremt-season (June–September) precipitation is projected to increase in central and northern regions but a decrease in precipitation over the southern part of the country.
2. A research made by *(Sintayehu Gebre, & Fulco Ludwig, 2015*).In order to understand the future impacts of climate change on four catchments (Gilgel Abay, Gumer, Ribb, and Megech) of the upper Blue Nile River basin using 50 Km by50 Km resolution GCMs output of RCP4.5 and RCP8.5 emission scenarios were used using Hydrologic (HEC-HMS) model for two future horizon of 2030`s (2035-2064) and 2070`s (2071-2100) and finds out that Runoff is expected to increase in the future. At 2030`s average annual runoff projection change may increase up to +55.7% for RCP4.5 and up to +74.8% for RCP8.5 scenarios. At 2070`s average annual runoff percentage change increase by +73.5% and by +127.4% for RCP4.5 and RCP8.5 emission scenarios, respectively.

As it is described in the result and discussion chapter the result of this thesis was found between the above mentioned pervious results, for RCP8.5 24% increase for (2051-2060) is obtained whereas According to sentayhu and Gebere,2015 for RCP 74.8% increase for (2035-2064) increase is obtained Even though, increasing future flow results were obtained, still there is great variation of results which may be due to selection of climate models for RCP data, the variation in the hydrological model, types of input data used ,method of bias correction adopted and the size of the catchment can be the main factor and requires further research findings throughout the the basin.

CHAPTER FIVE

5. CONCLUSION AND RECOMNDATION

5.1 CONCLUSION

Climate change has potential impacts on future hydrological and meteorological variables due to increased greenhouse emissions. In present study , the future impact of climate change on hydro-meteorological characteristics of the middle Abbay basin has been studied like: precipitation and Potential Evapotranspiration for 2030s (2031-2040),2050s (2051-2060) and 2090s (2091-2100) using data derived from an ensemble of downscaled climate data based on the coordinated regional climate downscaling experiment over African domain (CORDEX-Africa) with coupled Model Intercomparison project Phase5(CMIP5) simulations under representative concentration pathways viz. RCP2.6, RCP4.5 and RCP8.5 climate scenarios.

The SWAT2012 hydrological model was used to simulate stream flow in the basin to study impacts of climate change on future runoff. The model was calibrated and validated for the periods of 2001–2006 and 2007–2010 respectively, at 'Kesse' River gauging station located in the Abbay River. Three model performance indicators (Coefficient of determination; R^2, Nash and Sutcliff Efficiency;E_{NS} and percentage deviation; PBIAS) and graphical representations of differences between observed and simulated data were used to check the performance of the model.

The performance evaluation of the model confirmed that the statistical measure parameters for monthly simulation were very good with a values of R^2= 0.91, E_{NS} = 0.9 and PBIAS =10.3 for calibration period the corresponding value for validation period shows R^2= 0.76, E_{NS} = 0.75 and PBIAS =10.8. For daily simulation the values of those parameter resulted R^2= 0.83, E_{NS} = 0.81 and PBIAS =14.3% calibration period and R^2= 0.72, E_{NS} = 0.71 and PBIAS =16.8%

Bias-corrected CORDEX RCPs data for temperature and precipitation under RCP2.6, RCP4.5 and RCP8.5 were fed into SWAT model to simulate the stream flow for the future.

In this study, the simulated stream flow data was divided into three future periods (2030s, 2050s, and 2090s) and was compared with the baseline period (2001–2010). Different indicators: changes in mean annual, Seasonal, monthly and change in annual maximum and minimum flow were used to investigate the change in river flow under each RCP scenarios.

The main conclusions of the study are the following:-

1. The projected future precipitation and Potential Evapotranspiration increases for all future time under all RCPs (RCP2.6 RCP4.5 and RCP8.5) climate scenario. The rise in precipitation is expected to be more than the rise in Potential Evapotranspiration.

I. Annual Precipitation and Potential Evaporation Change

In the future, mean annual Precipitation and Potential Evapotranspiration will increase over the basin for all RCP scenarios. for RCP2.6 average annual precipitation may increases by (+9.4%), (+14.6%) and by (+20.7%) and the annual average Potential evapotranspiration may increase by (+3.8%), (+3.9%) and (+3.6%) for 2030`s, 2050`s and 2090`s future time respectively. For the 2nd emission scenario, RCP4.5 the mean annual precipitation may increase by (+9.9%), (+15.6%) and (+25.1%), and the mean annual Potential evapotranspiration may increase by (+4.8%), (+6.02%) and (+6.56%) for 2030`s, 2050`s and 2090`s respectively when compared to the base period. For the 3rd emission scenario, RCP 8.5 the mean annual precipitation may increase by (+18.1%), (+23.4%) and (+36.6%) and the mean annual Potential evapotranspiration may increase by (+4.3%), (+8.5%) and (+18.2%) for 2030`s, 2050`s and 2090`s, respectively.

II. Seasonal Precipitation and Potential Evaporation Change

The seasonal change for precipitation and Potential evaporation shows an increasing trend when compared to the base period values. For RCP2.6 the future precipitation shows an increasing trend with (+11.9%), (22.2%) and (36.9%) for precipitation and (+3.98%), (+5.39%) and (+3.98%) for PET during Belg(FMAM) season for 2030s, 2060s and 2090s respectively. And (+6.2%), (+9.9%) and (+13.6%) for precipitation and (+4.29%), (+3.27%) and (+3.43%) for PET during Kiremt(JJAS) season for 2030s, 2060s and 2090s respectively. And (+28.6%), (+36.3%) and (+46.9%) for precipitation and (+3.05%), (+2.84%) and (+3.26%) during Bega(ONDJ) season for the corresponding 2030s, 2060s and 2090s future time respectively.

For RCP4.5 the future seasonal precipitation and Potential evaporation shows an increasing trend compared to the base period with (+18.8%), (+28.6%) and (34.0%) for precipitation and (+4.56%), (+5.95%) and (+6.24%) for PET during Belg(FMAM) season in 2030s, 2060s and 2090s respectively. And (+8.1%), (+11.8%) and (+20.3%) for precipitation and +5.9%, +6.9% and +6.8% for PET during Kiremt (JJAS) season for 2030s, 2060s and 2090s respectively. And (+9.8%), (+24.2%) and (+45.7%) for precipitation and (+3.9%), (+5.3%) and (+6.7%) during Bega(ONDJ) season in the corresponding 2030s, 2060s and 2090s future time respectively.

For RCP8.5 the future seasonal precipitation and Potential evaporation shows an increasing compared to the base period with (+19.3%), (28.3%) and (42.6%) for precipitation and (+4.16%), (+8.6%) and (+18.4%) for PET during Belg(FMAM) season in 2030s, 2060s and 2090s respectively. And (+18.9%) + (21.7%) and (+34.7%) for precipitation and (+5.04%), (+9.0%) and (+19.1%) for PET during Kiremt (JJAS) season in 2030s, 2060s and 2090s respectively. And (+11%), (+28.6%) and (+42.0%) for precipitation and (+3.6%), (+7.9%) and (+17%) during Bega (ONDJ) season in 2030s, 2060s and 2090s future time respectively.

III. Monthly Precipitation and Potential Evaporation Change

For RCP2.6 The monthly average rainfall in the future time series of 2030s, 2050s and 2090s also shows in an increment relative to the base period with maximum increase in the month of December with (+95.89%) in 2090s and minimum change in June with (+3.8%) in 2030s.

Under RCP4.5 shows an increment during 2030s, 2050s and 2090s future time. Maximum increase rainfall is observed in the month of March with (+145.52%) in 2090s and minimum change is observed in July with (+0.31%) in 2030s. For RCP8.5 The monthly average rainfall in the future time series shows an increasing trend in all the month with maximum of increment in rainfall during the month of March with (+243.1%) in 2090s

2. According to the study, the results obtained for the change in future stream flow under different RCP climate scenarios show an increment compared to the base period stream flow

I. Annual Mean Stream flow Change

The result for projected mean annual stream flow shows an increasing trend under all RCP scenarios. For RCP2.6 the projected change shows (+7.8%), (+11.7%) and (+22.0%) for 2030s, 2050s and 2090s respectively. For RCP4.5 the results shows (+11.1%), (+14.5%) and (+24.5%) for 2030s, 2050s and 2090s respectively. For RCP8.5 the increase in runoff shows (+15.28%), (+23.64%) and (+41.24%) for 2030s, 2050s and 2090s respectively.

II. Seasonal Mean Stream flow Change

The result of the analysis for Seasonal flow shows an increase in water yield is likely for all seasons in the study area. For RCP2.6 the projected seasonal flow shows (+31.1%), (+36.7%) and (+62.6%) for Belg (FMAM) Season, for Kirmet (JJAS) season the results shows (+2.9%), (+7.8%) and (+12.9%) for Bega (ONDJ) season the increase in runoff shows (+13.3%), (+12.2%) and (+33.1%) for 2030s, 2050s and 2090s respectively.

The result of Seasonal flow for RCP4.5 shows (+10.1%), (+18.3%) and (+40.9%) for Belg (FMAM) Season, for Kirmet (JJAS) season the results shows (+7.7%), (+12.6%) and (+20.3%) and for Bega (ONDJ) season the increase in runoff shows (+23.5%), (+19.1%) and (+30.7) for 2030s, 2050s and 2090s respectively.

The result of Seasonal flow for RCP8.5 shows (+19.7%), (+34.9%) and (+66.6%) for Belg (FMAM) Season, for Kirmet (JJAS) season the results shows (+7.7%), (+12.6%) and (+20.3%) and for Bega (ONDJ) season the increase in runoff shows (+23.5%), (+19.1%) and (+30.7) for 2030s, 2050s and 2090s respectively.

III. Monthly Mean Stream flow Change

The result for projected mean monthly stream flow shows an increase in all the months in the future time period with (+16.1%), (+19.9%) and (+35.7%) for RCP2.6. for RCP4.5 the mean monthly stream flow shows (+15.2%) ,(+18.5%) and (+33%) and for RCP8.5 the corresponding mean monthly stream flow increase in the order of (+22.5%), (+32.5%) and (+60.9%) for 2030s, 2060s and 2090s.

IV. Monthly Maximum and Minimum Stream flow Change

For RCP2.6 maximum increment is expected in the month of May with (+98.5%) for 2090s and minimum increment in the month of August with (+0.5%) and a maximum decrease is expected in the month of July with (-0.2%) for 2030s. For RCP4.5 maximum monthly flow increase is expected in the month of March with (+52%) for 2090s and minimum increment in the month of august with (+5.3%) and maximum and minimum decrease is expected in the month May with (-6.5%) and (-2.5%) for 2050s and 2030s respectively. For RCP8.5 all month resulted in increment of flow for all period in the future with maximum increment in the month of December with (+138.6%) for 2090s and minimum increment in the month of August with (+16.9%) for 2030s.

V. Annual Extreme flow Change

The future annual maximum flow (peak flow) pattern shows an increasing trend in the future, for 2030s maximum increase in peak flow is expected in the year of 2035 with a value of (+21.94%) for RCP2.6, (+21.59%) for RCP4.5 and (+11.94%) for RCP8.5. But a deceasing trend is expected in the year 2036 with (-1.4%).The result of peak flow pattern for 2050s shows (+23%) for RCP2.6, (+20.6%) for RCP4.5 and (+21.4%) for RCP8.5. In 2090s the peak flow trend shows

(+26.7%) for RCP2.6, (+24%) for RCP4.5 and (28.1%) for RCP8.5 when compared to the peak flow during the base period.

The future annual minimum flow (Low flow) pattern shows both increasing and decreasing trend when compared with the low flow magnitude of the base period .For 2030s maximum increase in low flow is expected in the year of 2038 with a value of (+28.9%) for RCP2.6, (+43%) for RCP4.5 in the year of 2036 and (+75.8%) for RCP8.5 in the year of 2034. But a maximum deceasing trend is expected with (-45.8%) for RCP2.6 in 2036, (-32.5%) for RCP4.5 in 2037 and (-33.5%) for RCP8.5 in 2037. The result of maximum increase in minimum flow pattern for 2050s shows (+82.8%) for RCP2.6 in 2053, (+67.8%) for RCP4.5 in 2056 and (+86.1%) for RCP8.5 in 2055. In 2090s maximum increase in low flow with (+145.7%) for RCP2.6 in 2092, (+145.8%) for RCP4.5 in 2093 and (+281.2%) for RCP8.5 in 2094 is expected. But maximum decrease in low flow is expected only in 2096 with (-48.9%) for RCP2.6.

3. Finally the simulated stream flow was compared with the Precipitation projection under different RCP climate scenarios and it was found out that the increase in Precipitation will lead to an increase in stream flow. Therefore, this research concluded that a change in climate variables of precipitation and Potential Evapotranspiration would have an influence on the hydrology response in the selected Abay Basin (Upper Abbay basin).

5.2 RECOMMENDATION AND FURTHER RESEARCH NEEDS

- The increases in water availability will play significant benefits for small and large scale Irrigation activities in addition currently there are a lot of water resource projects being implemented in the main tributaries of Abay river .The increase in run off volume cloud possibly have a positive impact for the sustainability of existed and undergoing water development projects.
- The climate change may contribute in a positive direction for crop water availability for small scale farmers to harness water for their crop productivity, if and only if farmers are adopted them to cropping schedule. However, a precaution of mitigation and adaptation measures ought to be developed to control for possible flooding plains and low land areas of the basin.
- The result from the study has provided an insight on how hydrological response under changing climatic condition would impact water resource availability in the study area and therefore this information will be useful for development planners, decision makers and other participants when planning suitable water management polices to adapt the climate change impact.
- The future research should be directed towards the study on implication of climate change on the region which is directly linked with the livelihood of the local people living in the basin. This study will then be meaningful to society and so that they can either be well adapted to the forthcoming climatic condition or mitigate the adverse impacts of changing climate.
- Some of the result shows very high variation in peak and low flows which must raise alarm among water resource developers as these specific result must cause strategies to re-evaluate the design and operation of future and existing dams in the Abay river and to the major tributaries draining to Abay river.
- SWAT hydrological model has shown to be a robust tool in modeling impact of climate change with in the catchment area and therefore future researchers should utilize it more in research activities especially in water sector.

REFERENCE

1. Abbaspour KC (2012) User manual for SWAT-CUP 5.1.4. SWAT calibration and uncertainty analysis programs. Swiss Federal Institute of Aquatic Science and Technology, Eawag, Duebendorf
2. Awoke D. & Philip W. et al,: Modeling Agricultural Watersheds with the Soil and Water Assessment Tool (SWAT):Calibration and Validation with a Novel Procedure for Spatially Explicit HRUs, Environmental Management(2016) 57:894–911 DOI 10.1007/s00267-015-0636-4
3. Abdo, K. S., Fiseha, B. M., Rientjes, T. H. M., Gieske, A. S. M., and Haile, A. T.: Assessment of climate change impacts on the hydrology of Gilgel Abay catchment in Lake Tana basin, Ethiopia, Hydrological Processes,23,3661–3669, doi:10.1002/hyp.7363, 2009.
4. Aich, V., Liersch, S., Vetter, T., Huang, S., Tecklenburg, J., Hoffmann, P., Koch, H., Fournet, S., Krysanova, V., Müller, E. N., and Hattermann, F. F.: Comparing impacts of climate change on stream flow in four large African river basins, Hydrology and Earth System Sciences, 18, 1305–1321, doi:10.5194/hess-18-1305-2014, 2014.
5. BCEOM (1998) Abbay River Basin Integrated Development Master Plan Project, The Federal Democratic Republic of Ethiopia, Ministry of Water, Irrigation & Electricity.
6. Blue Nile Basin Atlas. (2009). Characterization and Atlas of the Blue Nile Basin and its Sub basins. Aster Denekew Yilma and Seleshi Bekele Awulachew. International Water Management Institute. January, 2009.
7. Booij, M.J.; Tollenaar, D.; van Beek, E.; Kwadijk, J.C.J. Simulating impacts of climate change on river discharges in the Nile basin. Phys. Chem. Earth 2011, 36, 696–709.
8. Deressa, T. T., Hassan, R. M., and Ringler, C.: Perception of and adaptation to climate change by farmers in the Nile basin of Ethiopia, The Journal of Agricultural Science, 149, 23–31, doi:10.1017/S0021859610000687, 2011.
9. Dile, Y. T., Berndtsson, R., and Setegn, S. G.: Hydrological Response to Climate Change for Gilgel Abay River, in the Lake Tana Basin Upper Blue Nile Basin of Ethiopia, PLOS ONE, 8, doi:10.1371/journal.pone.0079296, 2013.

10. Detlef P. van Vuuren & Jae Edmonds & Mikiko Kainuma & Keywan Riahi et al.: The representative concentration pathways: an overview, Climatic Change (2011) 109:5–31 DOI 10.1007/s10584-011-0148-z, 2011
11. Food and Agriculture Organization (FAO). Digital Soil Map of the World and Derived Soil Properties; Version 3.5; FAO: Rome, Italy, 1995.
12. Gebre SL, Ludwig F (2015) Hydrological Response to Climate Change of the Upper Blue Nile River Basin: Based on IPCC Fifth Assessment Report (AR5). J Climate Weather Forecasting 3: 121. doi:10.4172/23322594.1000121,2015
13. Höök, M.; Sivertsson, A.; Aleklett, K. Validity of the fossil fuel production outlooks in the IPCC emission scenarios. Nat. Resour. Res. 2010, 19, 63–81.
14. IPCC. Climate Change 2013: The Physical Science Basis; Contribution of Working Group I to the Fifth Assessment Report of the Intergovernmental Panel on Climate Change; Cambridge University Press: Cambridge, UK; New York, NY, USA, 2013;
15. IPCC (2014) Summary for Policymakers integrated view of climate change as the final part of the IPCC's Fifth Assessment Report (AR5).
16. IPCC (2014) Climate Change Synthesis Report
17. Luqman Atique, Irfan Mahmood and Farman Atique (2014) Disturbances in atmospheric radiative balance due to anthropogenic activities and its implication for climate change. American-Eurasian J Agric & Environ. Sci 14, 2014
18. Megersa, B., Markemann, A., Angassa, A., Ogutu, J. O., Piepho, H.-P., and Zarate, A. V.: Impacts of climate change and variability on cattle production in southern Ethiopia: Perceptions and empirical evidence, Agricultural System, 130, 23-34, dio: 10.5194/hess-16-391-2012
19. Meinshausen, M.; Smith, S.J.; Calvin, K.; Daniel, J.S.; Kainuma, M.L.T.; Lamarque, J.-F.; Matsumoto, K.; Montzka, S.A.; Raper, S.C.B.; Riahi, K.; et al. The RCP greenhouse gas concentrations and their extensions from 1765 to 2300. Clim. Chang. 2011, 109, 213.
20. Mengistu, D.T. and Sorteberg, A.: Sensitivity of SWAT simulated stream flow to climatic changes within the Eastern Nile River basin, HESS, 16, 391–407, doi:10.5194/hess-16-391-2012, 2012.
21. Moss RH. Edmonds JA, Hibbard KA, Manning MR, Rose SK et al. (2010) the next generation of Scenarios for climate change research and assessment nature.

22. Nash J.E., Sutcliff, J.V., 1970. River Flow Forecasting through Conceptual Models Part I- A discussion of Principles. Journal of Hydrology, 10:282-290.
23. Santhi, etal, (2001 a,b). Validation of SWAT model on a large river basin with point and non-point sources, Journal of the American Water Resources Association37:1169-1188
24. Taye, M. T. and Willems, P.: Temporal variability of hydro-climatic extremes in the Blue Nile basin, Water Resour Res, 48, doi: 10.1029/2011WR011466, 2012.
25. Taye, M. T., Willems, P., and Block, P.: Implications of climate change on hydrological extremes in the Blue Nile basin: A review, Journal of Hydrology: Regional Studies, 4, Part B, 280–293, doi:10.1016/j.ejrh.2015.07.001, 2015.
26. Teshager, A.D.; Gassman, P.W.; Secchi, S.; Schoof, J.T.; Misgna, G. Modeling agricultural watersheds with the soil and water assessment tool (swat): Calibration and validation with a novel procedure for spatially explicit hrus. Environ. Manag. 2016, 57
27. Teutschbein, C. and Seibert, J.: Bias correction of regional climate model simulations for hydrological climate-change impact studies: Review and evaluation of different methods, Journal of Hydrology, 456-457, 12–29, doi:10.1016/j.jhydrol.2012.05.052, 2012.
28. SWAT user manual (ARCSWAT User manual interference for SWAT2009).

Websites used for software downloads:

- SWAT (ARCSWAT2012) website http://www.brc.tamus.edu/swat/avswat.html [Accessed May 2017]
- Weather parameter calculator PCPSTAT (Williams, 1991) and dew point temperature calculator DEW02 programs http://www.brc.tamus.edu/swat/soft_links.html[Accessed July 2017]
- SWATCUP v5.1.6 website http://www.brc.tamus.edu/swat/swatcup.html

ANNEXES

Annex-1: stream flow Regression for Abay River at Kesse with Rib River at Addis Zemen Gauging Station

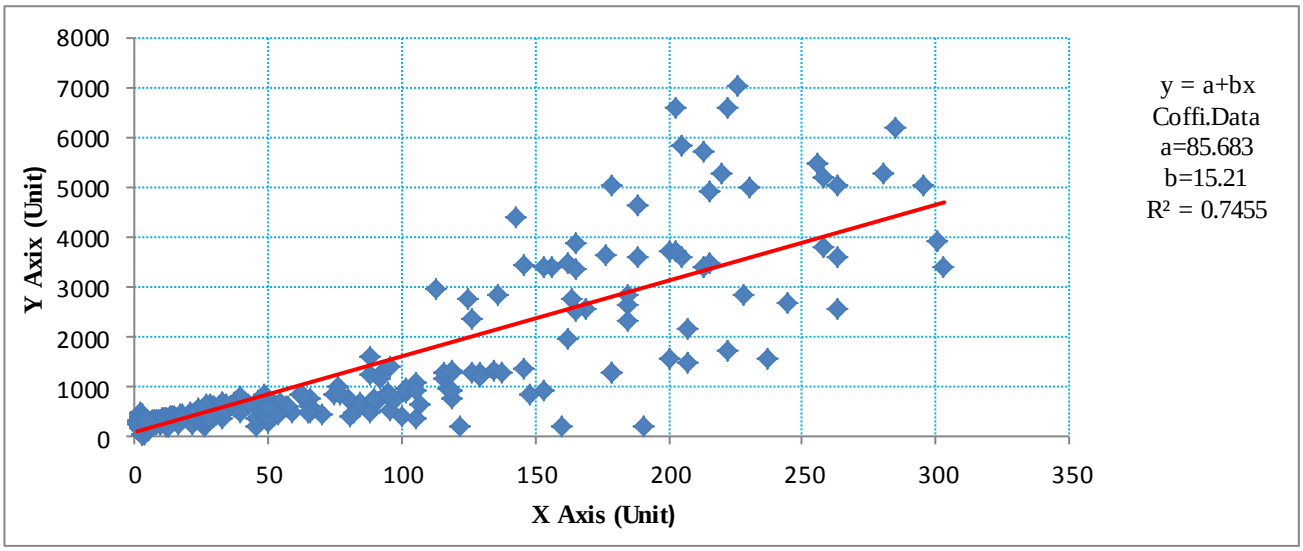

Annex-2: List of Parameters used for sensitivity analysis, Automatic model Calibration

Parameter Code	Rank	Parameter Description	File Location
CN2	1	Initial Curve No. at Moisture Condition II	.mgt
ALPHA_BF	2	Base flow alpha factor	.gw
GW_DELAY	3	Groundwater delay	.gw
GWQMN	4	Threshold depth of water in the shallow aquifer req'd for return flow	.gw
GW_REVAP	5	Groundwater revap coefficient	.gw
ESCO	6	Soil evaporation compensation factor	.hru
CH_N2	7	Manning's roughness value for main channel	.rte
CH_K2	8	Channel effective hydraulic conductivity	.rte
SOL_AWC	9	Available water capacity	.sol
SOL_K	10	Saturated hydraulic conductivity	.sol
HRU_SLP	11	Average slope steepness	.hru
SLSUBBSN	12	Average slope length	.hru
REVAPMN	13	Threshold water in the shallow aquifer for revap to occur	.gw

Annex-3: Description of Methods for Calibration Technique

Parameter Code	Change Method	Description for the Methods
CN2	r. Relative	**r**-Multiplying initial parameter by (1+ value)
ALPHA_BF	V. Replace	**V**-Replacement of parameter by value
GW_DELAY	V. Replace	**a**-Adding value to initial parameter
GWQMN	V. Replace	
GW_REVAP	a. absolute	
ESCO	V. Replace	
CH_N2	V. Replace	
CH_K2	V. Replace	
SOL_AWC	r. Relative	
SOL_K	r. Relative	
HRU_SLP	a. absolute	
SLSUBBSN	r. Relative	
REVAPMN	V. Replace	

Annex-4: consistency check for selected Rainfall Station in the study area

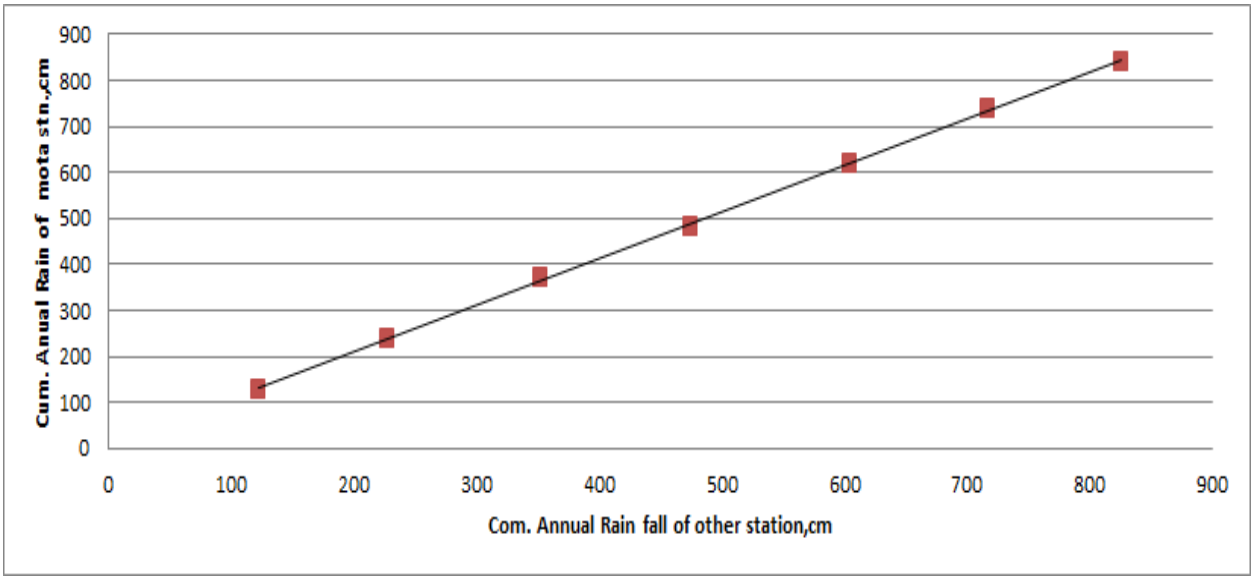

Annex:4.1 Double mass curve analysis for mota Rainfall Station

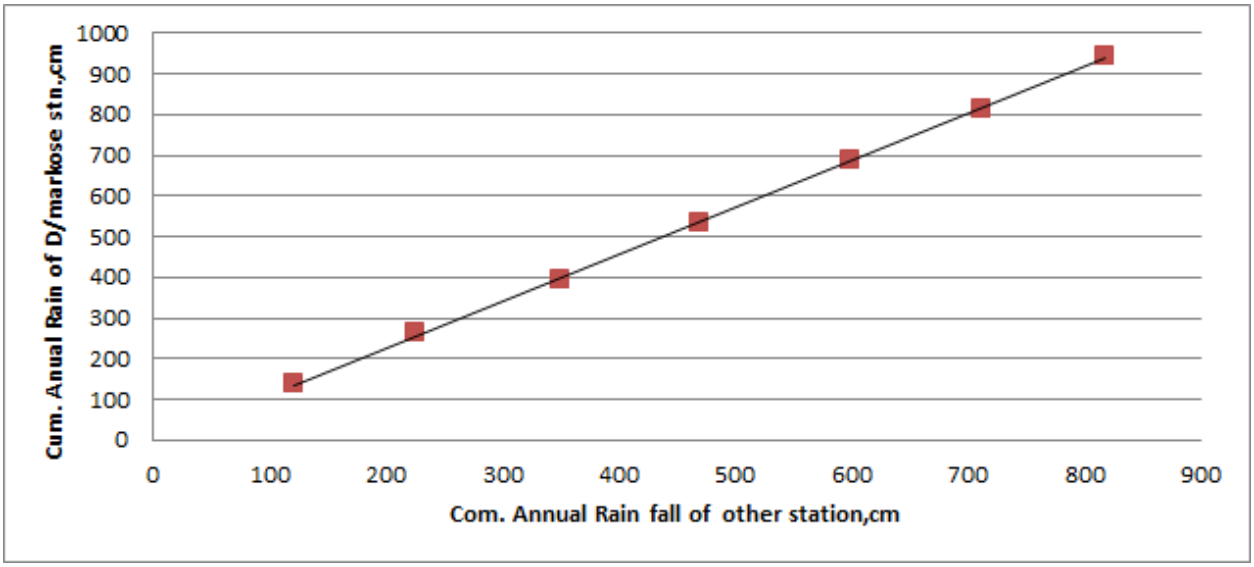

Annex:4.2 Double mass curve analysis for D/Markose Rainfall Station

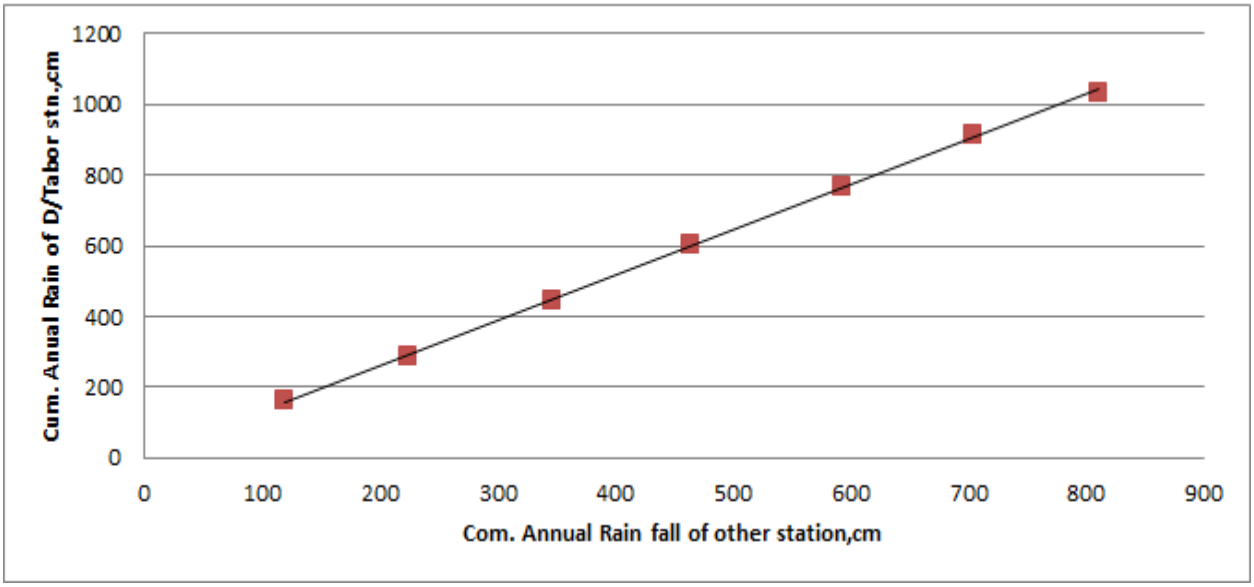

Annex:4.3 Double mass curve analysis for D/Tabour Rainfall Station

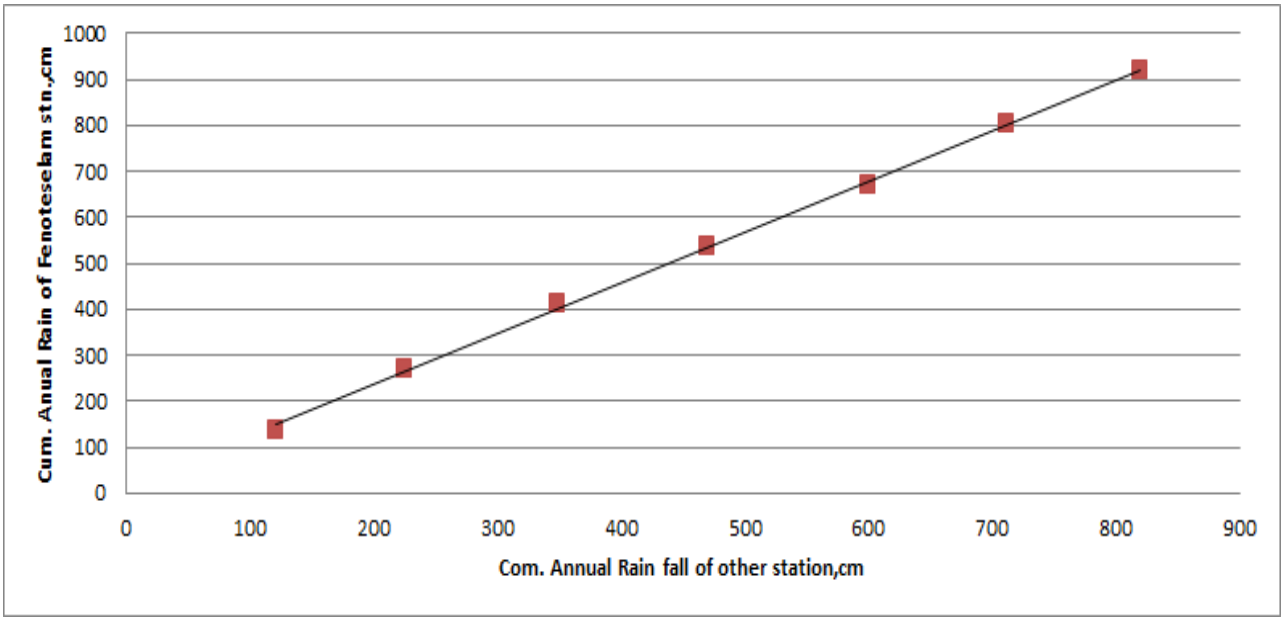

Annex:4.4 Double mass curve analysis for Finotselam Rainfall Station

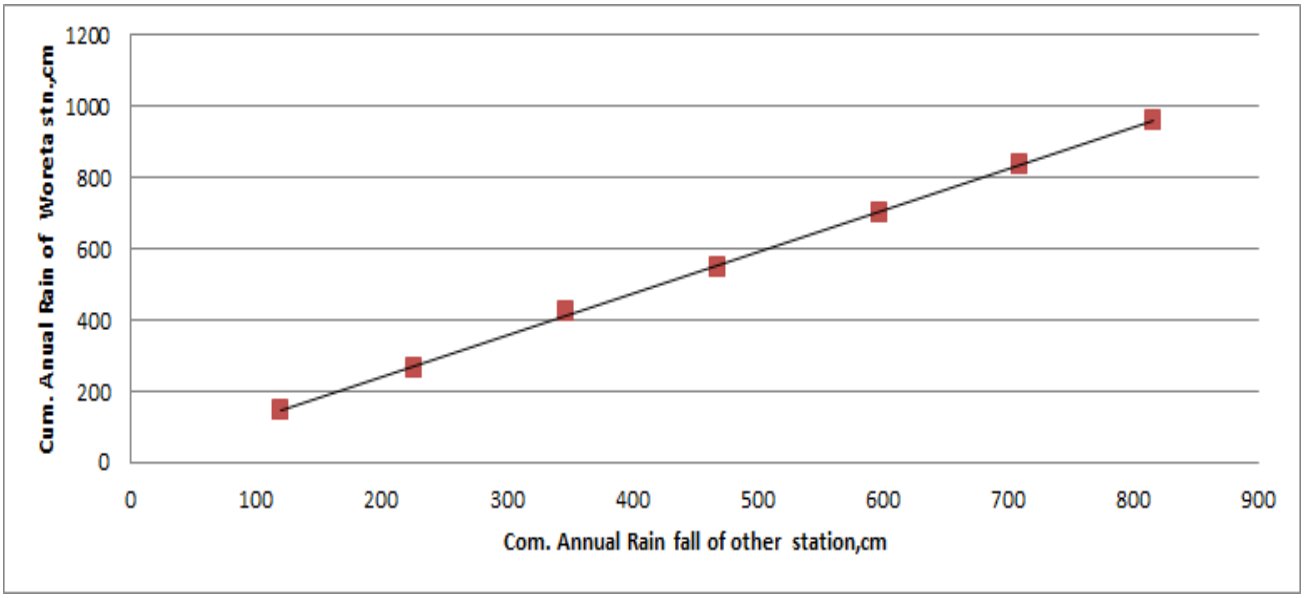

Annex: 4.5 Double mass curve analysis for Woreta Rainfall Station

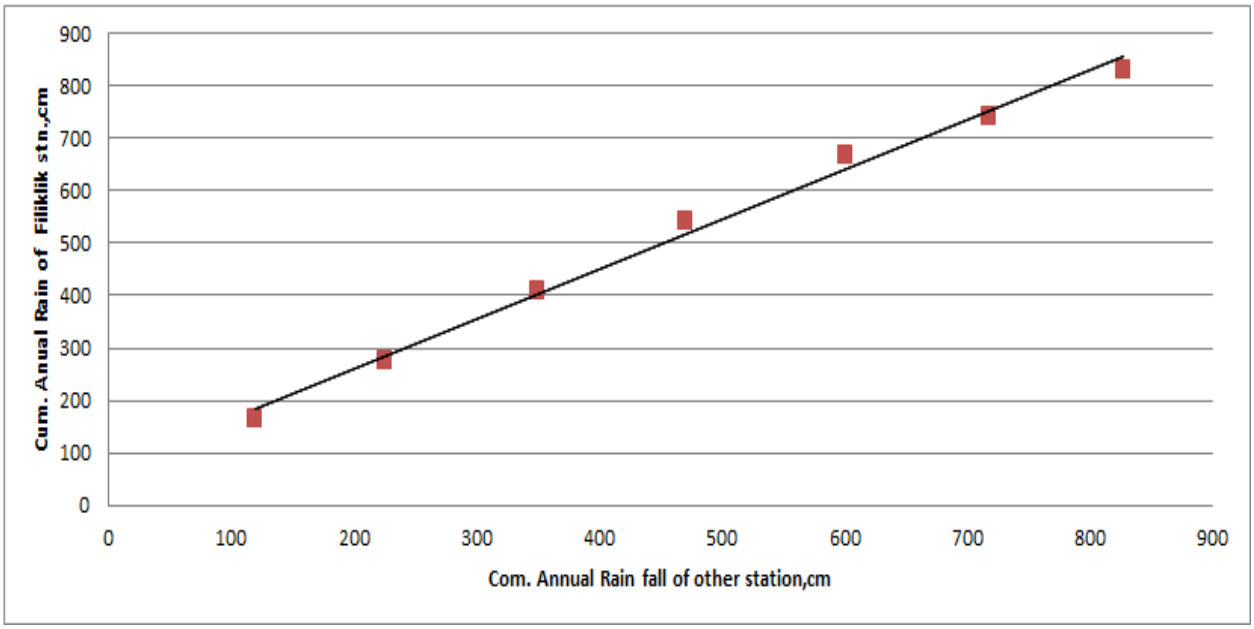

Annex: 4.6 Double mass curve analysis for Filiklik Rainfall Station

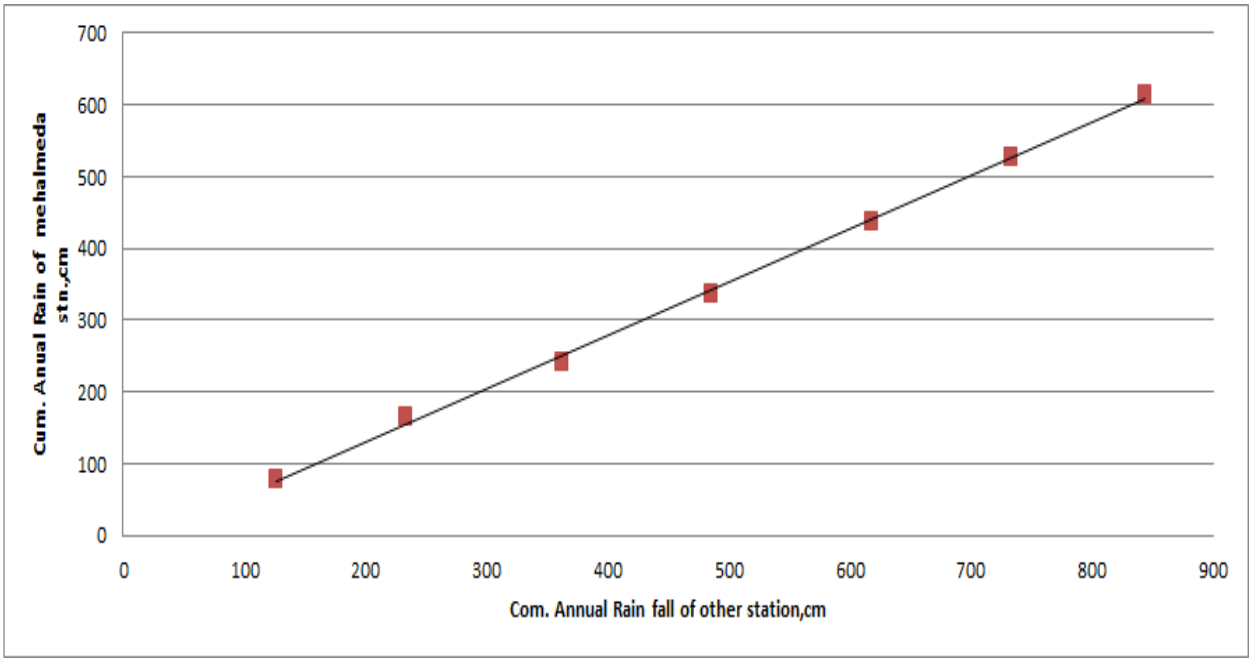

Annex: 4.7 Double mass curve analysis for MehalMeda Rainfall Station

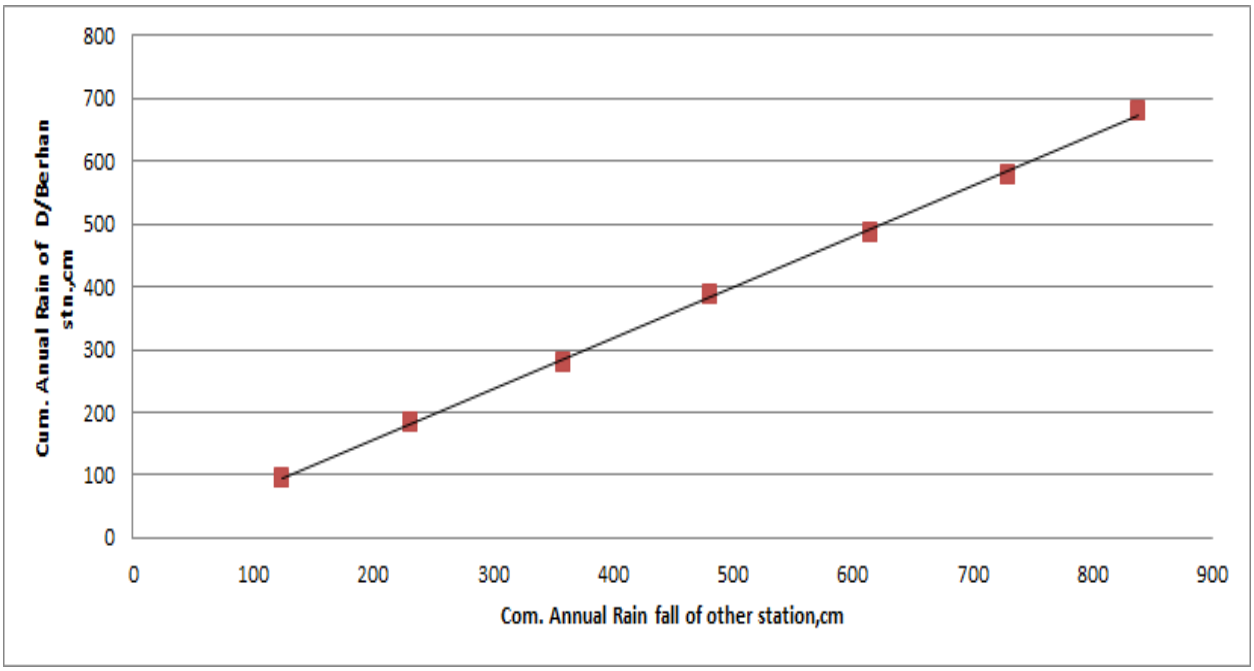

Annex: 4.8 Double mass curve analysis for DebreBerhan Rainfall Station

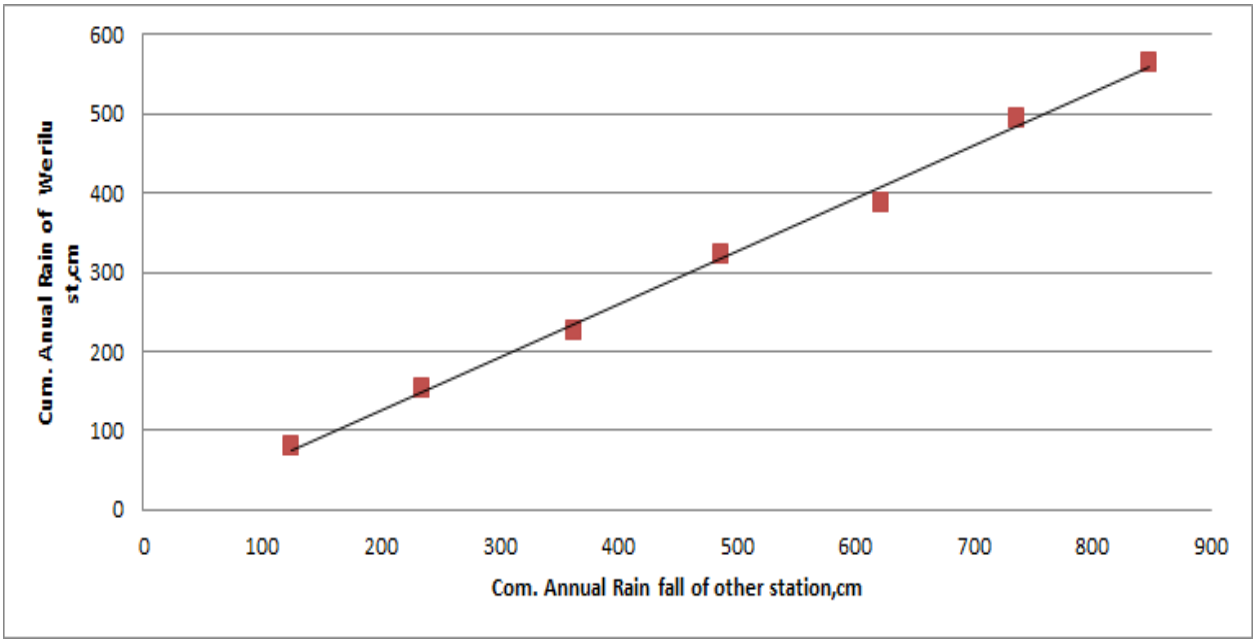

Annex: 4.9 Double mass curve analysis for Worilu Rainfall Station

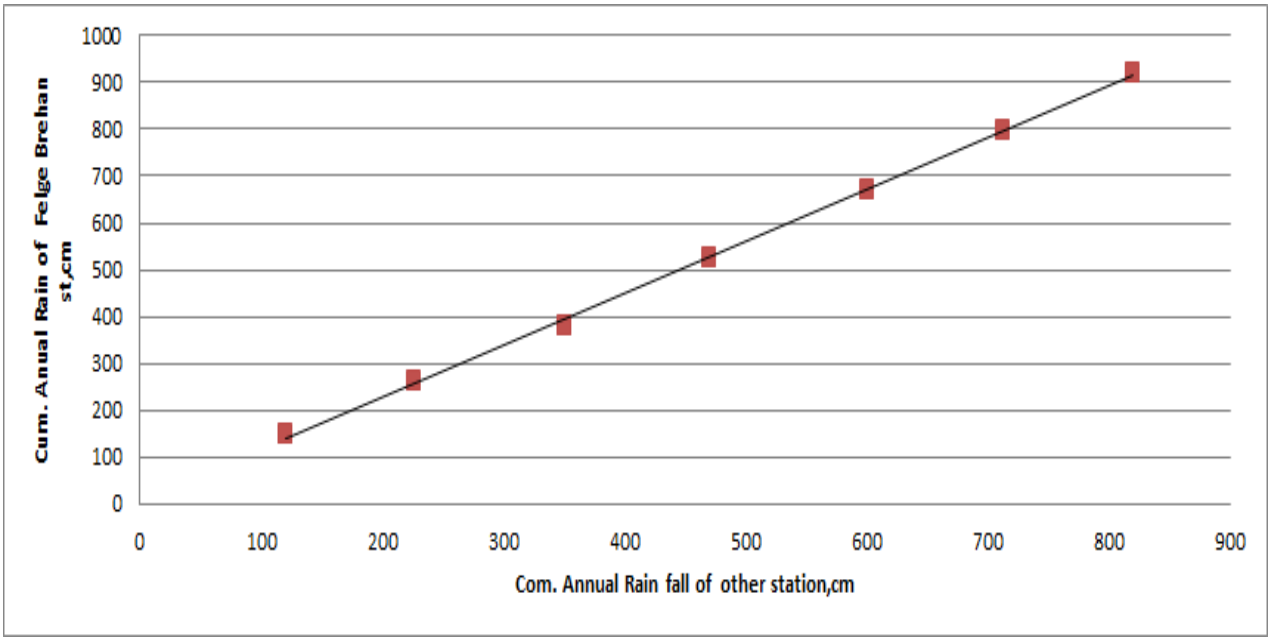

Annex: 4.10 Double mass curve analysis for FelegBrhan Rainfall Station

Annex: 5 Bias Correction for RCP Historical and Future time Rainfall data for selected Rainfall station

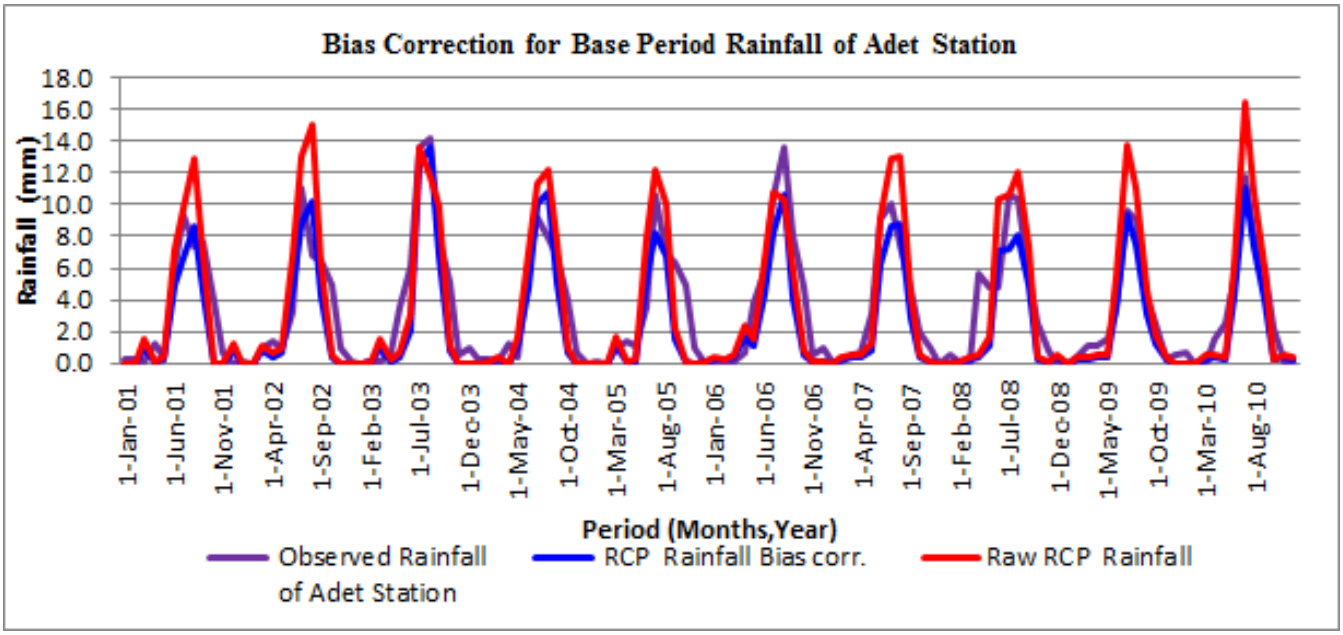

Annex: 5.1 Comparison of (Mean Daily Rainfall in Month) of Raw and Bias Corrected Rainfall data for the base period (2001-2010) for Adet Rainfall Station

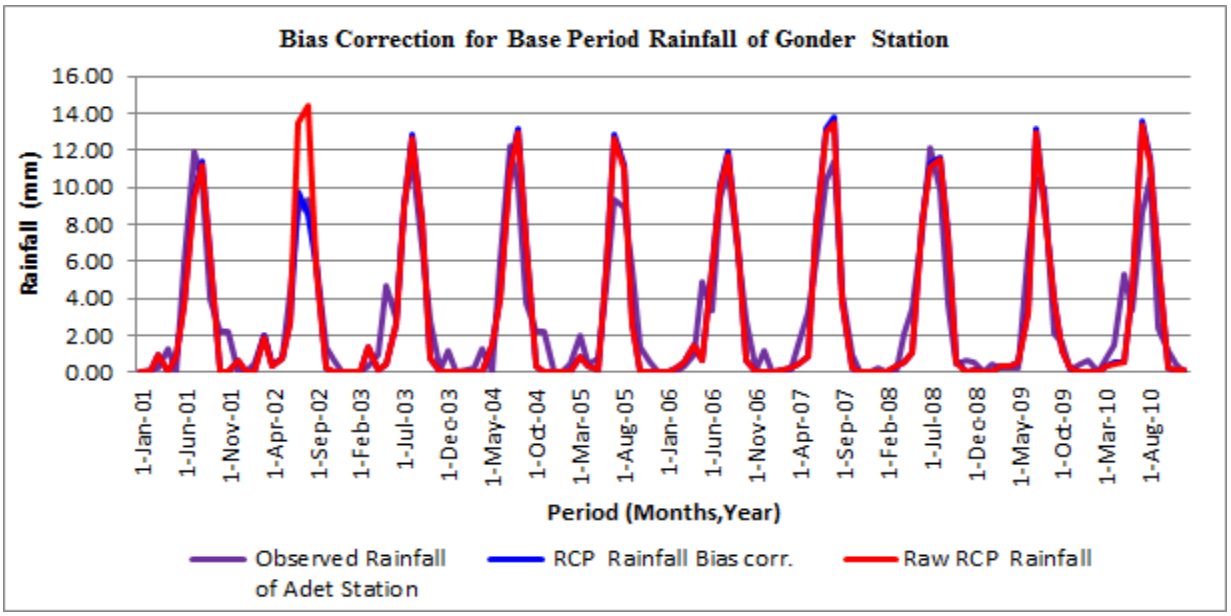

Annex: 5.2 Comparison of (Mean Daily Rainfall in Month) of Raw and Bias Corrected Rainfall data for the base period (2001-2010) for Gonder Rainfall Station

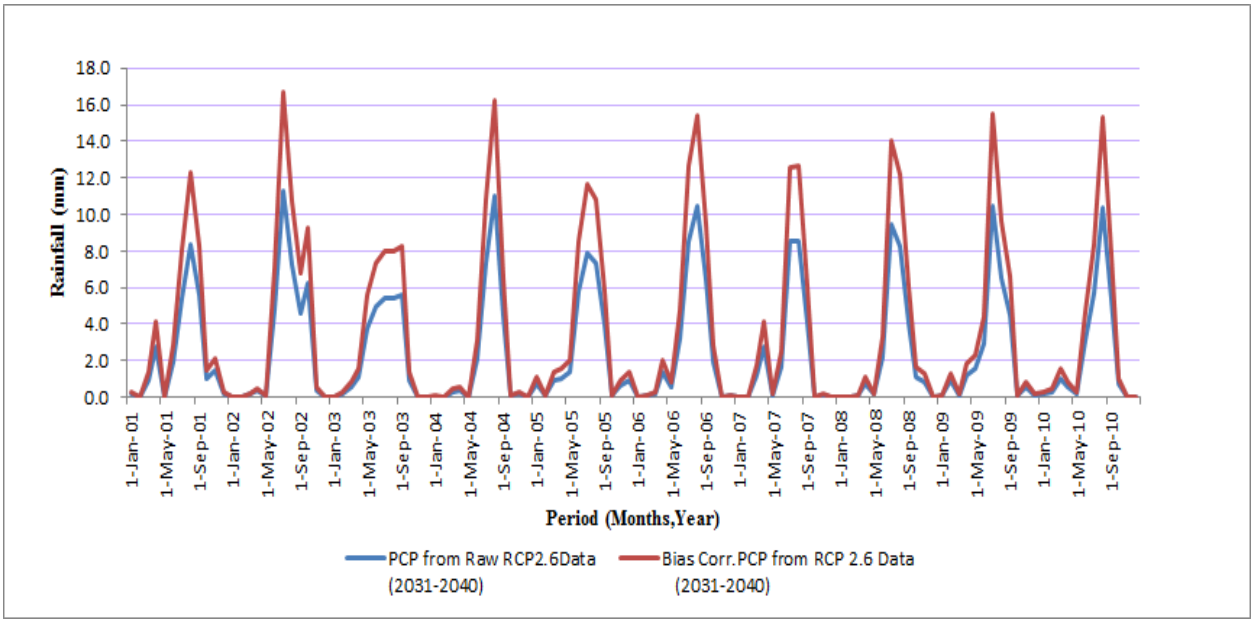

Annex: 5.3 Comparison of (Mean Daily Rainfall in Month) of Raw and Bias Corrected Rainfall data of RCP2.6 climate Data for (2031-2040) for Adet Rainfall Station

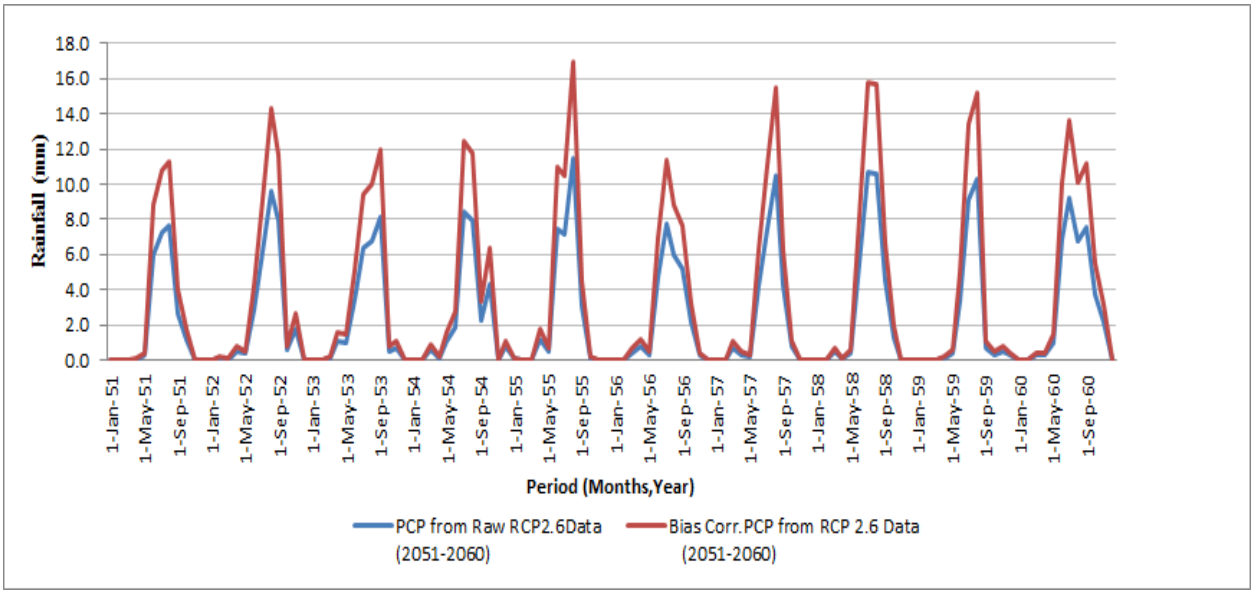

Annex: 5.4 Comparison of (Mean Daily Rainfall in Month) of Raw and Bias Corrected Rainfall data of RCP2.6 climate Data for (2051-2060) for Adet Rainfall Station

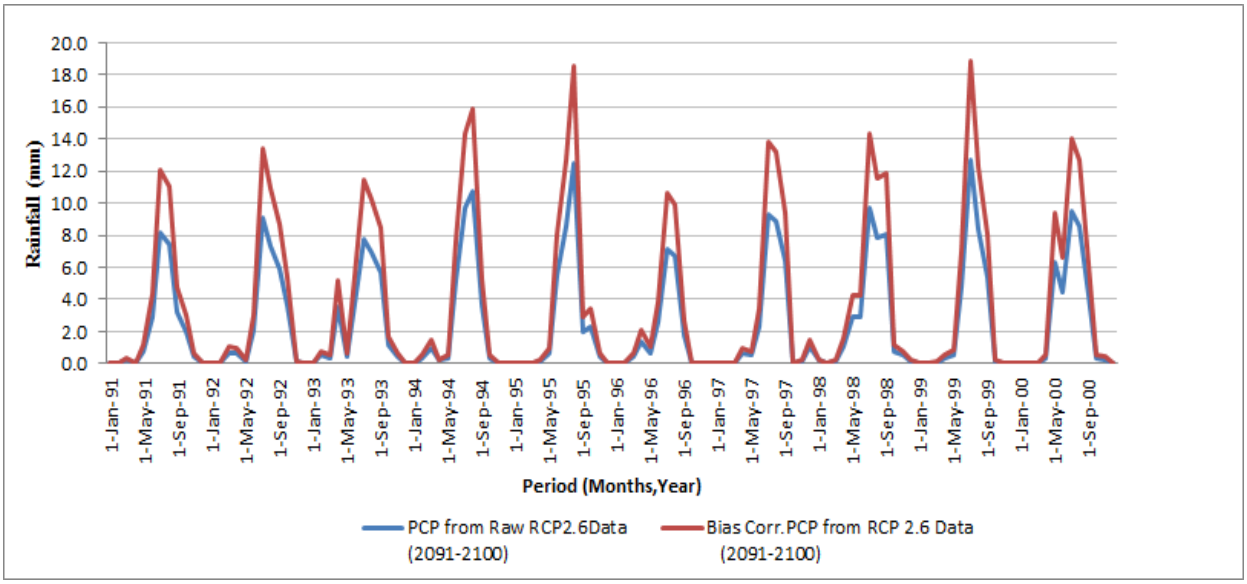

Annex: 5.5 Comparison of (Mean Daily Rainfall in Month) of Raw and Bias Corrected Rainfall data of RCP2.6 climate Data for (2091-2100) for Adet Rainfall Station

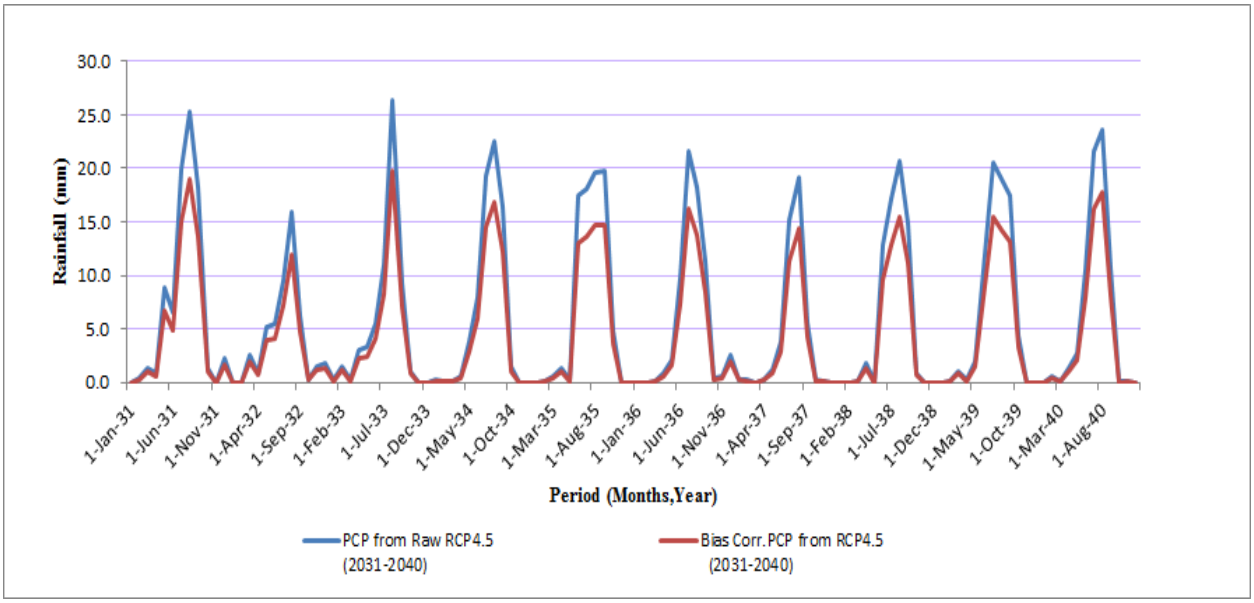

Annex: 5.6 Comparison of (Mean Daily Rainfall in Month) of Raw and Bias Corrected Rainfall data of RCP4.5 climate Data for (2031-2040) for Dangla Rainfall Station

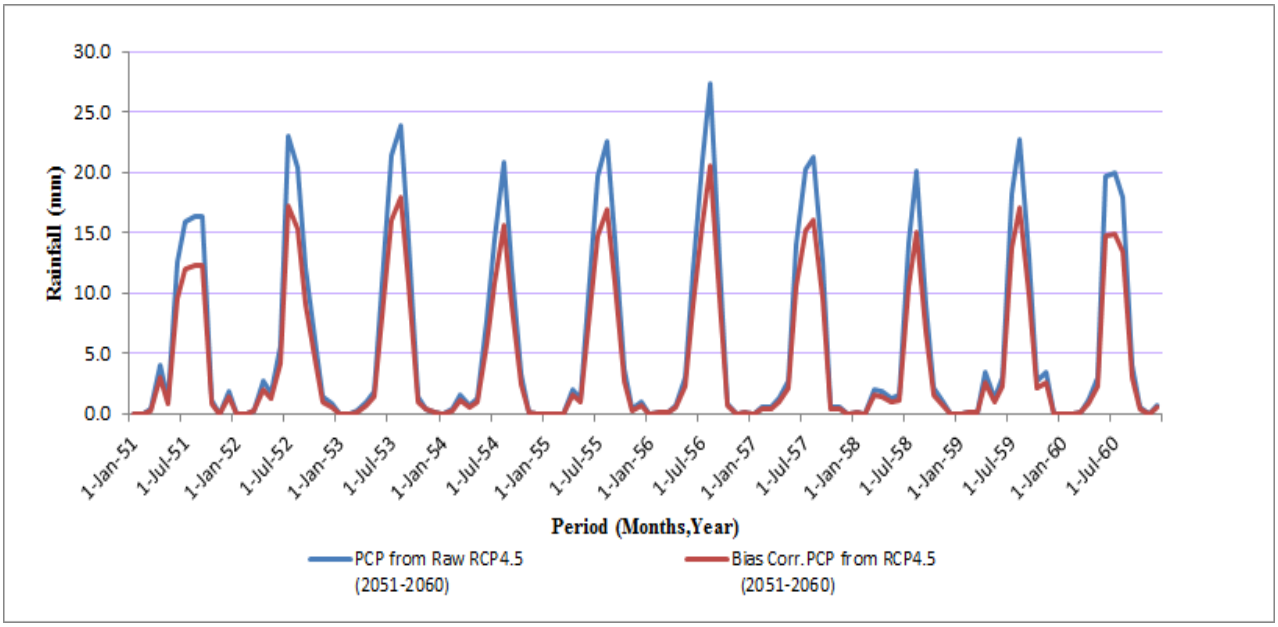

Annex: 5.7 Comparison of (Mean Daily Rainfall in Month) of Raw and Bias Corrected Rainfall data of RCP4.5 climate Data for (2051-2060) for Dangla Rainfall Station

Annex:6 Comparison of relative Change of future simulated runoff for a change in Precipitation and Potential Evapo-transpiration

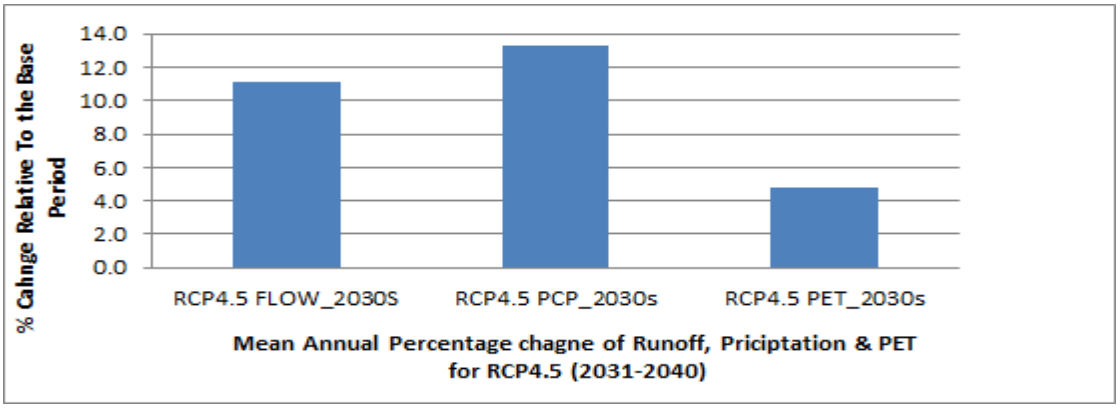

Annex: 6.1 comparisons of Percentage Change of Mean annual Simulated Runoff for a change in mean annual Rain Fall and potential Evapotranspiration for RCP4.5 (2031-2040)

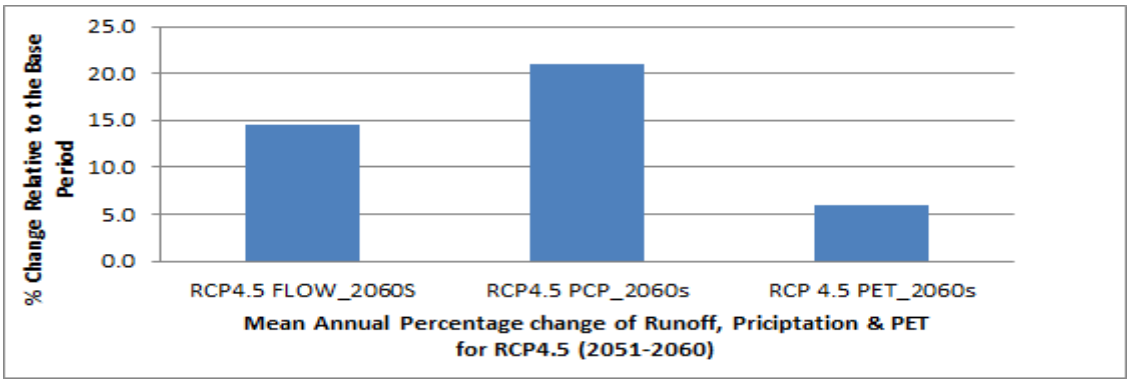

Annex: 6.2 comparison of Percentage Change of Mean annual Simulated Runoff for a change in mean annual Rain Fall potential Evapotranspiration for RCP4.5 (2051-2060)

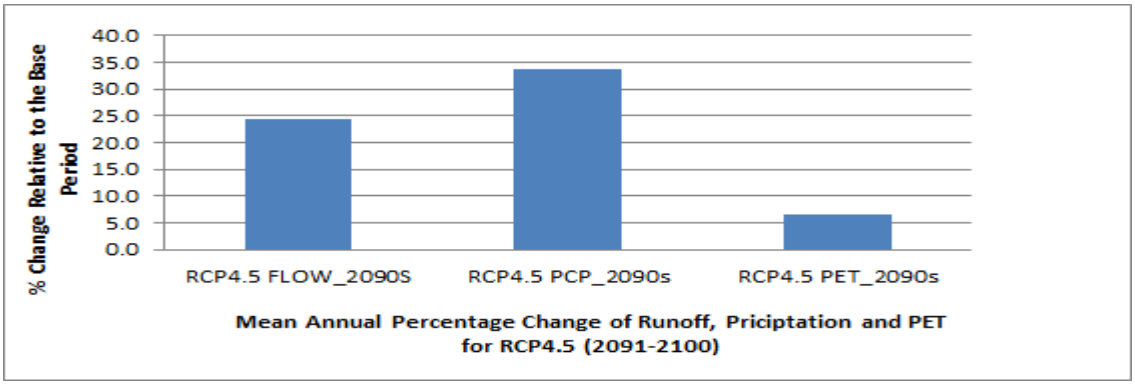

Annex: 6.3 comparison of Percentage Change of Mean annual Simulated Runoff for a change in mean annual Rain Fall potential Evapotranspiration for RCP4.5 (2091-2100)

Annex: 7 Land use classification as per BCEOM

A Agriculture: These are the areas identified as dominantly cultivated on the land cover map. Although animals play an important role in these areas, they are considered as secondary to cultivation. The key economic activity in these areas is cultivation, especially for grains, and these areas include sources of major surplus producing regions of the country. Crops include both large (Maize) and small (Wheat, Teff) grains.

AP-Agro pastoral: these areas are those defined as moderately cultivated on the land cover map, except as defined in the next unit. Only part of the area is cultivated; grazing activities are at least as important as cultivation.

AS-Agro-Sylvicultural: These are moderately cultivated areas mixed with significant forest, plantation or wood land, or forest/ wood land areas with extensive cultivation. Most of such areas will also be grazed. The units have been called Agro-Sylvicultural because of the importance of trees.

P-Pastoral: These are the grass land areas, generally above 1500m altitude. Pastoral areas are particularly difficult to define. Almost all areas are pastured to some degree. Most cultivated land is pastured after harvest; wood lands, bush lands and shrub lands are all grazed; animals may be found in high forest areas, even where relatively dense, seasonal wet lands are grazed during the dry season.

SP-Sylivo-Pastoral: These are the wood land, bush land and shrub land areas generally above 1500m these areas provide both grazing and wood resources.

S- Sylivicultural: These areas are essentially confined to the intact forest areas, plantations and high land wood lands. The term sylvicultural has been optimistically applied to all forest lands.

N.B:- BCEOM , French Engineering Consultants